TRANSFER OF HEAT AND MOMENTUM IN NON-UNIFORM TURBULENT FLOW

Thesis by

John Latimer Mason

In Partial Fulfillment of the Requirements

For the Degree of

Doctor of Philosophy

California Institute of Technology

Pasadena, California

1950

Acknowledgment

Financial support for this research program has been provided by the California Institute of Technology. Dr. B. H. Sage of the Department of Chemical Engineering has been responsible for the overall planning and supervision of the project. Darlton K. Breaux directed the experimental work with the heat transfer equipment, and Virgil J. Berry and Stuart D. Cavers cooperated in the taking of data. Franklin Page developed the method of correcting for the drift in the hot wire calibration. Harry W. Brough and Dr. Warren G. Schlinger were of material assistance in the work with the analog computer. Doris Moran assisted with the calculations.

The author is indebted to Dr. W. N. Lacey, Dr. D. M. Mason, and Dr. Sage for their helpful suggestions regarding the preparation of the manuscript. Special thanks are due Evelyn Anderson, Mary Lyon, and Katharine Schlinger for typing the manuscript.

Abstract

Determinations of pressure, temperature and velocity as functions of position in a non-uniform, steady, two dimensional, turbulently flowing air stream have been made under four different flow conditions.

Values of the eddy viscosity and eddy conductivity have been calculated and compared to those obtained under conditions of uniform flow. Bulk temperatures have been computed and compared with those obtained from existing empirical correlations.

The general problem of predicting temperature and velocity fields in non-uniform flow is discussed. Previous theoretical work is compared with the experimental results of this work. The further research necessary to solve this problem for the case of fully developed turbulent flow is outlined.

The partial differential equation for heat transfer has been solved for one of the above four flow conditions by means of an electrical analogy. Use has been made of eddy conductivity data obtained for uniform flow. This work is evaluated in light of the accompanying experimental results, and plans for further analog work are outlined.

TABLE OF CONTENTS

Introduction

During the past four years, a program of investigation into the nature of turbulent flow has been carried out at the California Institute. The purpose of this program is to verify the Reynolds analogy which is presumed to exist between the turbulent transfer of heat, momentum, and material (1). Experimental work accomplished up to this time has been primarily concerned with the transfer of heat and momentum.

Measurements of the turbulent flow of air have been made in a rectangular channel 12.4 in. wide, 0.7 in. high, and 13.4 in. long. Temperature and velocity distributions have been obtained in the wakes of heated cylinders (2) as well as in the unobstructed channel. All data have been taken midway between the vertical walls, so that the flow investigated has been very nearly two-dimensional.

Extensive measurements of uniform flow have been carried out by Corcoran (3), Page (4), and Cavers (5). (Flow is defined as uniform if the velocity and intensive fluid properties are independent of the downstream distance x.) The advantage of investigating uniform flow is that the differential equations of heat and momentum transfer are greatly simplified; parameters which describe the rates of transfer of heat and momentum may be readily calculated without the necessity of making invalidating assumptions. For two-dimensional steady uniform flow, the differential equation for momentum transfer may be expressed in the following simple form:

$$\tau_{yx} = y' \frac{dP}{dx} = \rho (\epsilon_m + \nu) \frac{du}{dy}, \qquad (1)$$

Under the same conditions the heat transfer equation is:

$$\dot{Q} = \sigma c_p (\epsilon_c + \varkappa) \frac{dt}{dy} \qquad (2)$$

The symbols used in these and succeeding equations are tabulated and defined in the table of nomenclature.

The turbulent contribution to the transfer of momentum is represented by the eddy viscosity; the turbulent contribution to the transfer of heat is represented by the eddy conductivity. Reynolds first hypothesized that, since transfer of heat and momentum takes place by the same process of turbulent mixing, the two eddy quantities ϵ_m and ϵ_c are equal. Experimental evidence (4), (5), indicates that the eddy quantities are not equal even under simple flow conditions; but they are of the same order of magnitude, and some progress has been made in predicting the ratio of the two quantities.

The quantities ν and $\varkappa$ are proportional to the transfer of momentum and heat by motion of the individual fluid molecules. A turbulently flowing stream may be divided into three sections according to the magnitudes of ν and $\varkappa$ relative to ϵ_m and ϵ_c, respectively. In the turbulent core $\nu \ll \epsilon_m$ and $\varkappa \gg \epsilon_c$; in the buffer layer $\nu \cong \epsilon_m$ and $\varkappa \cong \epsilon_c$; and in the laminar layer, the eddy quantities are zero.

The eddy quantities ϵ_m and ϵ_c differ fundamentally from their molecular analogs ν and $\varkappa$ in that they are not thermodynamic properties of the fluid, but vary from point to point in a flowing stream, even where the state of the fluid does not change. If these quantities are to be of engineering value, some means must be devised of

predicting them, either on the basis of a hypothesis which must finally be verified empirically, or directly from a correlation of experimental data. An example of the former is the Karman similarity theory (6). The latter is the method of approach of this research.

Calculations of ϵ_m and ϵ_c can be made for the case of uniform flow if four types of measurements are made: temperature, velocity, heat flux, and pressure gradient. Careful measurements of these quantities have been made for bulk air speeds ranging from 10 to 90 ft/sec.

The following conclusions seem indicated:

a. The eddy quantities ϵ_m and ϵ_c are independent of temperature or temperature gradient; they seem to be primarily a function of point velocity.

b. The eddy viscosity at midstream is not zero as is predicted by several investigators (7), (8).

These conclusions are drawn from measurements of uniform flow, but it seems reasonable to assume that they are valid for non-uniform flow as well.

The problem of turbulent flow is further complicated by the influence of wall roughness upon the turbulence and hence upon ϵ_m and ϵ_c . Results obtained in this research may or may not apply to flow in other smooth channels.

Some of the problems which arise in the treatment of non-uniform flow will now be discussed. Any flow in which there is an appreciable net transfer of heat to the fluid is of necessity non-uniform. The problem of determining the rate of heat transfer to a turbulently

flowing fluid is a formidable one, and is of paramount interest, both theoretically and industrially. The partial differential equation for heat transfer is non-linear. Analytical solutions are difficult even for the case of laminar flow.

The present engineering method of approach to the problem of turbulent heat transfer is by the use of overall coefficients. The numerical value of the heat transfer coefficient h may be calculated in terms of dimensionless ratios which describe the flow and the fluid properties. A large mass of heat transfer data has been correlated in the form of a relation between the Stanton, Prandtl, and Reynolds numbers (9):

$$St = 0.023 (R_e)^{-0.2} (P_r)^{-0.6} \qquad (3)$$

Correlations such as this, which apply to flow of a fluid in a pipe or between parallel plates, are extremely useful in calculation of overall rates of heat transfer, and the consequent evaluation of the bulk temperature of the flowing fluid. However, they are not adapted for calculation of point properties of a fluid. The eddy quantities show considerable promise for calculation of point properties, although their present use in engineering calculations is negligible.

The purpose of the investigation of uniform flow is to determine the behavior of the eddy quantities under simple flow conditions where they may be readily and accurately measured. Investigations of non-uniform flow permit computation of the eddy quantities under conditions of direct industrial importance, although the calculation procedure is unwieldy even after simplifying assumptions have been made.

The equation for heat transfer in two-dimensional steady non-uniform flow is:

$$\frac{\partial}{\partial y}\left[(\epsilon_c + K)\frac{\partial t}{\partial y}\right] = \frac{\partial t}{\partial x} \qquad (4)$$

This equation is derived in Appendix I.

In order to solve this equation to obtain t as a function of x and y, knowledge of the temperature boundary conditions, the velocity distribution, and the eddy conductivity distribution is necessary. Analytical solution of the above equation is definitely not feasible. Numerical methods are tedious and not generally satisfactory.

A method of solution which shows considerable promise is that of an electrical analogy. An electrical circuit is devised which obeys a differential equation analogous to Equation 4 when the latter is expressed in finite difference form. The heat transfer equation may then be solved by making measurements of electrical quantities which, upon conversion, give t as a function of x and y. The extent of agreement between an analog solution and a corresponding set of experimental measurements will indicate the validity of the eddy conductivity information used in obtaining the solution; the other variables may be accurately established.

Equipment

The experimental equipment used has been described in considerable detail elsewhere (10) and only a brief outline of its features will be presented here. A schematic diagram of the path followed by the working fluid (air) is shown in Fig. 1. Air is forced by the blower (C) through a Venturi meter, then through a turning section equipped with vanes to guide the flow, and then through a converging section (E) into the entrance of the channel. After its passage through the channel, the air is returned to the blower through another turning section.

The parallel plates which bound the working section above and below are of copper, 3/8 in. thick. The outside surfaces of the copper plates are in contact with independently circulating oil baths (Fig. 2). Electronic temperature control circuits permit maintenance of the oil baths and the entering air at predetermined temperatures. Oil bath and entering air temperatures are measured by means of platinum resistance thermometers. Temperatures and velocities* are measured by a 0.5 mil platinum wire 3/8 in. long which is positioned in the channel by means of a traversing mechanism. This dual use of the wire has led to its designation as the thermanemometer. To measure temperatures, the wire is used as a standard four-lead resistance thermometer. To measure velocities, use is made of the constant resistance technique of hot-wire anemometry. According to King's equation, the rate of energy dissipation from a hot wire is proportional to the temperature difference

---

*The wire actually measures the quantity $(u^2 + v^2)^{\frac{1}{2}}$ which is the magnitude of the velocity vector. In this work, the flow is practically horizontal and $(u^2 + v^2)^{\frac{1}{2}} \simeq u$.

between the wire and the air stream and to the square root of the velocity:

$$\frac{I^2 R_{HW}}{R_{HW} - R_A} = A + B\sqrt{u} \qquad (5)$$

The constants A and B in King's equation are determined experimentally by frequent calibration of the thermanemometer against a pitot tube. These instruments are mounted in the channel on piano wires (Fig. 3). The traversing mechanism which controls the movement of this assembly permits the hot wire to be elevated to within 0.001 in. of the upper wall and lowered to within about 0.015 in. of the lower wall. The side-walls of the working section may be moved horizontally to allow the traversing gear to be set at any desired downstream position. A sectional view and photograph of the traversing gear are shown in Figs. 3 and 4, respectively.

The static pressure is measured at a number of positions in the channel by means of pressure taps connected to a bank of manometers filled with kerosene. The absolute pressure at the upstream end of the channel is measured by means of a conventional mercury barometer; all other static pressures are measured relative to the upstream pressure. A cathetometer is used to measure the height of the columns of liquid in the manometers. The cathetometer and manometer bank are shown in Fig. 5. Pitot tube pressure measurements are made by means of a micromanometer (Fig. 6).

The resistances of the platinum thermometers are measured by Mueller bridges, one of which is also used to determine the resistance of the thermanemometer.

The circuit diagram for the thermanemometer is shown in Fig. 7. The energy input to the thermanemometer is adjusted so as to bring it to a predetermined resistance, which is attained by balancing a Wheatstone bridge which contains the thermanemometer as one leg. The voltages across a resistance in series with the thermanemometer and across the thermanemometer itself are measured by means of White and K-type potentiometers. The White potentiometer is also used to measure the voltage of thermocouples which are mounted in the copper plates at various distances downstream. Mueller bridges, potentiometers, and electronic control circuits for the oil baths and air are installed in the bench shown in Fig. 8.

The rate of heat transfer in uniform flow is measured by means of two calorimeters, which are installed at different downstream distances to check on the uniformity of the flow and the consistency of each calorimeter. The rate of electrical energy input necessary to maintain the temperature of the block equal to that of the surrounding plate is measured. Correction for energy losses to the surroundings (which are not large) permits calculation of the rate of heat transfer across the flowing stream. No calorimetric measurements were made under conditions of non-uniform flow.

Experimental Results

The experimental work reported herein consists of measurements of pressure, temperature, and velocity as a function of position in the channel. Results are summarized in Table I. The data are also presented graphically in Figs. 10-23.

Data were taken at two bulk velocities, U_B = 15 and 30 ft/sec,* for boundary conditions 100/85/100**. The other two boundary conditions, 115/100/85 and 100/100/85, were investigated at only one bulk velocity, U_B = 30 ft/sec.

Temperature traverses for each set of boundary conditions were made at downstream distances x = 23.22, 36.00, 50.00, 82.07, and 136.35 in., measured from the entrance to the channel at the upstream end of the copper plates. Velocity traverses were made at the first, third, and fifth of the above positions. Temperature measurements were made at shorter downstream intervals than velocity measurements because the temperature fields under investigation were more complex than the velocity fields.

The five temperature traverses for the case 100/85/100, U_B = 30 ft/sec, are shown in Fig. 10. The vertical isotherm t = 84.9°F is

- - - - - - - - - -

*These nominal values of U_B will be used for convenience. Values of the actual mass velocity and Reynolds number corresponding to these bulk velocities are listed in Table I.

**This description of the boundary conditions will be used throughout the discussion. The first number is the temperature of the upper oil bath; the second number is the bulk temperature of the entering air; the third number is the temperature of the lower oil bath. All temperatures are in °F.

the assumed temperature traverse for x = 0, the entrance to the channel. (A correction of -0.1°F has been applied to the bulk entering air temperature of 85.0°F to allow for the temperature drop in the converging section.) It is to be emphasized that this t vs. y curve is only an estimation of experimental conditions; no actual measurements of t and u were made for values of x smaller than 23.22 in., this being the farthest upstream that the traversing gear could be moved. However, the approximation of isothermal conditions at the entrance to the channel should be very good as a result of the passage of the air through the converging section. A very nearly constant velocity distribution should also prevail at x = 0 for the same reason, corresponding to potential flow.

The temperature traverses for 100/85/100, U_B = 15 ft/sec, are shown in Fig. 11. In this case the temperature drop in the converging section is negligible, and the bulk temperature of the entering air is taken as 85.0°F.

For both these cases, the temperature of the air will have no further tendency to change with downstream distance only when it reaches 100°F, the temperature of the plates. Uniform flow conditions would thus be represented in this case by an isothermal traverse at 100°F. Strictly speaking, uniformity would be attained only at an infinite downstream distance. It is not surprising that uniformity has not been approached very closely at x = 136.35 in. (the farthest distance downstream at which measurements were taken) for either U_B = ft/sec or U_B = 30 ft/sec.

The bulk temperatures corresponding to the traverses just discussed are presented in Table II. If variations in c_p and σ are neglected, the bulk temperature may be defined as:

$$t = \frac{\int_0^1 u\, t\, d(y/y_o)}{\int_0^1 u\, d(y/y_o)} \qquad (6)$$

It is the temperature which a given cross section of fluid would attain if it were removed from the channel and thoroughly mixed.

The velocity traverses for the above cases (100/85/100, U_B = 30 ft/sec; 100/85/100, U_B = 15 ft/sec) are presented graphically in Figs. 12 and 13. The data are also plotted in the dimensionless form u/u_m vs. y/y_o (Figs. 14 and 15). At U_B = 30 ft/sec for any value of y/y_o, u/u_m is somewhat larger for the traverse at x = 23.22 in. than for any of the other traverses. The relatively flat velocity distribution indicated by large values of u/u_m shows that the transition from potential flow at x = 0 to a fully developed turbulent velocity profile is not complete at x = 23.22 in.

The deviation of the remaining traverses from a single curve is small, and the random nature of the deviations indicates that they result from experimental uncertainty. Fully developed turbulent flow is evidently attained somewhere between x = 23.22 in. and x = 36.00 in. for U_B = 30 ft/sec. Fig. 15 indicates that fully developed turbulence is obtained upstream of x = 23.22 in. for U_B = 15 ft/sec.

Fully developed turbulent flow is obtained at a downstream distance beyond which the factors which describe the turbulence (such as intensity and scale) are uniform. Thus if for any value of x greater than x_c

$$\frac{\partial i_k}{\partial x} = 0 \qquad k = 1 \ldots \ell \qquad\qquad \frac{\partial a_k}{\partial x} = 0 \qquad k = 1 \ldots m \tag{7}$$

the turbulent flow is said to be fully developed at x_c. An alternate point of view is that the influence of the entrance conditions (such as the shape of the velocity profile at the entrance) is negligible for all values of $x = x_c$.

The influence of entrance conditions on the temperature profiles could have been eliminated by adding a conditioning section about four feet in length to the upstream end of the channel. This section would be geometrically similar to the remainder of the channel. Its distinguishing feature would be provision for control of the temperature of the copper plates separate from the plates bounding the main part of the channel. The temperature of the plates in the conditioning section would always be maintained at the temperature of the entering air. The air would enter this section approximately at potential flow; its velocity profile would become fully developed under isothermal conditions. The temperature boundary conditions would be applied at the downstream end of the conditioning section. In this way, temperature development would take place independently of velocity development. This design was not considered because the apparatus was built primarily for studies of uniform flow.

Fully developed turbulent flow does not imply uniformity, since the velocity must change with downstream distance whenever the density of the fluid is changing as a result of heat transfer.

Temperature and velocity data for the boundary conditions 115/100/85, U_B = 30 ft/sec, are presented in Figs. 16 and 17. Previous

data were taken at these boundary conditions at x = 136.35 in. as a part of the uniform flow program (4), (5). The data of Figs. 16 and 17 indicate that the assumption of uniformity is justified, since the flow is substantially uniform as far upstream as x = 50.00 in.

Uniformity is evidently established much more rapidly for the case 115/100/85 than for the case 100/85/100. For the latter case, the midline temperature must change by 15 degrees to reach the uniform value; in the former case no change in the midline temperature is necessary. The amount of change which the midline temperature must undergo is the factor which determines the distance downstream at which uniform conditions will be established in the case of symmetrical boundary conditions such as these.

The case 100/100/85 (Figs. 18 and 19) is intermediate between 115/100/85 and 100/85/100 in the distance downstream at which uniform flow is established. The flow is decidedly non-uniform at x = 136.35 in., but one would expect uniformity to be established at a finite downstream distance. Practically no heat is transferred from the upper wall for the traverses x = 23.22 in. and 36.00 in. A temperature gradient appears at the upper wall at x = 50.00 in., and becomes progressively larger for each remaining traverse.

Accuracy of Experimental Data

The bulk temperature of the air entering the channel and the temperature of the oil baths at the point of measurement were maintained within $\pm 0.02^{\circ}F$ of a predetermined value. It is believed that circulation of the oil (countercurrent to the flow of air) was sufficiently rapid so that the bulk temperature drop in each oil bath did not exceed $0.1^{\circ}F$ between the point of measurement of the oil temperature ($x = 156$ in.) and $x = 0$. However, the temperature of the inside surface of each copper plate was certainly less than the temperature of the oil bath with which it was in contact, the temperature drop being proportional to the flow of heat through the plates into the air stream.

Measurement of plate temperature by means of thermocouples indicates that the temperature drop through the plates may have been as much as $2.2^{\circ}F$ at the upstream end of the channel where the rate of heat transfer to the air stream was largest. Each thermocouple is installed in a well which extends to within a few hundredths of an inch of the air-side surface of the copper plate, but the thermocouple cannot be in contact with the plate; and it is estimated that any thermocouple reading may differ from the true temperature of the plate by as much as $\pm 0.5^{\circ}F$.

A knowledge of the rate of heat transfer through the plate would permit prediction of the temperature of the air-side surface of the copper plate from a knowledge of the temperature of the oil-side surface. But the oil-side temperature cannot be predicted

unless the thermal resistance of the oil film is known. The oil film resistances are different for the upper and lower baths; foreign matter is known to have settled from the upper oil bath onto the upper plate and presumably increases the film resistance. Because of these difficulties, no attempt was made to calculate air-side plate temperatures. It was believed that calculated values would be more in error than the thermocouple readings.

The location of the thermanemometer in the channel was known to within ± 0.005 in. for the x coordinate and ± 0.0015 in. for the y coordinate. The largest temperature gradients encountered in this work were approximately $200^{\circ}F/in.$; an error of 0.0015 in. in determining y would then correspond approximately to a temperature error of $0.3^{\circ}F$. However, large temperature gradients were found only near the walls where the uncertainty in determining y was less than the maximum value cited above. The temperature uncertainty as a result of uncertainty in thermanemometer position probably does not exceed $\pm 0.1^{\circ}F$ near the walls, and is less than this near the center of the stream. The corresponding uncertainty in velocity is ± 0.2 ft/sec.

Small vibrations of the hot wire about its equilibrium position resulted in corresponding fluctuations with time in the measured resistance of the wire. These fluctuations were of course largest near the walls where the temperature and velocity gradients were highest. If lag in the wire is neglected, no error will be introduced by these fluctuations with time, provided that an effective

time average of the resistance can be taken. However, the method of determining the mean value of the resistance was by means of a visual estimation of the mean position of a galvanometer needle. When the fluctuations were large, the mean position of the needle could not be accurately estimated. The resulting uncertainty in temperature and velocity measurements is estimated at $\pm 0.05^{\circ}F$ and ± 0.1 ft/sec, respectively.

A further possible complication is the lag of the thermanemometer behind the velocity fluctuation (11), but the resulting error is probably small and will not be considered further.

One of the most consistent sources of difficulty in the use of the thermanemometer is the tendency of the calibrations to change with time. It has been found that for a given air velocity the current required to maintain the thermanemometer at its operating temperature decreases with time. This phenomenon corresponds to a decrease in the heat transfer coefficient of the wire, and results in a change in the constants A and B* in Equation 5. It is believed that foreign material accumulates on the wire and inhibits heat transfer to the air stream. It has been found that heating the wire to a red glow for about 20 minutes causes the velocity calibration constants A and B to reassume approximately the values which they had when the wire was new. However, this reassumption is not quantitatively reliable, and so the wire was

---

*A and B will be referred to as constants even though they are functions of time.

calibrated as a velocity measuring device at frequent intervals and was burned off only when the rate of heat transfer from the wire became so low as to render it insensitive to changes in velocity. The constants A and B in Equation 5 were determined as functions of time by means of a standardized procedure (4).

The uncertainty in determining the air velocity by means of the thermanemometer is attributed to two factors:

a. The thermanemometer was calibrated only three times for each traverse. Considerable uncertainty exists in the delineation of curves such as A vs. θ and B vs. θ from only three experimental points. In order to avoid this difficulty, the assumption is made in the drift analysis procedure that the constants A and B change with time when and only when air is flowing through the channel. This assumption permits correlation of A and B as a function of time for several consecutive traverses, even when there are intervening idle periods. Unfortunately, it is often obviously impossible to correlate the traverses in this way, due perhaps to such factors as dislodgment of the foreign material from the thermanem - ometer during movement of the traversing gear.

b. Velocity measurements by means of the pitot tube, against which the hot wire was calibrated, are subject to considerable uncertainty, especially at low velocities.

The precision of the velocity measurements, that is, their consistency without regard to calibration errors, is estimated at $\pm$0.2 ft/sec. Their accuracy, however, is much lower; some of the velocities in traverses in which calibration difficulties were encountered may vary from the true value by as much as $\pm$0.5 ft/sec.

Unexpected difficulty was encountered in the change of temperature coefficient of resistance of the thermanemometer with time. The change was not large, and unlike the change in velocity calibration, it seemed to take place whether or not air was flowing through the channel. Fortunately the drift was nearly linear with time. This phenomenon appears to be unique; no such steady drift has taken place during other measurements on this project, and no mention of it has been found in the literature. A possible explanation for this drift is the diffusion along the wire of the solder which was used to connect the wire to the supporting needles.

The thermanemometer was calibrated as a temperature measuring device against a suitable standard in stagnant air at approximately 100°F. In the equation relating t and R

$$t = \alpha(\theta)\, R + \beta \qquad (8)$$

The coefficient $\alpha(\theta)$ was determined as a function of time by interpolation between the experimental calibrations with the assumption of constant β. A plot of $\alpha(\theta)$ vs. (θ) is shown in Fig. 24. The temperature error resulting from uncertainty in determining $\alpha(\theta)$ as a function of (θ) is estimated to be $\pm$0.05°F.

Additional physical phenomena introduce some uncertainty in the measurement of temperature by means of the thermanemometer. The first of these is the impact effect. The flow of air in the vicinity of the wire is obstructed by the wire; some of the air molecules are stopped completely, whereas others are slowed down. If the process is assumed to be adiabatic, the general energy balance for steady flow becomes

$$\Delta KE + \Delta H = 0 \tag{9}$$

If the air is assumed to be stopped completely, and if perfect gas behavior is assumed, Equation 9 becomes:

$$0 - \frac{u^2}{2g} + C_p \Delta t_s = 0 \tag{10}$$

or

$$\Delta t_s = \frac{u^2}{2gC_p} = t_s - t \tag{11}$$

where t_s is known as the stagnation temperature.

Equation 11 is obviously not a reliable measure of the temperature rise in the vicinity of the thermanemometer. Heat will be conducted from the vicinity of the wire to the main body of the stream. Most of the air near the wire is only slowed down, rather than stopped. The result is that the measured impact temperature rise Δt_i is only a fraction of the temperature rise Δt_s as calculated from Equation 11:

$$\frac{\Delta t_i}{\Delta t_s} = \omega \tag{12}$$

The quantity ω , known as the recovery factor, has been determined experimentally (12). A value of $\omega = 0.75$ has been used in correcting the experimentally measured temperatures. The maximum impact correction is 0.082°F at u = 36.0 ft/sec. Even if the value of ω used is appreciably in error, the resulting error in the temperature will not be large. The equation used for the impact correction is (13):

$$-\Delta t_i = 6.32 \times 10^{-5} u^2 \qquad (13)$$

A sizeable correction must be made for the heating effect of the Mueller bridge current which flows through the thermanemometer when its resistance is measured. King's equation is rewritten in the following form where $\Delta R = R_{HW} - R_A$ is replaced by $\frac{\Delta t}{\alpha}$:

$$\Delta t = \frac{\alpha I^2 R_{HW}}{A + B\sqrt{u}} \qquad (14)$$

R_{HW} is determined by direct measurement; I may be calculated from the Mueller bridge circuit constants; α , A, and B are determined from experimental calibration of the thermanemometer as a temperature and velocity measuring device. Substitution of these constants into Equation 14 gives the following:

$$\Delta t_b'' = \frac{1.04}{4.14 + \sqrt{u}} \qquad (15)$$

As predicted by Equation 15, $\Delta t_b''$ is a maximum (0.251°F) at zero air velocity. Since the thermanemometer was calibrated as a temperature measuring device at zero air velocity, this error is

introduced into all measurements, and the actual temperature correction is:

$$\Delta t'_b = 0.251 - \frac{1.04}{4.14+\sqrt{u}} \qquad (16)$$

This correction is subject to the assumption that the plot of $I^2R/R_{HW} - R_A = \Phi_o$ vs. $\sqrt{u}$ is a straight line as predicted by King's equation. It is especially important that the correction at zero air velocity be accurately known, since the thermanemometer was calibrated at this velocity.

A possible source of error in the bridge current correction is the loss of heat by conduction through the wire and into its supports. This heat loss will cause the wire to assume a somewhat lower mean temperature than that predicted by Equation 16. The mean temperature rise of the wire is calculated in Appendix II with the assumption that the ends of the wire are at the air temperature, which is reasonable in view of the excellent thermal contact between the ends of the wire and the supports. For any given air velocity, the mean temperature rise was found to be 90.7% of $\Delta t_b'$, the value predicted by Equation 16. The final expression for the bridge current correction is given by the equation

$$\Delta t'_b = \left(0.251 - \frac{1.04}{4.14+\sqrt{u}}\right) 0.907 \qquad (17)$$

The maximum correction for impact and bridge current as given by the sum of Equations 13 and 16 is +0.09°F. The uncertainty in this correction is estimated as $\pm$0.04°F, largely due to uncertainty in the recovery factor ω .

The uncertainty in temperature measurement as a result of the limit of precision of the Mueller bridge is $\pm 0.02^{\circ}F$. The overall temperature uncertainty is the root mean square of the individual uncertainties (14):

$$\delta t = \pm[0.02^2 \text{ (air temperature control)} + 0.10^2 \text{ (positioning of wire)} + 0.05^2 \text{ (calibration drift)} + 0.02^2 \text{ (Mueller bridge uncertainty)} + 0.04^2 \text{ (impact correction)} + 0.05^2]^{1/2} \text{ (wire vibration)} \quad (18)$$

$$\delta t = \pm 0.14^{\circ}F$$

This value is an indication of the probable difference between reported and true values of temperature; the precision or self-consistency of the temperature measurements is undoubtedly much better than this.

Gross Correlations: $\dot{Q}$ and h

The heat transfer coefficient has been calculated from Equation 3 for the boundary conditions 100/85/100, U_B = 15 and 30 ft/sec. The change in fluid properties between 85 and 100°F is so slight that the heat transfer coefficient at 100°F is only 0.3% higher than at 85°F. This small variation has been neglected. The values of h calculated from Equation 3, assumed uniform with respect to downstream distance, are:

$$h = 4.44 \text{ BTU/hr ft}^2 \text{ °F} \qquad (U_B = 15)$$
$$h = 7.62 \text{ BTU/hr ft}^2 \text{ °F} \qquad (U_B = 30)$$

Bulk temperatures have been calculated from the above heat transfer coefficients. An energy balance is taken on a segment of flowing fluid of cross-sectional area $y_o z$ and infinitesimal length dx:

$$d\dot{Q} = 2h\,z\,dx\,(t_w - t_B)\,\dot{m}\,c_p\,dt_B \qquad (19)$$

or, upon integration $$\frac{2h\,z\,x_1}{\dot{m}\,c_p} = \int_{(t_{B_o})_{x=o}}^{(t_{B_1})_{x=x_1}} \frac{dt_B}{t_w - t_B} \qquad (20)$$

Equation 20 has been used to calculate t_B for x 23.22, 36.00, 50.00, 82.07, and 136.35 in. on the basis of two assumptions:

a. The wall temperature, t_w, is uniform at 100°F.

b. The t_w - x distribution is as given by experimental thermocouple measurements (Fig. 42).

Case (a) was calculated in order to determine the magnitude of the error introduced by the assumption of a uniform wall temperature.

(Calculations made subsequently with the analog computer involved the assumption (a); the difference between (a) and (b) is useful in evaluation of the analog results.)

For the present calculation, then, (b) is the only case which should be expected to agree with experiment.

For the assumption (a), Equation 20 may be integrated readily. For the assumption (b), t_w is no longer constant, but is a known function of x. A laborious graphical integration is avoided by the assumption:

$$\frac{dt_w}{dt_B} = K_1 \qquad \text{, a constant} \qquad (21)$$

which is subsequently proved to be valid. This assumption amounts to determining t_B as a function of x for the case in which t_w varies with x as predicted by:

$$\frac{dt_w}{dx} = K_1 \frac{dt_B}{dx} \qquad (22)$$

This calculation (based on the assumption of Equation 21) will prove satisfactory if integration of Equation 22 gives wall temperatures which agree with the experimental values.

From Equation 21, it follows that:

$$\frac{d(t_w - t_B)}{K_1 - 1} = dt_B \qquad (23)$$

Equations 20 and 23 are combined to give:

$$\int_{(t_w - t_B)x=0}^{(t_w - t_B)x=x_1} \frac{d(t_w - t_B)}{t_w - t_B} = (K_1 - 1)\frac{2h\Sigma x_1}{\dot{m} C_p} \qquad (24)$$

Equation 24 is solved by successive approximations, the first approximation being $K_1 = 0$. The calculated bulk temperatures are listed in Table II for $U_B = 15$ and 30 ft/sec for comparison with the experimental values. The wall temperatures calculated from Equation 22 agree with the experimental values within 0.1°F, well within the accuracy of the experimental thermocouple measurements (Fig. 43). Thus the assumption of Equation 21 is justified.

Agreement between calculated and experimental bulk temperatures is not particularly good. However, the main source of disagreement is in the zone near the entrance to the channel, where the large temperature gradients and non-uniformity of the turbulence make the assumption of constant h quite invalid.

It is noteworthy that the calculated bulk temperatures are not even qualitatively correct for x = 23.22 and 36.00 in., since for these two downstream distances

$$(t_B)_{U_B=15} > (t_B)_{U_B=30} \qquad \text{(calculated)} \qquad (25)$$

$$(t_B)_{U_B=15} < (t_B)_{U_B=30} \qquad \text{(experimental)} \qquad (26)$$

The experimental results at x = 23.22 and 36.00 in. differ from those for the remaining traverses (x = 50.00, 82.07, and 136.35 in.), for which

$$(t_B)_{U_B=15} > (t_B)_{U_B=30} \qquad \text{(experimental)} \qquad (27)$$

as predicted by calculation from Equation 3.

This anomaly is doubtless due to entrance effects, the nature of which is not fully understood.

It appears that for U_B = 15 ft/sec, the heat transfer coefficient calculated from Equation 3 is essentially correct except for the region $0 < x < 23.22$ in., where the calculated values of h are too high. This statement follows from the approximately uniform difference between the calculated and experimental temperatures for each downstream distance, which indicates that practically all the error in calculation is introduced in the region $0 < x < 23.22$ in.

This conclusion is confirmed by the calculation of h as a function of x from the experimental bulk temperatures for U_B = 15 ft/sec. The values obtained range from h = 4.45 BTU/hr ft^2 ^oF at x = 23.22 in. to h = 5.05 BTU/hr ft^2 ^oF at x = 82.07 in., compared with the calculated value of h = 4.44 BTU/hr ft^2 ^oF, assumed uniform.

For U_B = 30 ft/sec, the situation is somewhat different. The calculated bulk temperature is too high for x = 23.22 and 36 in., and in agreement with experiment at the remaining downstream distances. Thus the calculated heat transfer coefficient (7.62 BTU/hr ft^2 ^oF) is too high upstream and too low downstream. Values of h calculated directly from the experimental bulk temperatures lead to the same conclusion; h ranges from 6.21 BTU/hr ft^2 ^oF at x = 23.22 in. to 8.83 BTU/hr ft^2 ^oF at x = 136.35 in., compared with the uniform calculated value of 7.62 BTU/hr ft^2 ^oF.

Table III contains values of $\frac{8}{Q}$ (as well as h) which are calculated from the experimental data.

Point Correlations: ϵ_m and ϵ_c

Values of ϵ_m and ϵ_c have been calculated for the case 100/85/100, U_B = 30 ft/sec. In addition, ϵ_c has been computed for the case 115/100/85, U_B = 30 ft/sec. Equations 176 and 179 (Appendix I) were integrated graphically to obtain the eddy quantities, which are listed in Table IV. Calculations of the eddy quantities were made only for $0.5 < y < 1.0$, symmetry being assumed for the remaining half of the channel, and for x = 23.22, 36, 50, 82.07, and 136.35 in., the downstream distances at which experimental data were taken.

One of the major difficulties in determining the eddy quantities in non-uniform flow is the lack of precision of the quantities $\partial u/\partial x$ and $\partial t/\partial x$, which are determined graphically from cross plots of the experimental temperatures and velocities. Uncertainties in the calibration for velocity or temperature will not affect the precision of each individual traverse, since any error introduced is essentially constant throughout the traverse. However, these uncertainties tend to change with time; the result is that the comparative precision of the traverses at successive downstream distances is affected adversely, and so is the accuracy of determination of $\partial u/\partial x$ and $\partial t/\partial x$. (The accuracy of the temperature and velocity data is not a factor in determining the accuracy of the derivatives of these quantities with respect to downstream distance; only the precision is important.)

The results of the calculations of ϵ_m and ϵ_c for 100/85/100 are in general good. The eddy viscosity changes very little with

downstream distance, the maximum change being only 2%; accordingly, the values of ϵ_m vs. y/y_o have been correlated in Fig. 27 by means of a single curve. The values of ϵ_m calculated for $y/y_o = 1$ are very nearly zero, the maximum deviation being only 0.005×10^{-3} ft^2/sec. This deviation is less than 3% of the kinematic viscosity at the wall. The eddy viscosity attains its maximum value approximately at $y/y_o = 0.8$. The midstream eddy viscosity is about 80% of the maximum value. The calculated values of ϵ_m agree well with the results obtained for uniform flow (4).

The eddy conductivity distribution calculated for the same case (100/85/100, U_B = 30 ft/sec) is similar to the eddy viscosity distribution. A definite increase in the eddy conductivity with downstream distance is noted. This increase amounts to as much as 80% (for a given value of y/y_o) between x = 23.22 and 136.35 in. This increase seems excessive compared to the nearly uniform distribution of eddy viscosity.

The eddy conductivities calculated for 115/100/85, U_B = 30 ft/sec, show the same general behavior as the eddy conductivities discussed above. They increase with downstream distance. They pass through a maximum approximately at $y/y_o = 0.8$. However, quantitative agreement between the eddy conductivities for the two cases is not good. The values of ϵ_c are nearly twice as high for the boundary conditions 100/85/100 as for 155/100/85. It would be expected that the eddy conductivities would be equal, or nearly so, for these two cases, since they differ only in temperature, which is presumed to exert little or no influence on ϵ_c.

Difficulties were encountered in the calculation of ϵ_c for the case 115/100/85. Since in this case $\partial t/\partial y$ is not zero at $y/y_o = 0.5$, Equation 178 (Appendix I) must be integrated from the wall where ϵ_c is known to vanish:

$$(\epsilon_c + \kappa) \frac{\partial t}{\partial y}\Big]_{y_1} = \kappa \frac{\partial t}{\partial y}\Big]_{y_o} = \int_{y_o}^{y_1} u \frac{\partial t}{\partial x}\, dy \qquad (28)$$

or

$$\epsilon_c = \frac{\int_{y_o}^{y_1} u \frac{\partial t}{\partial x}\, dy + \kappa \frac{\partial t}{\partial y}\Big]_{y_o}}{\frac{\partial t}{\partial y}\Big]_{y_1}} - \kappa \qquad (29)$$

Unfortunately, too few laminar layer data were obtained to permit accurate evaluation of $\partial t/\partial y$ at the wall. Hence the accuracy of the eddy conductivities calculated from Equation 29 is low. However, the precision is good for the determination of ϵ_c as a function of y for a given value of x, since the uncertainty in $\partial t/\partial y$ at the wall will introduce a constant error in ϵ_c.

Prediction of Temperature and Velocity Fields in Non-Uniform Flow

In a previous section the concept of fully developed turbulent flow was discussed. According to this notion, the shape of the velocity profile is independent of entrance conditions for all values of x greater than x_c, the distance downstream at which the turbulent flow is said to be fully developed. In other words, the dimensionless quantity u/u_m is a function of only the y coordinate for $x > x_c$. The independence of u/u_m of the downstream distance has been experimentally verified by this research. The data indicate that for U_B = 30 ft/sec, x_c is between 23.22 and 36 in., and that for U_B = 15 ft/sec, x_c is less than 23.22 in.

The velocity field in non-uniform flow may be predicted (for $x > x_c$) from a knowledge of the functional relationship

$$\frac{u(x,y)}{u_m(x,y)} = f_u(y) \qquad (30)$$

*

if the maximum velocity $u_m(x)$ is also known. To determine $u_m(x)$, knowledge of the mass velocity G and the temperature and pressure fields $t = t(x,y)$ and $P = P(x,y)$ is necessary. The latter two quantities determine the specific weight: $\sigma = \sigma(P,t) = \sigma(x,y)$. Then

$$G = \int_0^{'} \sigma u \; d\left(\frac{y}{y_0}\right) \qquad (31)$$

$$G = \int_0^{'} \sigma f_u(y) u_m(x) \, d\left(\frac{y}{y_0}\right) \qquad (32)$$

---

*For a given fluid at a fixed Reynolds number, f_u and f_t are functions of y only. The dependence of f_u and f_t on fluid properties and flow conditions will be discussed below.

$$u_m(x_1) = \frac{G}{\int_0^1 \sigma(x_1, y) f_u(y)\, d(y/y_0)} \tag{33}$$

$$u(x_1, y_1) = f_u(y_1) \frac{G}{\int_0^1 \sigma(x_1, y) f_u(y)\, d(y/y_0)} \tag{34}$$

Attention will now be directed to the problem of determination of the temperature field in non-uniform flow for $x > x_c$. The quantity $t_w - t / t_w - t_c$ has been plotted vs. y/y_0 for all temperature traverses taken at U_B = 30 ft/sec (Fig. 28). It is found that within experimental error the points lie on a single curve. Furthermore, this curve very nearly coincides with the curve u/u_m vs. y/y_0, (Fig. 14) which is reproduced in Fig. 28 for comparison. Similarly, $t_w - t / t_w - t_c$ has been plotted vs. y/y_0 for U_B = 15 ft/sec (Fig. 29). The points are again correlated by a single curve, which nearly coincides with the curve u/u_m vs. y/y_0 for the same bulk velocity.

From a knowledge of the functional relationship*

$$\frac{t_w - t(x,y)}{t_w - t_c(x)} = f_t(y) \tag{35}$$

the temperature field $t = t(x,y)$ may be predicted if the centerline temperature $t_c = t_c(x)$ is known. The centerline temperature may be related to the bulk temperature as follows:

$$t_B(x) = \frac{\int_0^1 \frac{u}{u_m}\, t\, d\left(\frac{y}{y_0}\right)}{\int_0^1 \frac{u}{u_m}\, d\left(\frac{y}{y_0}\right)} \tag{36}$$

---

*See footnote, previous page.

$$t_B(x) = \frac{-\int_o^{'} \frac{u}{u_m} \frac{t_w - t}{t_w - t_c} \, d\left(\frac{y}{y_o}\right) + \int_o^{'} \frac{u t_w}{t_w - t_c} \, d\left(\frac{y}{y_o}\right)}{\int_o^{'} \frac{u/u_m}{t_w - t_c} \, d\left(\frac{y}{y_o}\right)} \tag{37}$$

$$t_B(x) = - \frac{\int_o^{'} f_u(y) \, f_t(y) \, d\left(y/y_o\right)}{\int_o^{'} \frac{f_u(y)}{t_w - t_c} \, d\left(y/y_o\right)} + t_w \tag{38}$$

$$\frac{t_w - t_B(x)}{t_w - t_c(x)} = \frac{\int_o^{'} f_u(y) \, f_t(y) \, d\left(y/y_o\right)}{\int_o^{'} f_u(y) \, d\left(y/y_o\right)} \tag{39}$$

Equations (34), (35), and (39) may be solved simultaneously* for t(x,y) and u(x,y) from a knowledge of the following quantities:

$$G = \text{constant} \tag{40}$$

$$t_w = t_w(x) \tag{41}$$

$$t_B = t_B(x) \tag{42}$$

$$P = P(x) \tag{43}$$

$$\frac{u(x,y)}{u_m(x,y)} = f_u(y) \tag{44}$$

$$\frac{t_w(x) - t(x,y)}{t_w(x) - t_c(x)} = f_t(y) \tag{45}$$

The pressure P is assumed to be a function of x only, and since it enters only in determination of σ, may be assumed constant. The

---

*A trial solution is involved. A good first approximation for flow of a gas is $t_w - t_B / t_w - t_c$ 0.85. This ratio is nearly independent of G.

mass velocity G and the wall temperature $t_w(x)$ are independent variables. The bulk temperature of the air may be calculated from empirical correlation such as Equation 3.

The discussion of the last several pages will be summarized in the next three paragraphs. It has been found experimentally that for air at a given Reynolds number the velocity field $u(x,y)$ can be represented as a product of a function of x only $\left[u_m(x)\right]$, and a function of y only $\left[f_u(y)\right]$. Similarly, the quantity $\left[t_w(x) - t(x,y)\right]$ may be represented as the product of a function of x only, $\left[t_w(x) - t_c(x)\right]$, and a function of y only, $\left[f_t(y)\right]$.

It has been shown that if G, t_w, t_B, and P are known, the functions $\left[u_m(x)\right]$ and $\left[t_w(x) - t_c(x)\right]$ may be eliminated from Equations 30 and 35, respectively. Furthermore, G, t_w, t_B, and P are either known or readily determinable functions, and so the problem of determining the velocity and temperature fields has been reduced the determination of the functions $f_u(y)$ and $f_t(y)$. The advantage is obvious; the number of dimensions involved has been reduced from two to one.

However, this discussion is valid only for fully developed turbulent flow. It must fail where entrance effects are appreciable, that is, where x is less than x_c. No attempt has been made to apply this treatment to non-symmetrical cases such as 115/100/85 or 100/100/85.

A theoretical approach to this problem by Martinelli (15) indicates that the functions of f_u and f_t depend on the Reynolds number as well as the vertical position in the channel. In addition, f_t, depends on the Prandtl number:

$$f_u = f_u\,(Re, y) \tag{46}$$

$$f_t = f_t\,(Re, Pr, y) \tag{47}$$

According to Martinelli's treatment, the dimensionless velocity and temperature distributions f_u and f_t coincide at Pr = 1:

$$f_u = f_t \tag{48}$$

$$f_u\,(Re, y) = f_t\,(Re, 1, y) \tag{49}$$

The Prandtl number for air at 100°F is 0.71, and the dimensionless temperature and velocity distributions predicted by Martinelli for air are thus nearly identical.

As mentioned previously, the functions f_u and f_t have been calculated from the experimental data for air at two bulk velocities, $U_B = 15$ and 30 ft/sec. These experimentally determined functions f_u and f_t and their corresponding theoretical values predicted by Martinelli are compared in Figs. 28 and 29. Agreement between theory and experiment is reasonably good.

The problem of predicting temperature and velocity fields in non-uniform turbulent flow is not finally solved. Martinelli's admirable theoretical approach cannot be relied on for quantitative information, largely because of the assumption

$$\frac{\partial t}{\partial x} \neq f(y) \tag{50}$$

which he had to make in order to integrate the differential equation for heat transfer.

It is the writer's belief that the best approach to this problem is the experimental determination of the function $f_t(y,Re,Pr)$ for a variety of values of the Reynolds and Prandtl numbers. The function $f_u(y,Re)$ is already well defined by such familiar expressions as the universal equations for turbulent velocity distribution (16):

$$u^+ = y^+ \qquad 0 \leq y^+ \leq 5 \tag{51}$$

$$u^+ = -3.05 + 5.00 \ln y^+ \qquad 5 \leq y^+ \leq 30 \tag{52}$$

$$u^+ = 5.5 + 2.5 \ln y^+ \qquad 30 \leq y^+ \tag{53}$$

Furthermore, since f_u and f_t coincide at Pr = 1, the most exhaustive investigations of f_t should be made at Prandtl numbers differing appreciably from unity. Since heat transfer to oils (Pr = 100) and to liquid metals (Pr = 0.01 for mercury) has important industrial applications, the determination of f_t for widely varying Prandtl numbers will be of immediate practical value. The experimental work reported herein is only a first step in this direction.

It will be noted that this method of approach does not require the knowledge of ϵ_m or ϵ_c as a function of x and y.

No established method exists at present for the prediction of temperature and velocity fields for downstream distances x less than x_c. In fact, the calculation even of bulk temperatures in this region by existing correlations, such as Equation 3, is not very reliable. The experimental work carried out in this research contributes little to solution of the problem, since physical limitations of the apparatus were such that no measurements of temperature or velocity could be made for values of x less than 23.22 in., at which point the transition to fully developed turbulent flow was practically complete.

Since the region in which x less than x_e is by definition a region wherein the entrance conditions affect the flow, experimental results obtained in one channel will not be applicable to other channels unless entrance conditions are identical.

For the transition from isothermal potential flow to fully developed turbulent flow, the dimensionless temperature and velocity distributions at the limits of the transition region are:

$$\frac{u}{u_m} = \frac{t_w - t}{t_w - t_c} \qquad (x = 0) \qquad (54)$$

$$\frac{u}{u_m} = \frac{t_w - t}{t_w - t_c} = f_u(y) = f_t(y) \qquad (x = x_c) \qquad (55)$$

For Pr = 1 (Approximated by air and other gases) $u/u_m = t_w - t / t_w - t_c$ at both ends of the transition region. It is possible that this equality holds throughout the transition region. Experimental measurements of the simultaneous developments of temperature and velocity

profiles will be necessary to test this hypothesis.

Studies of the development of the turbulent temperature and velocity profiles independently of each other could be made by means of equipment described in a previous section, in which the velocity profile is allowed to attain full development under isothermal conditions upstream of the point of application of the temperature boundary conditions.

Solution of the Heat Transfer Equation by Electrical Analogy

If conduction in the direction of flow is neglected, and if $c_p\sim$ is assumed constant, the heat conduction equation becomes:

$$\frac{\partial}{\partial y}\left[(\epsilon_c + K)\frac{\partial t}{\partial y}\right] = u\frac{\partial t}{\partial x} \tag{56}$$

This equation is derived in Appendix I.

A quantity $\bar{\phi}(y)$, designated the thermal resistance, is defined as follows:

$$\bar{\phi}(y) = \int_{0.5}^{y/y_0} \frac{d(y/y_0)}{\epsilon_c + K} \tag{57}$$

so that $$\frac{d\bar{\phi}}{d\,y/y_0} = \frac{1}{\epsilon_c + K} \tag{58}$$

Equation 56 can be expressed in terms of $\bar{\phi}$ as follows:

$$\frac{\partial^2 t}{\partial \bar{\phi}^2} = y_0^2(\epsilon_c + K)u\frac{\partial t}{\partial x} \tag{59}$$

The steps by which Equation 59 follows from Equations 56 and 57 are non-essential and have been omitted.

The left side of Equation 59 is now expressed in finite difference form:

$$\frac{\dfrac{t_{p+1} - t_p}{\Delta\bar{\phi}} - \dfrac{t_p - t_{p-1}}{\Delta\bar{\phi}}}{\Delta\bar{\phi}} = y_0^2(\epsilon_c + K)u\frac{\partial t}{\partial x} \tag{60}$$

$$p = 1,2,3.....n$$

The points p = 1,2,3.....n are spaced at equal intervals of $\Delta\bar{\phi}$.

$$\Delta \bar{\Phi} = \frac{\bar{\Phi}(\bar{y}_o)}{n-1} \tag{61}$$

The value of n (the total number of points) is quite arbitrary. As n is increased, Equation 60 approaches Equation 59 more and more closely. It is important to remember that the points $p = 1,2,3.....n$ divide the channel between $y/y_o = 0.5$ and $y/y_o = 1.0$ into (n-1) sections of equal thermal resistance.

We now proceed to develop the electrical analog of Equation 60 by considering unsteady flow of current through the network shown in Fig. 30. The sum of the currents leading into any junction j must be zero:

$$\frac{E_{j+1} - E_j}{\Delta R} - \frac{E_j - E_{j-1}}{\Delta R} = C_j \frac{dE_j}{d\theta} \tag{62}$$

A comparison of Equations 60 and 62 shows that they are of the same form. The analogous quantities are: temperature, $\bar{t} \sim$ voltage, E; thermal resistance, $\bar{\Phi}$, $\sim$ electrical resistance, R; downstream distance, x, $\sim$ time, θ; and $(\epsilon_c + K) u \bar{y}_o^2 \Delta \bar{\Phi} \sim$ capacitance, C.

At any one time, junctions $j = 1,2,3.....n$ of the electrical network represent a set of vertical points $p = 1,2,3.....n$ in the flow channel all of which are at a particular downstream distance x. For the actual analog circuit, n = 25. Point p = 1 is located at the wall of the channel ($y/y_o = 1$); point p = 25 is at the center of the stream ($y/y_o = 0.5$). The analog circuit thus represents

only half the channel, symmetry being assumed with respect to the axis $y/y_o = 0.5$. The values of y/y_o corresponding to the intervening points p = 2,3,4....24 are obtained by plotting ϕ vs. y/y_o and determining the values of y/y_o for successive equal intervals of ϕ.

The factor of proportionality between downstream distance x in the heat transfer equation and its electrical analog, time, is designated as λ. This quantity may be determined by a balance of the dimensions of Equations 60 and 62:

$$\frac{\Delta R C_j}{y_o^2 (\Delta \phi)^2 (\epsilon_c + K)_p u_p} = \lambda \frac{\partial u}{\partial t} \qquad (63)$$

Only two of the quantities ΔR, λ, $C_1, C_2, C_3 \ldots\ldots C_{24}$ may be chosen arbitrarily; the rest are fixed by Equation 63. In practice, the magnitude of the components was dictated by the range of values available in the analog circuit.

This analog circuit is adaptable only to cases for which both $(\epsilon_c + K)$ and u are assumed to be functions of y only. It would be necessary to vary the circuit resistances and capacitances with time to allow for a variation of $(\epsilon_c + K)$ and u with downstream distance x.

Before Sw 1 (Fig. 31) is closed, the circuit is quiescent. All junctions are at ground potential, which will be assigned the value zero. When Sw 1 is closed, the battery voltage E_1 appears at junction j = 1. This voltage will remain constant as long as Sw 1 remains closed. The boundary conditions thus imposed on

on Equation 62 are:

$$E = E(\theta, j) \qquad j = 1, 2, 3 \ldots 25 \tag{64}$$

$$E(\theta, 1) = E_1 \tag{65}$$

$$E(0, j) = 0 \qquad j \neq 1 \tag{66}$$

A temperature t_1 is now assigned to the voltage E_1 and another temperature t_o to the ground potential of zero. A linear relationship between the two variables being assumed, t is thus defined in terms of E. Equation 58 is now subject to the following boundary conditions which correspond to Equations 64 - 66:

$$t = t(x, p) \qquad p = 1, 2, 3, \ldots 25 \tag{67}$$

$$t(x, 1) = t_1 \tag{68}$$

$$t(0, p) = t_o \qquad p \neq 1 \tag{69}$$

Since each point p 1,2,3.....25 corresponds to a particular value of y/y_o, the above boundary conditions may be expressed as follows:

$$t = t(x, y) \tag{70}$$

$$t(x, y_o) = t_1 \tag{71}$$

$$t(x, 0) = t_1 \tag{72}$$

$$t(0, y) = t_o \tag{73}$$

Knowledge of E_j as a function of time will then permit determination of t_p (for p = j) as a function of x:

$$t_p(x) = t_o + \frac{E_j(\theta)}{E_1}(t_1 - t_o) \qquad (74)$$

for which $t_p(x)$ denotes t as a function of x for a particular value of y/y_o. In practice E_j for j = 1,2,3.....n is recorded by photographing an oscilloscope trace. (See Figs. 32 - 35) The vertical axis of an oscilloscope trace represents voltage; the horizontal axis, time. (The oscilloscope trace is formed by the motion of a small beam of light at a constant horizontal speed.)

The actual problem investigated by the analog computor was the case 100/85/100, U_B = 30 ft/sec. The eddy conductivity information used in the analog work was obtained from uniform flow measurements at U_B = 30 ft/sec (4) The measurements from which these eddy conductivities are calculated are designated in (4) as "Test 40"; this terminology will be continued.

One of the purposes of this investigation is to test the applicability of eddy conductivity information obtained from uniform flow measurements to non-uniform flow problems.

Subsequent calculations of ϵ_c directly from the experimental data for 100/85/100, U_B = 30 ft/sec, give results which do not agree with the uniform eddy conductivities. This lack of agreement is no cause for concern, however; ϵ_c is a very sensitive variable and errors in its assumed distribution may not affect the validity of the analog solution. Furthermore, the accuracy of

determination of ϵ_c for non-uniform flow is decidedly less than for uniform flow; it is possible that the uniform values of (Test 40) are as representative of actuality for the case 100/85/100 U_B = 30 ft/sec as the values calculated directly from the non-uniform experimental data.

At any rate, limitations of the analog circuit force the assumption that

$$\epsilon_c \neq f(x) \tag{75}$$

and the non-uniform values of ϵ_c could not have been used on this account.

The velocity distribution used in the analog solution was that of Fig. 14 which is determined from the experimental data for 100/85/100, U_B = 30 ft/sec.

$$u \neq f(x) \tag{76}$$

is also necessary for this analog solution. The average of the experimental maximum velcities, 34.87 ft/sec, was taken as representative of the entire channel, and a single u - y relationship determined from this value and Fig. 14.

The analog circuit components were computed from the experimental values of ϵ_c and u by Equation (63). The eddy conductivities of Test 40 were not accurately determined near the wall, due to uncertainty in determining the large temperature gradients in that region. Accordingly, several different interpolations were made of the $\epsilon_c - y$ curve between its known limiting behavior at

the wall (namely $\epsilon_c = 0$) and the nearest accurately calculated point at $\frac{y}{y_0} = 0.96$. The way in which this interpolation is made is important, since it defines the thermal resistance in the region in which it is highest.

Three interpolations, labeled A,B, and C, are shown in the plot of ϵ_c vs. $\frac{y}{y_0}$ in Fig. 31. Case A was drawn in only as an upper limit beyond which the curve could not possibly go; it was not thought to be a very probable distribution, since it shows $\epsilon_c > 0$ throughout the laminar layer. Case C follows from the assumption of $\epsilon_c = 0$ throughout the laminar layer with a discontinuous slope at $y^+ = 5$ ($\frac{y}{y_0} = 0.008$), the outer limit of the laminar layer. Case B was intermediate between cases A and C. Case D was drawn in light of more recent eddy conductivity information and will be discussed below.

Solutions of the heat transfer problem were carried out for cases B and C. No significant difference was found between the solutions for the two cases, indicating that the thermal resistances for the two cases are, for practical purposes, identical.

Five representative oscilloscope traces are shown in Figs. 32 - 36. (These are for Case C about which the subsequent discussion will be concerned.) As indicated above, the oscilloscope traces are curves of voltage vs. time which may be converted into temperature vs. downstream distance by use of Equation 74 and the following:

$$\theta = \lambda x \tag{77}$$

Fig. 32 represents t vs. x (or more precisely, the electrical analogs of these quantities, E vs. θ) for $y/y_o = 0.5$. Figs. 33, 34, and 35 represent t vs. x for $y/y_o = 0.643$, 0.821, and 0.964 respectively.

Fig. 36 differs from Figs. 32 - 35 in that it is a trace of E_{12} vs. θ , which is equivalent to a plot of the temperature difference across a known thermal resistance vs. distance downstream. Since this thermal resistance is adjacent to the wall, the temperature drop determined from Fig. 37 can be used to calculate the rate of heat transfer from the wall to the air stream as well as the heat transfer coefficient h:

$$\dot{q}_w = K \left(\frac{\partial t}{\partial y}\right)_{y=y_o} \tag{78}$$

$$h = \dot{q}_w / t_w - t_B \tag{79}$$

These quantities are plotted vs. downstream distances in Fig. 37. Values of h determined in this way are listed in Table III. These are compared with those calculated from the analog bulk temperatures (see below) by means of Equation 20.

Plots of t ^oF vs. x (in) corresponding to Figs. 32 - 35 are shown in Figs. 38 - 41 respectively. In all, 25 such traces have been obtained, one for each junction j. The temperature information obtained from these traces has been cross-plotted to give t vs. y/y_o at the five values of x at which experimental measurements were made. These temperature traverses are plotted in Fig. 42, and

the data are listed in Table V. Bulk temperatures have been calculated from these data and are included in Table II for ready comparison with the experimental results.

Agreement between the experimental temperature traverses (Fig. 10) and those obtained by analog solution (Fig. 42) is only fair.

Three reasons are presented for this lack of agreement. It is probable that all are significant factors:

a. Failure of Case C to represent the actual eddy conductivity distribution near the wall. Since predicted temperatures exceed experimental temperatures throughout the channel, the values of ϵ_c predicted by Case C are apparently too high. Information which has recently become available (5) indicates that the eddy conductivity distribution is better represented by the curve in Fig. 32, labeled D. The total thermal resistances for the two cases are related as follows:

$$\frac{\phi_D}{\phi_C} = 1.14 \qquad (80)$$

Case D is seen to have an appreciably higher thermal resistance than Case C and should give correspondingly lower temperatures.

b. Failure of any uniform eddy conductivity distribution to apply in the transition region between potential and fully developed turbulent flow. As indicated in a previous section, conditions near the channel entrance are

very complex. It is assumed that the intensity of turbulence increases from a rather small value at $x = 0$ to a much larger, essentially uniform value at $x = x_c$, at which point the transition to fully developed turbulent flow is complete. If this assumption is correct, the eddy conductivity must show a corresponding increase with downstream distance. Therefore, the assumption of a uniform eddy conductivity distribution equal to that obtained in fully developed turbulent flow will lead to predicted rates of heat transfer which are much too high in the transition region.

c. Disagreement between the boundary conditions imposed on the analog circuit and those obtained experimentally. The analog solution of course applies to the case where the plates are maintained isothermal at 100°F. As previously mentioned, the measured plate temperatures are appreciably lower than 100°F, due to the temperature drop through the plates. This drop is largest near $x = 0$ where the rate of heat transfer is highest. Plate temperatures (air side) as measured by thermocouples are plotted vs. x in Fig. 43. The temperature at $x = 0$ is seen to be 97.7°F, and that at $x = 136.35$ in. is 99.5°F. Obviously, if the analog solution is to be directly comparable to the experimental work, the analog boundary conditions must be made to coincide with the experimental values.

An attempt has been made to correct for this discrepancy between analog and experimental boundary conditions. The bulk temperature of the air has been calculated by use of Equation 3 on the basis (1) of a uniform wall temperature of 100°F and (2) experimental t_w - x distribution as given by thermocouple measurements. The difference in the temperatures thus attained represents a correction for lack of agreement of the boundary condition $t_w = 100^\circ$ with the experimental boundary condition. This correction is applied to the analog bulk temperature: $\Delta t_B^A = \Delta t_B^E$

It is not presumed that this correction is anything better than a reasonable approximation to reality. The corrected analog bulk temperatures (Table II) are still higher than the experimental values. This discrepancy is attributed primarily to (a) and (b), above, since the effect of (c) has largely been eliminated by the correction just discussed.

In an effort to resolve these difficulties (a), (b), and (c), a new set of analog measurements is planned. The temperature at the wall will coincide with the experimental curve (Fig. 43). In the analog circuit (Fig. 30) the point j = 1 corresponds to the wall. The voltage imposed at j = 1 must be made to vary with time in a manner analogous to the actual variation of temperature with distance downstream as shown by Fig. 43. A variable voltage may be imposed on the circuit by means of an arbitrary function generation.

In this proposed set of measurements, the eddy conductivity distribution of Case D (Fig. 31) will be utilized. As outlined

above, this information is believed to be the best presently available.

In order to determine the error introduced by assumption of uniform eddy conductivities in the transition region ($0 \leq x \leq x_c$) two analog solutions are planned. The first of these will be for initial conditions corresponding to an experimental traverse at a value of $x > x_c$. ($x = 36.00$ in. has been proposed.) The voltage corresponding to this experimental temperature distribution will be applied to the circuit points $j = 1.....25$ (each of which corresponds to a different value of η/η_o) until equilibrium is attained. The voltages will then be removed from all points except $j = 1$; the time of removal will correspond to a downstream distance of $x = 36.00$ in. The voltage at $j = 1$ must be varied with time to account for the known change in wall temperature with downstream distance. Oscilloscope traces of E vs. θ, representing t as a function x, will be obtained in the usual manner.

The other analog solution will cover the entire channel. The initial condition will correspondto the isothermal entrance of air at $t = 85^{\circ}F$. This initial condition is identical with that of the solution already carried out for case C.

If both of the two planned solutions agree with experiment, it can be concluded that case D is an accurate representation of the eddy conductivity distribution, and that its anticipated failure in the transition region has not taken place. If, as is expected, satisfactory agreement with experiment is obtained for

the solution beginning at x = 36.00 in. but not for the solution beginning at x = 0, the uniform eddy conductivity distribution will be proved satisfactory for solutions of problems involving fully developed turbulent flow, but not for flow in the transition region $x < x_c$.

If agreement is not satisfactory for the solution beginning at x = 36.00 in., Case D is an erroneous representation of the eddy conductivity.

Conclusion

Experimental measurements of temperature and velocity in non-uniform turbulent flow have been made at two Reynolds numbers and three sets of temperature boundary conditions. Values of the eddy viscosity, the eddy conductivity, and the heat transfer coefficient have been calculated from the experimental measurements.

It has been found that in the region of fully developed turbulence the eddy viscosity is substantially uniform. The eddy conductivity increases appreciably with downstream distance in the same region.

The values of bulk temperature calculated from the experimental measurements are in reasonably good agreement with the predictions of Equation 3 for the region of fully developed turbulence. However, Equation 3 is unreliable for calculations of bulk temperature in the transition region.

The problem of determining the temperature and velocity fields in non-uniform flow has been approached in two ways:

a. It has been found that for the fully developed turbulent flow at a fixed mass velocity, the dimensionless velocity and temperature distributions, f_u and f_t, can be expressed as functions of only the vertical position in the channel. These functions have been determined for air for two Reynolds numbers (9750 and 19,290) and have been found to vary only slightly with the Reynolds number over this limited range. The desirability of the

experimental determination of these functions at Prandtl numbers differing appreciably from unity has been indicated.

b. The partial differential equation for heat transfer has been solved by means of an electrical analogy, and the results compared with experimental data. Agreement between the analog solution and the experimental results is only fair; this has been attributed to the inaccuracy of the eddy conductivity information utilized in the solution. Further analog work is planned in which more accurate information regarding the eddy conductivity distribution near the wall will be used.

Appendix I. Theoretical Background

Equations of Motion

In this section the equations of motion of a fluid in laminar flow will be developed by use of Newton's second law. These equations will then be generalized so as to apply to turbulent flow. The first step in the development of these equations is to consider the forces which may act on a body of fluid. Forces arising from gravitational or other fields will be neglected.

In order to apply the laws of statics to the body of fluid, it is convenient to consider a separating surface S through the body, and to evaluate the force per unit area exerted by the particles to the right of S on those to the left. If one can determine the stress for every conceivable surface S_1, S_2,..... which may be passed through a point A, the problem of delineating the state of stress at A is evidently solved. It can be demonstrated in a relatively simple manner (16) that knowledge of the stresses for three mutually perpendicular surfaces S_x, S_y, and S_z through A yields sufficient information completely to characterize the state of stress at A.

The stress vectors for the three mutually perpendicular surfaces S_x, S_y, and S_z are P_x, P_y, and P_z, respectively. Each vector may be resolved into components as follows:

$$\begin{matrix} P_x: \\ P_y: \\ P_z: \end{matrix} \begin{pmatrix} \tau_{xx} & \tau_{xy} & \tau_{xz} \\ \tau_{yx} & \tau_{yy} & \tau_{yz} \\ \tau_{zx} & \tau_{zy} & \tau_{zz} \end{pmatrix} \tag{81}$$

for which τ_{xy} represents the y component of the stress on the surface normal to the x axis. The three stresses with repeated subscripts are normal stresses; the other six are tangential or shearing stresses. It may be readily proved (16) that the shearing stresses with reversed subscripts are equal. Thus $\tau_{xy} = \tau_{yx}$; $\tau_{xz} = \tau_{zx}$; and $\tau_{yz} = \tau_{zy}$.

Consider an infinitesimal volume element of dimensions dx, dy, and dz:

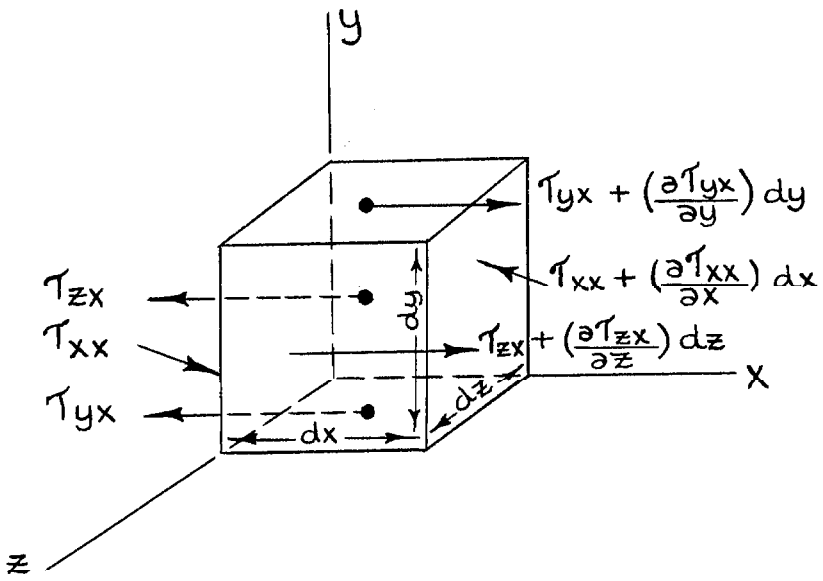

This volume element moves with the fluid. The net force on this volume element is to be evaluated. The x component of the force on each of the six faces of the volume element is obtained by multiplying the x component of the stress by the area of the face:

left yz face: $-\tau_{xx}\, dy\, dz$

right yz face: $\left[\tau_{xx} + \left(\frac{\partial \tau_{xx}}{\partial x}\right) dx\right] dy\, dz$

lower xz face: $-\tau_{yx}\, dx\, dz$

upper xz face: $\left[\tau_{yx} + \left(\frac{\partial \tau_{yx}}{\partial y}\right) dy\right]$

front xy face: $-\tau_{zx}\,dx\,dy$

rear xy face: $\left[\tau_{zx} + \left(\frac{\partial \tau_{zx}}{\partial z}\right) dz\right] dx\,dy$

The sum of these six terms is the x component of the net force on the volume element:

$$F_x = \left(\frac{\partial \tau_{xx}}{\partial x} + \frac{\partial \tau_{yx}}{\partial y} + \frac{\partial \tau_{zx}}{\partial z}\right) dx\,dy\,dz \qquad (82)$$

The corresponding expressions for the y and z components of force are:

$$F_y = \left(\frac{\partial \tau_{xy}}{\partial x} + \frac{\partial \tau_{yy}}{\partial y} + \frac{\partial \tau_{zy}}{\partial z}\right) dx\,dy\,dz \qquad (83)$$

$$F_z = \left(\frac{\partial \tau_{xz}}{\partial x} + \frac{\partial \tau_{yz}}{\partial y} + \frac{\partial \tau_{zz}}{\partial z}\right) dx\,dy\,dz \qquad (84)$$

The change in shape of the volume element as a result of the above forces will now be considered. The x component of velocity, u, is expanded in a Taylor series in the neighborhood of a point $\underline{A}$ (x_a, y_a, z_a):

$$u(x,y,z) = u(x_a\, y_a\, z_a) + \frac{\partial u}{\partial x}(x - x_a) + \frac{\partial u}{\partial y}(y - y_a) + \frac{\partial u}{\partial z}(z - z_a) \qquad (85)$$

Only the linear terms of the series have been retained since these will suffice to describe the behavior of the fluid in the immediate neighborhood of $\underline{A}$. From this and similar expressions which may be written for the y and z components of velocity, it appears that the character of the motion of $\underline{A}$ may be described by the following nine partial derivatives:

$$\begin{Bmatrix} \frac{\partial u}{\partial x} & \frac{\partial v}{\partial x} & \frac{\partial w}{\partial x} \\ \frac{\partial u}{\partial y} & \frac{\partial v}{\partial y} & \frac{\partial w}{\partial y} \\ \frac{\partial u}{\partial z} & \frac{\partial v}{\partial z} & \frac{\partial w}{\partial z} \end{Bmatrix}$$

The three diagonal members of the above matrix, $\partial u/\partial x$, $\partial v/\partial y$, and $\partial w/\partial z$ represent the rate of change in shape of a fluid element by extension in the direction of each of the coordinate axes:

$$e_x = \frac{\partial u}{\partial x} \qquad \text{(along x axis)} \qquad (86)$$

$$e_y = \frac{\partial v}{\partial y} \qquad \text{(along y axis)} \qquad (87)$$

$$e_z = \frac{\partial w}{\partial z} \qquad \text{(along z axis)} \qquad (88)$$

The remaining six terms of the matrix represent rates of angular rotation about the various coordinate axes. For example, $\partial v/\partial x$ measures the rate of rotation about the z axis of lines which were originally parallel to the x axis; correspondingly, $\partial u/\partial y$ measures that rate of rotation about the z axis of lines originally parallel to the y axis. The sum of these derivatives gives the rate of angular deformation of an element in the xy plane:

$$\gamma_{xy} = \frac{\partial v}{\partial x} + \frac{\partial u}{\partial y} \qquad (89)$$

Similar expressions may be written for the rates of deformation in the xz and yz planes respectively:

$$\gamma_{xz} = \frac{\partial u}{\partial z} + \frac{\partial w}{\partial x} \qquad (90)$$

$$\gamma_{yz} = \frac{\partial w}{\partial y} + \frac{\partial v}{\partial z} \qquad (91)$$

It is now assumed that stress is proportional to rate of strain. The factor of proportionality is μ, the coefficient of viscosity.

The resulting equations for the three shear stresses are:

$$\tau_{xy} = \mu \gamma_{xy} = \mu \left(\frac{\partial v}{\partial x} + \frac{\partial u}{\partial y} \right) \tag{92}$$

$$\tau_{xz} = \mu \gamma_{xz} = \mu \left(\frac{\partial u}{\partial z} + \frac{\partial w}{\partial x} \right) \tag{93}$$

$$\tau_{yz} = \mu \gamma_{yz} = \mu \left(\frac{\partial w}{\partial y} + \frac{\partial v}{\partial z} \right) \tag{94}$$

The three normal stresses are:

$$\tau_{xx} = -p' + 2\mu \frac{\partial u}{\partial x} \tag{95}$$

$$\tau_{yy} = -p' + 2\mu \frac{\partial v}{\partial y} \tag{96}$$

$$\tau_{zz} = -p' + 2\mu \frac{\partial v}{\partial z} \tag{97}$$

in which p' is the true pressure, a thermodynamic property of the fluid independent of flow conditions.

Equations 95-97 may be expressed in terms of a mean pressure, p, which is defined as follows:

$$p = -\frac{1}{3} (\tau_{xx} + \tau_{yy} + \tau_{zz}) \tag{98}$$

A combination of the above four equations yields:

$$p' = p + \frac{2}{3} \mu \left(\frac{\partial u}{\partial x} + \frac{\partial v}{\partial y} + \frac{\partial w}{\partial z} \right) \tag{99}$$

The equations for the normal stresses, rewritten in terms of the mean pressure p are:

$$\tau_{xx} = -p - \frac{2}{3} \mu \left(\frac{\partial u}{\partial x} + \frac{\partial v}{\partial y} + \frac{\partial w}{\partial z} \right) + 2\mu \frac{\partial u}{\partial x} \tag{100}$$

$$\tau_{yy} = -p - \frac{2}{3} \mu \left(\frac{\partial u}{\partial x} + \frac{\partial v}{\partial y} + \frac{\partial w}{\partial z} \right) + 2\mu \frac{\partial u}{\partial y} \tag{101}$$

$$\tau_{zz} = -p - \frac{2}{3}\mu\left(\frac{\partial u}{\partial x} + \frac{\partial v}{\partial y} + \frac{\partial w}{\partial z}\right) + 2\mu\frac{\partial w}{\partial z} \qquad (102)$$

The pressures p' and p differ by terms which vanish in the case of steady incompressible flow, since under these conditions the continuity equation becomes:

$$\frac{\partial u}{\partial x} + \frac{\partial v}{\partial y} + \frac{\partial w}{\partial z} = 0 \qquad (103)$$

An element of arbitrariness is involved in the definition of p as the arithmetic mean of the three normal stresses. One advantage of this definition is that p is independent of the choice of coordinate axes (17). The mean pressure p is that which would be measured by determining the mean value of the normal forces on three mutually perpendicular planes which move with the fluid. It is not to be confused with the so-called "stagnation pressure" which is measured by a fixed impact tube.

The equations relating stress and rate of strain may be expressed more compactly in matrix form:

$$\begin{Bmatrix} \tau_{xx} & \tau_{xy} & \tau_{xz} \\ \tau_{yx} & \tau_{yy} & \tau_{yz} \\ \tau_{zx} & \tau_{zy} & \tau_{zz} \end{Bmatrix} = -\begin{Bmatrix} p' & 0 & 0 \\ 0 & p' & 0 \\ 0 & 0 & p' \end{Bmatrix} + \mu\begin{Bmatrix} \frac{\partial u}{\partial x} & \frac{\partial v}{\partial x} & \frac{\partial w}{\partial x} \\ \frac{\partial u}{\partial y} & \frac{\partial v}{\partial y} & \frac{\partial w}{\partial y} \\ \frac{\partial u}{\partial z} & \frac{\partial v}{\partial z} & \frac{\partial w}{\partial z} \end{Bmatrix} + \mu\begin{Bmatrix} \frac{\partial u}{\partial x} & \frac{\partial u}{\partial y} & \frac{\partial u}{\partial z} \\ \frac{\partial v}{\partial x} & \frac{\partial v}{\partial y} & \frac{\partial v}{\partial z} \\ \frac{\partial w}{\partial x} & \frac{\partial w}{\partial y} & \frac{\partial w}{\partial z} \end{Bmatrix} \qquad (104)$$

The matrix formulation is in this case a shorthand way of expressing the desired functional relationship between each of the terms which

occupy equivalent positions in the various matrices. Thus, Equation 104 is the equivalent of Equations 92-97.

Newton's second law, written for the x component of force on a volume element of constant mass, is:

$$F_x = \frac{D(mu)}{D\theta} = \frac{D(\rho u dx dy dz)}{D\theta} = \rho dx dy dz \frac{Du}{D\theta} \quad (105)$$

in which $D/D\theta$, the fluid derivative, is defined as:

$$\frac{D}{D\theta} = \frac{\partial}{\partial\theta} + u\frac{\partial}{\partial x} + v\frac{\partial}{\partial y} + w\frac{\partial}{\partial z} \quad (106)$$

Equations 82 and 105 are combined and (dxdydz) cancelled from both sides:

$$\frac{\partial \tau_{xx}}{\partial x} + \frac{\partial \tau_{yx}}{\partial y} + \frac{\partial \tau_{zx}}{\partial z} = \rho \frac{Du}{D\theta} \quad (107)$$

The analogous expressions for the y and z components of force are:

$$\frac{\partial \tau_{xy}}{\partial x} + \frac{\partial \tau_{yy}}{\partial y} + \frac{\partial \tau_{zy}}{\partial z} = \rho \frac{Dv}{D\theta} \quad (108)$$

$$\frac{\partial \tau_{xz}}{\partial x} + \frac{\partial \tau_{yz}}{\partial y} + \frac{\partial \tau_{zz}}{\partial z} = \rho \frac{Dw}{D\theta} \quad (109)$$

These equations were first derived by Navier (18) and Stokes (19).

Turbulent steady flow will now be considered. Under these conditions, the instantaneous velocity at any point may be resolved into components u_i, v_i, and w_i, which are represented as the sum of a mean velocity and a fluctuating velocity:

$$u_i = u + u' \quad (110)$$

$$v_i = v + v' \quad (111)$$

$$w_i = w + w' \quad (112)$$

The time average of each fluctuating component must be zero, since by definition $u_i = u$, etc.

Equations 107-109 may be applied directly to turbulent flow if the steady velocities u, v, and w encountered in laminar flow and appearing in these equations are replaced by the instantaneous turbulent velocities u_i, v_i, and w_i. The equations of motion of a turbulently flowing fluid are as follows:

$$\frac{\partial \tau_{xx}}{\partial x} + \frac{\partial \tau_{yx}}{\partial y} + \frac{\partial \tau_{zx}}{\partial z} = \frac{Du_i}{D\theta} \qquad (113)$$

$$\frac{\partial \tau_{xy}}{\partial x} + \frac{\partial \tau_{yy}}{\partial y} + \frac{\partial \tau_{zy}}{\partial z} = \frac{Dv_i}{D\theta} \qquad (114)$$

$$\frac{\partial \tau_{xz}}{\partial x} + \frac{\partial \tau_{yz}}{\partial y} + \frac{\partial \tau_{zz}}{\partial z} = \frac{Dw_i}{D\theta} \qquad (115)$$

If u in Equation 113 is replaced by its equivalent $(u + u')$, and the time average of each term taken, the result is:

$$\overline{(u+u')\frac{\partial}{\partial x}(u+u')} + \overline{(v+v')\frac{\partial}{\partial y}(u+u')} + \overline{(w+w')\frac{\partial}{\partial z}(u+u')} = 1/\rho\left[\frac{\partial \tau_{xx}}{\partial x} + \frac{\partial \tau_{xy}}{\partial y} + \frac{\partial \tau_{xz}}{\partial z}\right] \qquad (116)$$

or,

$$\left[\begin{array}{l} \overline{u\frac{\partial u}{\partial x}} + \overline{u'\frac{\partial u}{\partial x}} + \overline{u\frac{\partial u'}{\partial x}} + \overline{u'\frac{\partial u'}{\partial x}} \\ + \overline{v\frac{\partial u}{\partial y}} + \overline{v'\frac{\partial u}{\partial y}} + \overline{v\frac{\partial u'}{\partial y}} + \overline{v'\frac{\partial u'}{\partial y}} \\ + \overline{w\frac{\partial u}{\partial z}} + \overline{w'\frac{\partial u}{\partial z}} + \overline{w\frac{\partial u'}{\partial z}} + \overline{w'\frac{\partial u'}{\partial z}} \end{array}\right] = 1/\rho\left[\frac{\partial \tau_{xx}}{\partial x} + \frac{\partial \tau_{xy}}{\partial y} + \frac{\partial \tau_{xz}}{\partial z}\right] \qquad (117)$$

Terms of the type $\overline{u'\partial u/\partial x}$ vanish since $\overline{u'\,\partial u/\partial x} = \overline{u'\,\partial u/\partial x} = 0$. Similarly, terms of the type $\overline{u\partial u'/\partial x}$ also vanish since $\overline{u\partial u'/\partial x} = \overline{u\partial u'/\partial x} = 0$. If these and similar terms are eliminated from Equation 117, the result is:

$$\rho u\frac{\partial u}{\partial x} + \rho v\frac{\partial u}{\partial y} + \rho w\frac{\partial u}{\partial z} + \rho\overline{u'\frac{\partial u'}{\partial x}} + \rho\overline{v'\frac{\partial v'}{\partial x}} + \rho\overline{w'\frac{\partial w'}{\partial x}} = \frac{\partial \tau_{xx}}{\partial x} + \frac{\partial \tau_{xy}}{\partial y} + \frac{\partial \tau_{xz}}{\partial z} \tag{118}$$

The steady-flow continuity equation applies to both the instantaneous and the mean velocities; hence it also applies to the fluctuating velocities:

$$\frac{\partial \rho u'}{\partial x} + \frac{\partial \rho v'}{\partial y} + \frac{\partial \rho w'}{\partial z} = 0 \tag{119}$$

$$u'\frac{\partial \rho u'}{\partial x} + u'\frac{\partial \rho v'}{\partial y} + u'\frac{\partial \rho w'}{\partial z} = 0 \tag{120}$$

The result of adding Equations 118 and 120 is:

$$\rho u\frac{\partial u}{\partial x} + \rho v\frac{\partial u}{\partial y} + \rho w\frac{\partial u}{\partial z} + \frac{\partial \rho\overline{u'u'}}{\partial x} + \frac{\partial \rho\overline{u'v'}}{\partial y} + \frac{\partial \rho\overline{u'w'}}{\partial z} = \frac{\partial \mathcal{T}_{xx}}{\partial x} + \frac{\partial \mathcal{T}_{xy}}{\partial y} + \frac{\partial \mathcal{T}_{xz}}{\partial z} \tag{121}$$

The analogous equations resulting from a balance of y and z components of force are:

$$\rho u \frac{\partial v}{\partial x} + \rho v \frac{\partial v}{\partial y} + \rho w \frac{\partial v}{\partial z} + \frac{\partial \rho \overline{v'u'}}{\partial x} + \frac{\partial \rho \overline{v'v'}}{\partial y} + \frac{\partial \rho \overline{v'w'}}{\partial z} = \frac{\partial \tau_{xy}}{\partial x} + \frac{\partial \tau_{yy}}{\partial y} + \frac{\partial \tau_{yz}}{\partial z} \tag{122}$$

$$\rho u \frac{\partial w}{\partial x} + \rho v \frac{\partial w}{\partial y} + \rho w \frac{\partial w}{\partial z} + \frac{\partial \rho \overline{w'u'}}{\partial x} + \frac{\partial \rho \overline{w'v'}}{\partial y} + \frac{\partial \rho \overline{w'w'}}{\partial z} = \frac{\partial \tau_{xz}}{\partial x} + \frac{\partial \tau_{yz}}{\partial y} + \frac{\partial \tau_{zz}}{\partial z} \tag{123}$$

It is more convenient to use the mean velocities u, v, and w than the instantaneous velocities u', v', and w'. Equations 107-109 may be written in terms of the mean velocity if the laminar stresses

τ_{xx}, τ_{xy} ..... are replaced by a set of turbulent stresses

τ'_{xx}, τ'_{xy} ..... Equations 107-109 then become:

$$\frac{\partial \tau'_{xx}}{\partial x} + \frac{\partial \tau'_{xy}}{\partial y} + \frac{\partial \tau_{xz}'}{\partial z} = \rho \frac{Du}{D\theta} \tag{124}$$

$$\frac{\partial \tau_{xy}}{\partial x} + \frac{\partial \tau_{yy}}{\partial y} + \frac{\partial \tau_{yz}}{\partial z} = \rho \frac{Dv}{D\theta} \tag{125}$$

$$\frac{\partial \tau_{xz}}{\partial x} + \frac{\partial \tau_{yz}}{\partial y} + \frac{\partial \tau_{zz}}{\partial z} = \rho \frac{Dw}{D\theta} \tag{126}$$

A comparison of Equations 121-123 with Equations 124-126 leads to the following results:

$$\tau_{xx'} = \tau_{xx} - \rho\,\overline{u'u'} \tag{127}$$

$$\tau'_{yy} = \tau_{yy} - \rho\,\overline{v'v'} \tag{128}$$

$$\tau'_{zz} = \tau_{zz} - \rho\,\overline{w'w'} \tag{129}$$

$$\tau'_{xy} = \tau_{xy} - \rho\,\overline{u'v'} \tag{130}$$

$$\tau_{xz} = \tau_{xz} - \rho\,\overline{u'w'} \tag{131}$$

$$\tau'_{yz} = \tau_{yz} - \rho\,\overline{v'w'} \tag{132}$$

in which the unprimed stresses result from the molecular viscosity of the fluid and are defined in Equations 92-97.

The turbulent contribution to the stress will now be described in terms of the eddy viscosity, ϵ_m . The primed stresses are redefined by a set of equations analogous to 92-94 and 100-102, in which μ is replaced by $(\mu+\rho\epsilon_m)$: The resulting equations are:

$$\tau_{xx}' = -p - \frac{2}{3}(\mu+\rho\epsilon_m)\left(\frac{\partial u}{\partial x}+\frac{\partial v}{\partial y}+\frac{\partial w}{\partial z}\right)+2(\mu+\rho\epsilon_m)\frac{\partial u}{\partial x} \tag{133}$$

$$\tau_{yy}' = -p - \frac{2}{3}(\mu+\rho\epsilon_m)\left(\frac{\partial u}{\partial x}+\frac{\partial v}{\partial y}+\frac{\partial w}{\partial z}\right)+2(\mu+\rho\epsilon_m)\frac{\partial v}{\partial y} \tag{134}$$

$$\tau_{zz}' = -p - \frac{2}{3}(\mu+\rho\epsilon_m)\left(\frac{\partial u}{\partial x}+\frac{\partial v}{\partial y}+\frac{\partial w}{\partial z}\right)+2(\mu+\rho\epsilon_m)\frac{\partial w}{\partial z} \tag{135}$$

$$\tau_{xy}' = (\mu+\rho\epsilon_m)\left(\frac{\partial v}{\partial x}+\frac{\partial u}{\partial y}\right) \tag{136}$$

$$\tau_{xz}' = (\mu+\rho\epsilon_m)\left(\frac{\partial u}{\partial z}+\frac{\partial w}{\partial x}\right) \tag{137}$$

$$\tau_{yz}' = (\mu+\rho\epsilon_m)\left(\frac{\partial w}{\partial y}+\frac{\partial v}{\partial z}\right) \tag{138}$$

For laminar flow ϵ_m is zero and Equations 133-138 reduce to Equations 92-94 and 100-102.

Comparison of Equations 127-132 with Equations 133-138 yields a set of relations all of which must be satisfied simultaneously by the eddy viscosity:

$$-\overline{u'u'} = 2\epsilon_m \frac{\partial u}{\partial x} - \frac{2}{3}\epsilon_m \left(\frac{\partial u}{\partial x} + \frac{\partial v}{\partial y} + \frac{\partial w}{\partial z}\right) \tag{139}$$

$$-\overline{v'v'} = 2\epsilon_m \frac{\partial v}{\partial y} - \frac{2}{3}\epsilon_m \left(\frac{\partial u}{\partial x} + \frac{\partial v}{\partial y} + \frac{\partial w}{\partial z}\right) \tag{140}$$

$$-\overline{w'w'} = 2\epsilon_m \frac{\partial w}{\partial z} - \frac{2}{3}\epsilon_m \left(\frac{\partial u}{\partial x} + \frac{\partial v}{\partial y} + \frac{\partial w}{\partial z}\right) \tag{141}$$

$$-\overline{u'v'} = \epsilon_m \left(\frac{\partial v}{\partial x} + \frac{\partial u}{\partial y}\right) \tag{142}$$

$$-\overline{u'w'} = \epsilon_m \left(\frac{\partial u}{\partial z} + \frac{\partial w}{\partial x}\right) \tag{143}$$

$$-\overline{v'w'} = \epsilon_m \left(\frac{\partial w}{\partial y} + \frac{\partial v}{\partial z}\right) \tag{144}$$

A case of steady uniform flow will now be considered. Consider isothermal two-dimensional flow between parallel plates. Evidently $v = w = 0$, and u depends on y only. Equations 139-144 then reduce to:

$$-\overline{u'u'} = 0 \tag{145}$$

$$-\overline{v'v'} = 0 \tag{146}$$

$$-\overline{w'w'} = 0 \tag{147}$$

$$-\overline{u'v'} = \epsilon_m \frac{\partial u}{\partial y} \tag{148}$$

$$-\overline{u'w'} = 0 \tag{149}$$

$$-\overline{v'w'} = 0 \tag{150}$$

The first three of the above equations indicate that the mean square of each fluctuating velocity is zero, and hence that the fluctuations all vanish. Since turbulent flow is based on the existence of these fluctuations, it would seem that the concept of a single entity,

eddy viscosity, which satisfies equations 139-144 is too restrictive, at least in some cases. (Since the case in which it has been shown to be too restrictive is simple, it might be inferred that it is too restrictive in all cases.)

This fact has been implicitly recognized; some investigators have attempted to replace the scalar ϵ_m by a vector of components ϵ_{m_x}, ϵ_{m_y} and ϵ_{m_z} for use according to the direction of momentum transfer. The normal components of turbulent stress can be defined in this way without difficulty; ϵ_m would be replaced by ϵ_{m_x}, ϵ_{m_y} and ϵ_{m_z} in Equations 133, 134, and 135, respectively.

However, ambiguity results if the tangential components of turbulent stress are defined in this way. Equation 136 can be written in two ways:

$$-\overline{u'v'} = \epsilon_{m_y}\left(\frac{\partial v}{\partial x} + \frac{\partial u}{\partial y}\right) \quad \begin{matrix}\text{(turbulent transfer of momentum} \\ \text{in y direction)}\end{matrix} \tag{151}$$

$$-\overline{v'u'} = \epsilon_{m_x}\left(\frac{\partial v}{\partial x} + \frac{\partial u}{\partial y}\right) \quad \begin{matrix}\text{(turbulent transfer of momentum} \\ \text{in x direction)}\end{matrix} \tag{152}$$

Since $u'v' = v'u'$ $\epsilon_{m_x} = \epsilon_{m_y}$ and representation of the eddy viscosity as a vector quantity is in general unsatisfactory.

A more general way of representing the eddy viscosity is in terms of the nine components of a tensor:

$$\begin{Bmatrix} \underline{\epsilon}_{m_{xx}} & \underline{\epsilon}_{m_{xy}} & \underline{\epsilon}_{m_{xz}} \\ \underline{\epsilon}_{m_{yx}} & \underline{\epsilon}_{m_{yy}} & \underline{\epsilon}_{m_{yz}} \\ \underline{\epsilon}_{m_{zx}} & \underline{\epsilon}_{m_{zy}} & \underline{\epsilon}_{m_{zz}} \end{Bmatrix}$$

where $\underline{\epsilon}_{m_{xy}} = \underline{\epsilon}_{m_{yx}}$; $\underline{\epsilon}_{m_{xz}} = \underline{\epsilon}_{m_{zx}}$; $\underline{\epsilon}_{m_{yz}} = \underline{\epsilon}_{m_{zy}}$, as in the case of the

stress tensor. The turbulent analog of Equation 104 then becomes:

$$\begin{Bmatrix} \tau_{xx} \tau_{xy} \tau_{xz} \\ \tau_{yx} \tau_{yy} \tau_{yz} \\ \tau_{zx} \tau_{zy} \tau_{zz} \end{Bmatrix} = - \begin{Bmatrix} p' & 0 & 0 \\ 0 & p' & 0 \\ 0 & 0 & p' \end{Bmatrix} + \begin{Bmatrix} \underline{\epsilon}_{m_{xx}} & \underline{\epsilon}_{m_{xy}} & \underline{\epsilon}_{m_{xz}} \\ \underline{\epsilon}_{m_{yx}} & \underline{\epsilon}_{m_{yy}} & \underline{\epsilon}_{m_{yz}} \\ \underline{\epsilon}_{m_{zx}} & \underline{\epsilon}_{m_{zy}} & \underline{\epsilon}_{m_{zz}} \end{Bmatrix} \left[\begin{Bmatrix} \frac{\partial u}{\partial x} & \frac{\partial v}{\partial x} & \frac{\partial w}{\partial x} \\ \frac{\partial u}{\partial y} & \frac{\partial v}{\partial y} & \frac{\partial w}{\partial y} \\ \frac{\partial u}{\partial z} & \frac{\partial v}{\partial z} & \frac{\partial w}{\partial z} \end{Bmatrix} + \begin{Bmatrix} \frac{\partial u}{\partial x} & \frac{\partial u}{\partial y} & \frac{\partial u}{\partial z} \\ \frac{\partial v}{\partial x} & \frac{\partial v}{\partial y} & \frac{\partial v}{\partial z} \\ \frac{\partial w}{\partial x} & \frac{\partial w}{\partial y} & \frac{\partial w}{\partial z} \end{Bmatrix} \right] \quad (153)$$

Since six components of the eddy viscosity tensor are independent, some of them may vanish independently of the others, and relations such as Equations 145-150 may be fulfilled.

It has been shown that representation of the eddy viscosity by means of a scalar in isothermal two-dimensional uniform steady flow forces the assumption that $\overline{u'u'} = 0$; $\overline{v'v'} = 0$; $\overline{w'w'} = 0$. Even though these normal stress terms do not actually vanish in turbulent flow, they are usually quite small compared to the pressure p', and hence may be neglected in Equations 127-129. It is concluded that turbulent flow may for all practical purposes be described in terms of a single scalar eddy viscosity, even though this point of view is theoretically incorrect.

Energy Balance

The equation of heat transfer for a flowing fluid will be developed by use of the general energy balance for steady flow, neglecting radiation. Consider a fixed infinitesimal volume element of dimensions dy, dy, and dz:

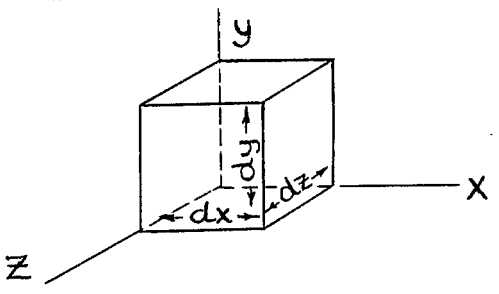

The general energy balance (20) for this volume element may be expressed as:

$$d\underline{\dot{H}} + d\underline{\dot{PE}} + d\underline{\dot{KE}} = \dot{q} \qquad (154)$$

For flow through the two yz faces, the rate of accumulation of enthalpy is:

$$\frac{\partial}{\partial x}(\sigma u H)\, dx\, dy\, dz$$

The net rate of accumulation of enthalpy for the six faces of the volume element is:

$$\underline{d\dot{H}} = \left[\frac{\partial}{\partial x}(\sigma u H) + \frac{\partial}{\partial y}(\sigma v H) + \frac{\partial}{\partial z}(\sigma w H)\right] dx\, dy\, dz \qquad (155)$$

which may be expanded to give:

$$\underline{d\dot{H}} = \left[\sigma\left(u\frac{\partial H}{\partial x} + v\frac{\partial H}{\partial y} + w\frac{\partial H}{\partial z}\right) + H\left(\frac{\partial \sigma u}{\partial x} + \frac{\partial \sigma v}{\partial y} + \frac{\partial \sigma w}{\partial z}\right)\right] dx\, dy\, dz \qquad (156)$$

The three terms which are multiplied by H vanish in light of the steady-flow continuity equation, $\left(\frac{\partial \sigma u}{\partial x} + \frac{\partial \sigma v}{\partial y} + \frac{\partial \sigma w}{\partial z}\right) = 0$

Equation 156 then becomes:

$$\underline{d\dot{H}} = \sigma\left(u\frac{\partial H}{\partial x} + v\frac{\partial H}{\partial y} + w\frac{\partial H}{\partial z}\right) dx\, dy\, dz \qquad (157)$$

Perfect gas behavior is now assumed, for which $dH = c_p dT$. Equation 157 becomes:

$$\underline{d\dot{H}} = c_p \sigma\left(u\frac{\partial T}{\partial x} + v\frac{\partial T}{\partial y} + w\frac{\partial T}{\partial z}\right) dx\, dy\, dz \qquad (158)$$

Expressions similar to Equation 157 may be written involving the potential energy and the kinetic energy:

$$d\,\underline{\dot{P}E} = \sigma\left(u\frac{\partial PE}{\partial x} + v\frac{\partial PE}{\partial y} + w\frac{\partial PE}{\partial z}\right)dx\,dy\,dz \qquad (159)$$

$$d\,\underline{\dot{K}E} = \sigma\left(u\frac{\partial KE}{\partial x} + v\frac{\partial KE}{\partial y} + w\frac{\partial KE}{\partial z}\right)dx\,dy\,dz \qquad (160)$$

If the y axis is assumed to be vertical $\partial PE/\partial x = \partial PE/\partial z = 0$; $\partial PE/\partial y = 1$; and Equation 159 simplifies to:

$$d\,\underline{\dot{P}E} = \sigma v\,dx\,dy\,dz \qquad (161)$$

The rate of conduction of heat into the volume element is obtained by use of the fundamental conduction equation:

$$\underline{\dot{Q}} = \frac{\partial}{\partial x}\left(K\,dy\,dz\frac{\partial T}{\partial x}\right)dx + \frac{\partial}{\partial y}\left(K\,dx\,dz\frac{\partial T}{\partial y}\right)dy + \frac{\partial}{\partial z}\left(K\,dx\,dy\frac{\partial T}{\partial z}\right)dz \qquad (162)$$

or

$$\underline{\dot{Q}} = \left[\frac{\partial}{\partial x}\left(K\frac{\partial T}{\partial x}\right) + \frac{\partial}{\partial y}\left(K\frac{\partial T}{\partial y}\right) + \frac{\partial}{\partial z}\left(K\frac{\partial T}{\partial z}\right)\right] \qquad (163)$$

If the above values for dH, dKE, dPE, and q are substituted into the Equation 154 and dxdydz cancelled from each term, the result is:

$$C_p\sigma\left(u\frac{\partial T}{\partial x} + v\frac{\partial T}{\partial y} + w\frac{\partial T}{\partial z}\right) + \sigma v + \sigma\left(u\frac{\partial KE}{\partial y} + v\frac{\partial KE}{\partial y} + w\frac{\partial KE}{\partial z}\right)$$

$$= \frac{\partial}{\partial x}\left(K\frac{\partial T}{\partial x}\right) + \frac{\partial}{\partial y}\left(K\frac{\partial T}{\partial y}\right) + \frac{\partial}{\partial z}\left(K\frac{\partial T}{\partial z}\right) \qquad (164)$$

The kinetic and potential energy terms are usually small and may be neglected. Equation 164 then becomes:

$$c_p \sigma \left(u \frac{\partial t}{\partial x} + v \frac{\partial t}{\partial y} + w \frac{\partial t}{\partial z}\right) = \frac{\partial}{\partial x}\left(K \frac{\partial t}{\partial x}\right) + \frac{\partial}{\partial y}\left(K \frac{\partial t}{\partial y}\right) + \frac{\partial}{\partial z}\left(K \frac{\partial t}{\partial z}\right) \quad (165)$$

This equation is valid for laminar flow. Representation of the instantaneous temperature as the sum of a mean temperature t and a fluctuating component t' leads to the derivation of the analog of Equation 165 for turbulent heat transfer. The steps in the derivation are quite similar to those in the derivation of the equations for momentum transfer and have been omitted. Turbulent fluctuations in c_p, σ and K are neglected. The resulting equation for heat transfer is:

$$c_p \sigma \left(u \frac{\partial t}{\partial x} + v \frac{\partial t}{\partial y} + w \frac{\partial t}{\partial z}\right) = \frac{\partial}{\partial x}\left(K \frac{\partial t}{\partial x}\right) + \frac{\partial}{\partial y}\left(K \frac{\partial t}{\partial y}\right) + \frac{\partial}{\partial z}\left(K \frac{\partial t}{\partial z}\right)$$

$$- c_p \left(\frac{\partial \sigma \overline{u't'}}{\partial x} + \frac{\partial \sigma \overline{v't'}}{\partial y} + \frac{\partial \sigma \overline{w't'}}{\partial z}\right) \quad (166)$$

The eddy conductivity ϵ_c is now defined so that Equation 165 is valid for turbulent heat transfer if K is replaced by $(\epsilon_c + K)\sigma c_p$. According to this definition, ϵ_c must satisfy all the following relations:

$$-\overline{u't'} = \epsilon_c \frac{\partial t}{\partial x} \quad (167)$$

$$-\overline{v't'} = \epsilon_c \frac{\partial t}{\partial y} \quad (168)$$

$$-\overline{w't'} = \epsilon_c \frac{\partial t}{\partial z} \quad (169)$$

The scalar ϵ_c is sometimes replaced by a vector of components ϵ_{cx}, ϵ_{cy} and ϵ_{cz} for use according to the direction of heat

transfer:

$$-\overline{u't'} = \epsilon_{cx}\frac{\partial t}{\partial x} \tag{170}$$

$$-\overline{v't'} = \epsilon_{cy}\frac{\partial t}{\partial y} \tag{171}$$

$$-\overline{w't'} = \epsilon_{cz}\frac{\partial t}{\partial z} \tag{172}$$

This vectorial representation of ϵ_c (unlike that of its analog, ϵ_m) is theoretically satisfactory, but is of little practical use, since sufficient information to evaluate the eddy conductivity in terms of components is not readily available in most cases. Scalar representation for both the eddy quantities is used in this research.

For the special case of two-dimensional steady flow, the equations of motion and heat transfer may be simplified considerably, since all derivatives with respect to z and θ vanish. Equation 124 then becomes:

$$\frac{\partial \tau_{x\,x'}}{\partial x} + \frac{\partial \tau_{x\,y}}{\partial y} = \rho\left(u\frac{\partial u}{\partial x} + v\frac{\partial u}{\partial y}\right) \tag{173}$$

Equations 133 and 136 are differentiated and combined with Equation 173:

$$-\frac{\partial p}{\partial x} - \frac{2}{3}\frac{\partial}{\partial x}\left[\rho\left(\nu+\epsilon_m\right)\left(\frac{\partial v}{\partial x}+\frac{\partial u}{\partial y}\right)\right] + 2\frac{\partial}{\partial x}\left[\rho\left(\nu+\epsilon_m\right)\frac{\partial u}{\partial x}\right]$$

$$+\frac{\partial}{\partial y}\left[\rho\left(\nu+\epsilon_m\right)\left(\frac{\partial v}{\partial x}+\frac{\partial u}{\partial y}\right)\right] = \rho\left(u\frac{\partial u}{\partial x} + v\frac{\partial u}{\partial y}\right) \tag{174}$$

A further simplification results if it is assumed that v = 0.

Equation 174 then becomes:

$$\frac{\partial}{\partial y}\left[\rho\left(\nu+\epsilon_m\right)\frac{\partial u}{\partial y}\right]+\frac{4}{3}\frac{\partial}{\partial x}\left[\rho\left(\nu+\epsilon_m\right)\frac{\partial u}{\partial x}\right]-\frac{\partial p}{\partial x}=\rho u\frac{\partial u}{\partial x} \quad (175)$$

The term $\frac{4}{3}\frac{\partial}{\partial x}\left[\rho\left(\nu+\epsilon_m\right)\frac{\partial u}{\partial x}\right]$ is small compared with the remaining terms in Equation 175 and will be neglected. The resulting equation, solved for the eddy viscosity, is:

$$\epsilon_m = \frac{\int_0^{y'}\left[\rho u\frac{\partial u}{\partial x}+\frac{\partial p}{\partial x}\right]dy'}{\rho\frac{\partial u}{\partial y'}}-\nu \quad (176)$$

for which the origin is taken at the axis of flow where du/dy = 0.

The heat-transfer equation for two-dimensional steady flow reduces to:

$$c_p\sigma u\frac{\partial t}{\partial x}=\frac{\partial}{\partial x}\left[c_p\sigma\left(\epsilon_c+K\right)\frac{\partial t}{\partial x}\right]+\frac{\partial}{\partial y}\left[c_p\sigma\left(\epsilon_c+K\right)\frac{\partial t}{\partial y}\right] \quad (177)$$

This equation may be simplified if it is assumed that $c_p\sigma$ is constant and that the term $\frac{\partial}{\partial x}\left[c_p\sigma\left(\epsilon_c+K\right)\frac{\partial t}{\partial x}\right]$, which represent heat transfer in the direction of flow, is negligible. The resulting simplified equation is:

$$u\frac{\partial t}{\partial x}=\frac{\partial}{\partial y}\left[\left(\epsilon_c+K\right)\frac{\partial t}{\partial y}\right] \quad (178)$$

which may be solved for ϵ_c :

$$\epsilon_c = \frac{\int_o^y u \frac{\partial t}{\partial x} dy}{\frac{\partial t}{\partial y}} - k \qquad (179)$$

The origin is again taken at the axis of flow.

It is possible that for fully developed turbulence, the eddy quantities are independent of downstream distance. The conditions which must be fulfilled to obtain uniformity of the eddy quantities will now be considered. If the density is assumed constant, Equation 176 may be rewritten as follows:

$$\epsilon_m = \frac{\frac{1}{u_m}\int_o^y \left(u \frac{\partial u}{\partial x} + \frac{1}{\rho} \frac{\partial p}{\partial x}\right) dy}{\rho \frac{\partial u}{\partial y}} - \nu \qquad (180)$$

The maximum velocity u_m is a function of x only and may be moved inside differentials and integrals with respect to y without complication:

$$\epsilon_m = \frac{\int_o^y \left(\frac{u}{u_m} \frac{\partial u}{\partial x} + \frac{1}{\rho u_m} \frac{\partial p}{\partial x}\right) dy}{\rho \frac{\partial}{\partial y}\left(\frac{u}{u_m}\right)} - \nu \qquad (181)$$

The denominator of Equation 181 is a function of y only, since for fully developed turbulence $\partial/\partial x(u/u_m) = \partial f_u/\partial x = 0$. In the numerator, $\partial P/\partial x$ and $1/\rho u_m$ can be considered to be functions of

y only, the former on the assumption of a constant pressure gradient, the latter from the continuity equation for two-dimensional steady flow, vertical velocities being neglected. Since u/u_m is also a function of y only, the eddy viscosity will be a function of only the y coordinate for fully developed turbulence if the following requirements are met:

$$\rho = \text{constant} \tag{182}$$

$$\partial^2 u/\partial x^2 = 0 \tag{183}$$

Equation 179 may be rewritten as follows:

$$\epsilon_c + K = \frac{y_o^2 \int_o^{y'/y_o} \frac{u}{u_m} \frac{\partial}{\partial x}\left[\frac{t - t_w}{t_c - t_w}(t_c - t_w) + t_w\right] d\left(y'/y_o\right)}{\frac{1}{u_m}\frac{\partial}{\partial (y'/y_o)}\left[\frac{t_w - t}{t_w - t_c}(t_w - t_c) + t_w\right]} \tag{184}$$

Since t_w = constant and both $\partial f_t/\partial x$ and $\partial t_c/\partial y$ are equal to zero, Equation 184 becomes:

$$\epsilon_c + K = \frac{\int_o^{y'/y_o} y_o^2 f_u f_t \frac{\partial t_c}{\partial x} d\left(y'/y_o\right)}{\frac{t_w - t_c}{u_m} \quad \frac{\partial f_t}{\partial y'/y_o}} \tag{185}$$

or

$$\epsilon_c + K = \frac{y_o^2 u_m \frac{\partial t_c}{\partial x}}{t_w - t_c}\left[\frac{\int_o^{y'/y_o} f_u f_t \, d\left(y'/y_o\right)}{\frac{\partial f_t}{\partial (y'/y_o)}}\right] \tag{186}$$

The bracketed term in the above expression is a function of y only, but of the remaining quantities u_m, $\partial t/\partial x$, and t_c are all

functions of x. The necessary condition for uniformity of the eddy conductivity is:

$$\frac{\partial}{\partial x}\left[\frac{u_m \frac{\partial t_c}{\partial x} y_o^2}{t_w - t_c}\right] \tag{187}$$

Appendix II. Thermanemometer Correction

This section is devoted to the estimation of the effect of conduction of heat from the thermanemometer by its supporting needles. This effect need not be considered for velocity measurements, since it is accounted for by the calibration. However, the correction for the heating of the thermanemometer during temperature measurements due to the Mueller Bridge current is influenced by this effect.

The ends of the wire will be assumed to be at zero temperature, which is also the temperature of the free air stream. The heat transfer coefficient from the wire to the air stream is determined by application of Equation 5 (King's Equation) at zero air velocity.

An energy balance on an infinitesimal element of wire of length dx gives:

$$\frac{E^2}{R}\,\frac{dx}{2L} + \frac{d}{dx}\left[K\,\frac{\pi D^2}{4}\,\frac{dt}{dx}\right]dx = h\pi D t\,dx \qquad (188)$$

The first term of Equation 188 represents the heat developed in the element of wire due to the flow of current; the second term is the gain in heat of the element by conduction; the third term represents the heat loss from the element to the air stream by convection.

Equation 188 may be simplified by the introduction of constants B' and C':

$$B'\frac{d^2t}{dx^2} - C't = -1 \qquad (189)$$

where $$B' = \frac{K\pi D^2 R L}{2E^2} \qquad (190)$$

and $$C' = \frac{2\pi D h R L}{E^2} \qquad (191)$$

The general solution of this equation is:

$$t = M e^{\sqrt{\frac{C'}{B'}}x} + N e^{\sqrt{\frac{C'}{B'}}x} + \frac{1}{C'} \qquad (192)$$

The constants M and N are determined from the boundary conditions:

$$t(o) = 0$$

$$\frac{dt}{dx} = 0 \quad (x = e) \qquad (193)$$

Equations 192 and 193 are combined to give:

$$M + N + \frac{1}{C'} = 0 \qquad (194)$$

$$M e^{L\sqrt{\frac{C'}{B'}}} = N e^{-L\sqrt{\frac{C'}{B'}}} \qquad (195)$$

whence

$$M = -\frac{1}{C'\left(1 + e^{2L\sqrt{C'/B'}}\right)} \qquad (196)$$

$$N = -\frac{e^{2L\sqrt{C'/B'}}}{C'\left(1 + e^{2L\sqrt{C'/B'}}\right)} \qquad (197)$$

The resulting equation is:

$$t = 1/C'\left[1 - \frac{e^{\sqrt{C'/B'}x} + e^{\sqrt{C'/B'}(2L-x)}}{1 + e^{2L\sqrt{C'/B'}}}\right] \qquad (198)$$

The mean temperature of the wire is determined by integration:

$$\bar{t} = \frac{\int_0^L t \, dx}{L} \tag{199}$$

$$\bar{t} = \frac{1}{C'} \left\{ 1 - \frac{\sqrt{B'/C'} \left[e^{L\sqrt{C'/B'}} - 1 \right] + e^{2L\sqrt{C'/B'}} \sqrt{B'/C'} \left[1 - e^{-L\sqrt{C'/B'}} \right]}{L \left[1 + e^{2L\sqrt{C'/B'}} \right]} \right\} \tag{200}$$

Since $e^{L\sqrt{C'/B'}} \gg 1$ and $e^{-L\sqrt{C'/B'}} \ll 1$, Equation 200 simplifies to:

$$\bar{t} = \frac{1}{C'} \left\{ 1 - \frac{\sqrt{B'/C'} \left[e^{L\sqrt{C'/B'}} + e^{2L\sqrt{C'/B'}} \right]}{L \, e^{2L\sqrt{C'/B'}}} \right\} \tag{201}$$

Since $e^{2L\sqrt{C'/B'}} \gg e^{L\sqrt{C'/B'}}$, Equation 201 reduces to:

$$\bar{t} = \frac{1}{C'} \left\{ 1 - \frac{1}{L} \sqrt{B'/C'} \right\} \tag{202}$$

The numerical values of the constants are now obtained:

$$\sqrt{\frac{B'}{C'}} = \sqrt{\frac{KD}{4h}} = \frac{1}{595.3}$$

$$L = 0.015625$$

$$C = \left[\frac{E^2}{2\pi D h R L} \right]^{-1} = \frac{1}{0.251}$$

Then $\bar{t} = 0.251 \left\{ 1 - 0.093 \right\} = 0.251 \left\{ 0.907 \right\}$ (203)

This result shows that the mean temperature rise of the wire at zero air velocity is 90.7% of the rise which would take place in the absence of heat conduction from the ends of the wire.

This result is applicable to hot wire corrections for bridge current temperature rise at any air velocity (even though it was

derived for the correction at zero air velocity) if the slight variation of the heat transfer coefficient with velocity is neglected.

Nomenclature

$\underline{A}$	A point of coordinates (x_a, y_a, z_a)
A	Dimensional constant in thermanemometer velocity calibration equation
B	Dimensional constant in thermanemometer velocity calibration equation
B'	Dimensional constant in equation for heat flow along a wire
C'	Dimensional constant in equation for heat flow along a wire
D	Diameter of wire, ft.
E	Electrical potential difference, volts
E_j	Potential difference between junction j of analog circuit and ground
E_{12}	Potential difference between junctions 1 and 2 of analog circuit
e	Base of natural logarithms
e_x	Rate of change in shape of fluid element by extension in direction of x axis, sec^{-1}
F_x	Component of force acting in x direction, lb
f_t	Dimensionless temperature distribution function, $(t_w - t)/(t_w - t_c)$
f_u	Dimensionless velocity distribution function, u/u_m
f(x)	A function of x
G	Mass velocity, lb/sec ft^2
g	Acceleration due to gravity, ft/sec^2
H	Specific enthalpy, BTU/lb
$\underline{\dot{H}}$	Rate of enthalpy transport, BTU/sec
h	Heat transfer coefficient, BTU/hr ft^2 ^oF
I	Current, amperes
i	An intensity factor of turbulence
K	Thermal conductivity, BTU ft/sec ft^2 ^oF
K_1	Dimensionless constant

KE	Specific kinetic energy, ft lb/lb
$\dot{KE}$	Rate of kinetic energy transport, ft lb/sec
k	Dummy index
L	Length of wire, ft
l	The number of turbulent intensity factors existing in a particular flow situation
m	The number of turbulent scale factors existing in a particular flow situation
$\dot{m}$	Weight rate of flow, lb/sec
M	Constant of integration, Equation 192
N	Constant of integration, Equation 192
n	A number
P'	Thermodynamic pressure, lb/ft^2 or lb/in^2
P	Mean pressure in a flowing fluid, lb/ft^2 or lb/in^2
P_x	Stress vector for surface normal to x axis, lb/ft^2 or lb/in^2
p	A point in the channel equivalent to a particular value of y/y_o, and analogous to a junction j of the analog circuit
$\dot{PE}$	Rate of potential energy transport, ft lb/sec
$\dot{Q}$	Rate of heat transfer, BTU/sec
$\dot{Q}$	Rate of heat transfer per unit area, BTU/sec ft^2
$\dot{Q}_w$	Rate of heat transfer per unit area from wall to air stream, BTU/sec ft^2
R	Resistance, ohms
R_A	Resistance of thermanemometer at air stream temperature, ohms
R_{HW}	Resistance of thermanemometer at its operating temperature, ohms
S_x	Surface normal to x axis
s	A scale factor of turbulence
t	Time average temperature, ^oF
t'	Temperature fluctuation, ^oF

t_i	Instantaneous temperature, ^oF
$\bar{t}$	Mean temperature of wire (averaged over its length), ^oF
t_B	Bulk air temperature, ^oF
t_c	Centerline temperature, ^oF
$t_p(x)$	Temperature as a function of x for a point p in the channel, corresponding to a particular value of y/y_o
t_w	Wall temperature, ^oF
Δt_B^A	Correction to be added to analog bulk temperature, ^oF
Δt_B^E	Bulk temperature calculated from assumption (2), page 48, minus bulk temperature calculated from assumption (1), page 48
Δt_b	Correction of thermanemometer for bridge current heating
$\Delta t_b'$	Intermediate value of bridge current heating correction, ^oF
$\Delta t_b''$	Intermediate value of bridge current heating correction, ^oF
Δt_i	Impact temperature correction, ^oF
Δt_s	Stagnation temperature rise, ^oF
δt	Uncertainty in temperature, ^oF
u^*	Friction velocity, $\sqrt{\tau_{yx}/\rho}$, ft/sec
U_B	Bulk air velocity, ft/sec
u, v, w	Time average velocities in x, y, and z directions, ft/sec
u', v', w'	Fluctuating velocities in x, y, and z directions, ft/sec
u_i, v_i, w_i	Instantaneous velocities in x, y, and z directions, ft/sec
u_m	Maximum velocity in x direction, ft/sec
x	Longitudinal coordinate of channel, origin at channel entrance, ft or in.
y	Vertical coordinate in channel, origin at lower wall, ft or in.
z	Lateral coordinate in channel, origin at longitudinal midline, ft or in.

x_c Downstream distance for fully developed turbulence, ft or in.

y' Vertical coordinate in channel, origin at $y/y_o = 0.5$, ft or in.

y_o Channel height, ft or in.

Greek letters

α Dimensional constant in thermanemometer temperature calibration equation

β Dimensional constant in thermanemometer temperature calibration equation

γ Rate of change in shape of a fluid element by angular deformation, sec^{-1}

ϵ_c Eddy conductivity, ft^2/sec

ϵ_m Eddy viscosity, ft^2/sec

$\underline{\epsilon_m}$ Sum of eddy and kinematic viscosities, ft^2/sec

θ Time, sec

κ Thermometric conductivity, ft^2/sec

λ Factor relating time to downstream distance (analog computer), sec/ft

μ Absolute viscosity, lb sec/ft^2

ν Kinematic viscosity, ft^2/sec

ρ Specific mass, lb sec^2/ft^4

σ Specific weight, lb/ft^3

τ_{yx} x component of stress vector for surface normal to y axis (laminar flow), lb/ft^2 or lb/in^2

τ'_{yx} Turbulent stress component: sum of laminar stress τ_{yx} and eddy stress $-\rho\overline{u'v'}$, lb/ft^2 or lb/in^2

$\tau^{o\prime}_{yx}$ Turbulent stress component at wall, lb/ft^2 or lb/in^2

ϕ Thermal resistance, sec/ft^2

ϕ_o Thermanemometer velocity function, $I^2R_{HW}/(R_{HW} - R_A)$, amp^2

Dimensionless quantities:

Pr	$\nu/\varkappa$
Re	DU_B/ν
St	$h/c_p G$
u^+	u/u^*
y^+	$(y_o-y)u^*/\nu$

Symbols:

$\cong$	Same order of magnitude
$\approx$	Approximately equal to
$\sim$	Analogous to
$\ll$	Much less than
$\overline{u'v'}$	Time average of the product $u'v'$

List of Figures

22. Pressure vs. Downstream Distance, P lbs/in.^{2} vs. x in., 115/100/85, U_B = 30 ft/sec

23. Pressure vs. Downstream Distance, P lbs/in.^{2} vs. x in., 100/100/85, U_B = 15 ft/sec

24. Slope of Thermanemometer Calibration Equation, ^oF/ohm vs. Time , days

25. Experimental and Calculated Bulk Temperatures t_B ^oF vs. x in., 100/85/100, U_B = 30 ft/sec

26. Experimental and Calculated Bulk Temperatures t_B ^oF vs. x in., 100/85/100, U_B = 15 ft/sec

27. Eddy Viscosity Distribution, ft^2/sec vs. y/y_o

28. Theoretical and Experimental Dimensionless Temperature and Velocity Distributions, u/u_m and $t_w - t/t_w - t_c$ vs. y/y_o, 100/85/100, U_B = 30 ft/sec

29. Theoretical and Experimental Dimensionless Temperature and Velocity Distributions, u/u_m and $t_w - t/t_w - t_c$ vs. y/y_o, 100/85/100, U_B = 15 ft/sec

30. Circuit Diagram, Analog Equipment

31. Eddy Conductivity Distribution Used in Analog Solutions (Test 40), ft^2/sec vs. y/y_o

32. Oscilloscope Trace, E vs. , y/y_o = 0.500

33. Oscilloscope Trace, E vs. , y/y_o = 0.643

34. Oscilloscope Trace, E vs. , y/y_o = 0.821

35. Oscilloscope Trace, E vs. , y/y_o = 0.964

36. Oscilloscope Trace E_{12} vs.

37. Analog Solution: Heat Transfer and Heat Transfer Coefficient vs. x

38. Analog Solution: t^oF vs. x in., y/y_o = 0.500

39. Analog Solution: t^oF vs. x in., y/y_o = 0.643

40. Analog Solution: t^oF vs. x in., y/y_o = 0.821

41. Analog Solution: t^oF vs. x in., y/y_o = 0.964

42. Analog Solution: Temperature Distribution vs. y/y_o

43. Wall Temperatures, t_w °F, vs. Downstream Distance, x in. for 100/85/100, U_B = 15 and 30 ft/sec

Note: Each of the figures listed below presents two or more traverses which are nearly identical. The curves have been separated by displacing the origin of each successive traverse as follows: Figs. 12, 17, 19, 10 ft/sec; Fig. 13, 5 ft/sec; Figs. 16, 18, 2°F. For all figures the plotted scale of t or u is valid for the traverse at x=23.22 in.

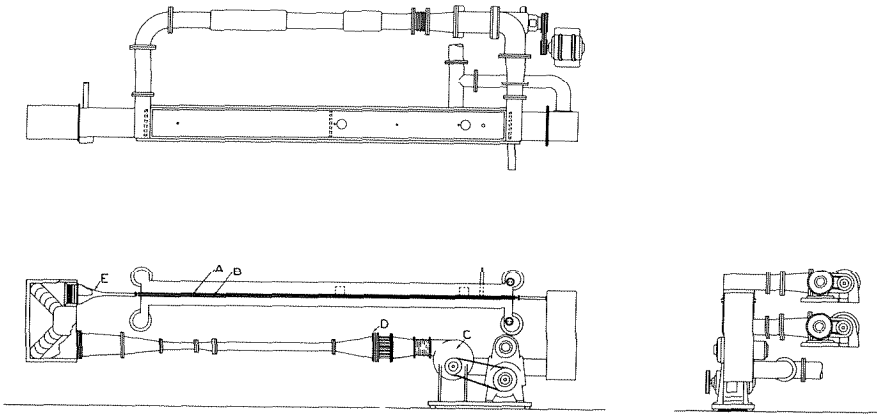

Fig. 1. General View of Equipment

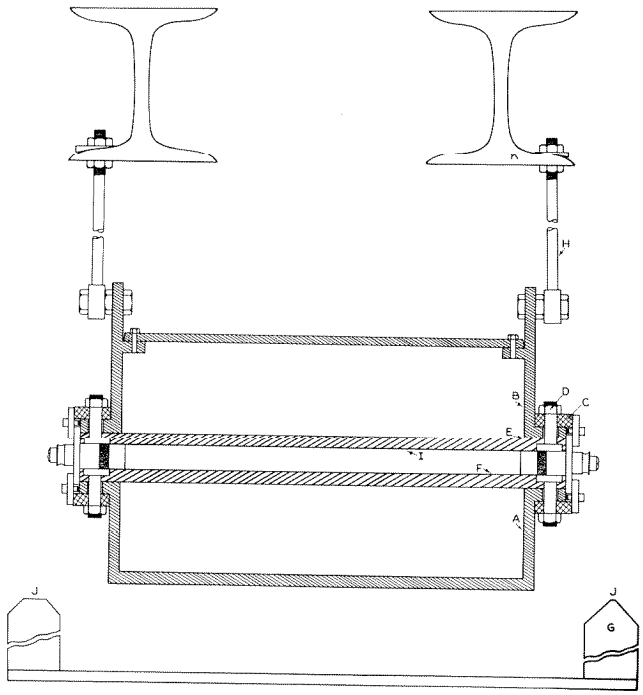

Fig. 2. End View of Channel

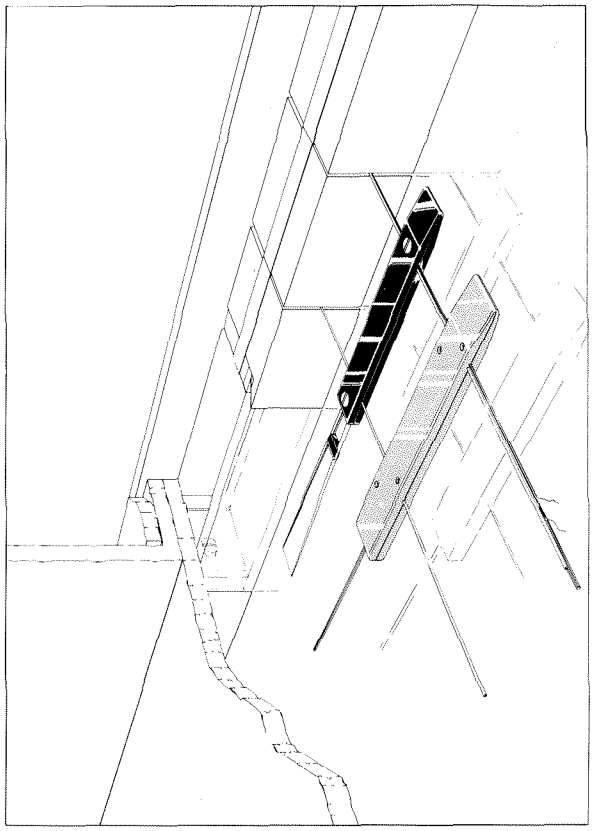

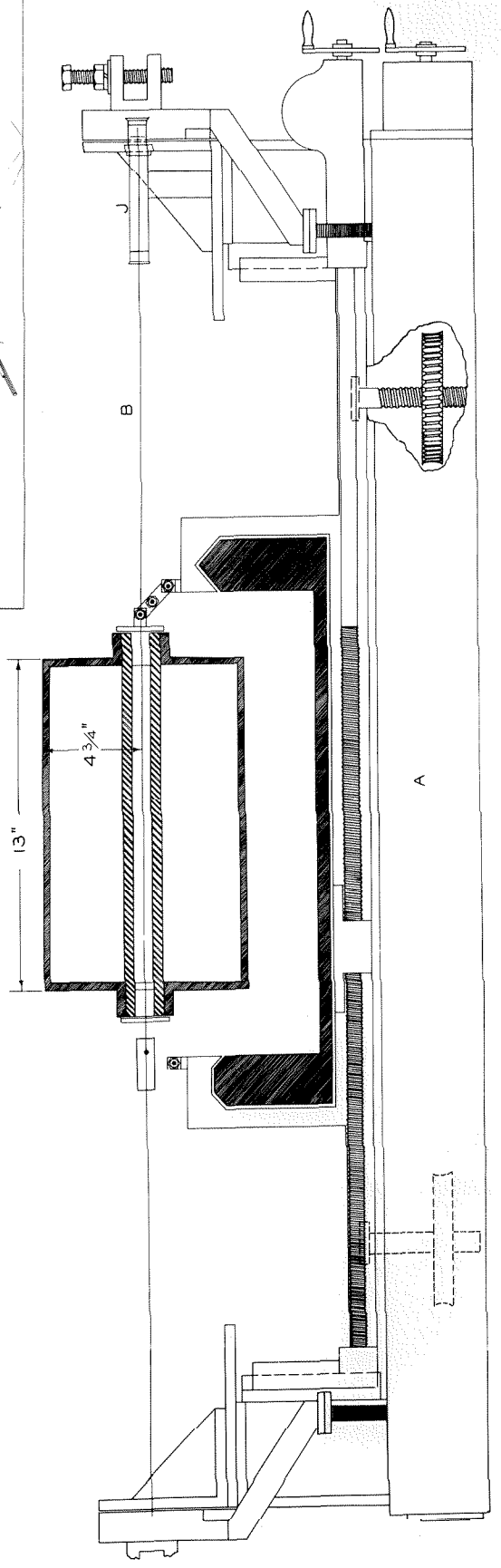

Fig. 3

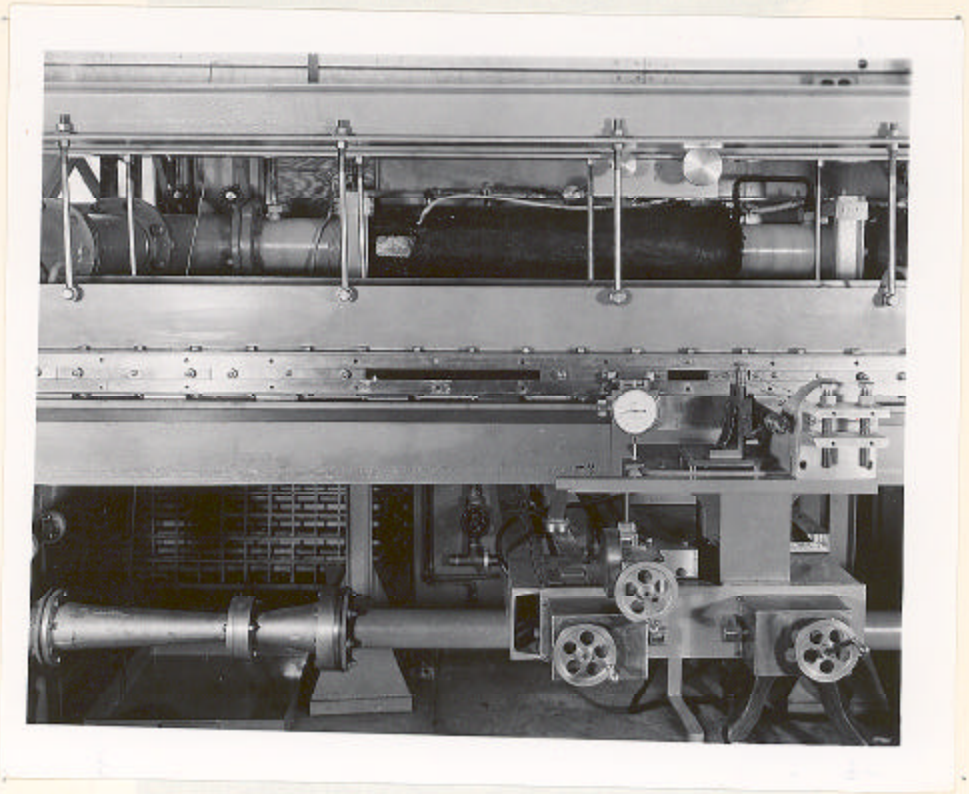

Fig. 4. Traversing Gear and Channel

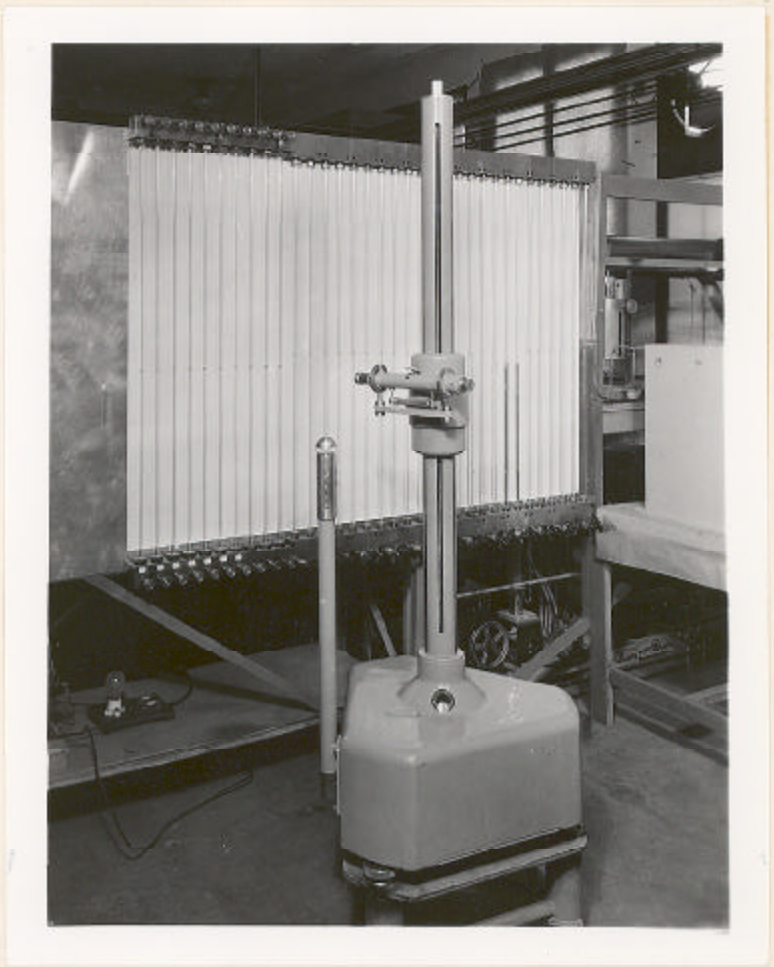

Fig. 5. Cathetometer and Manometer Bank

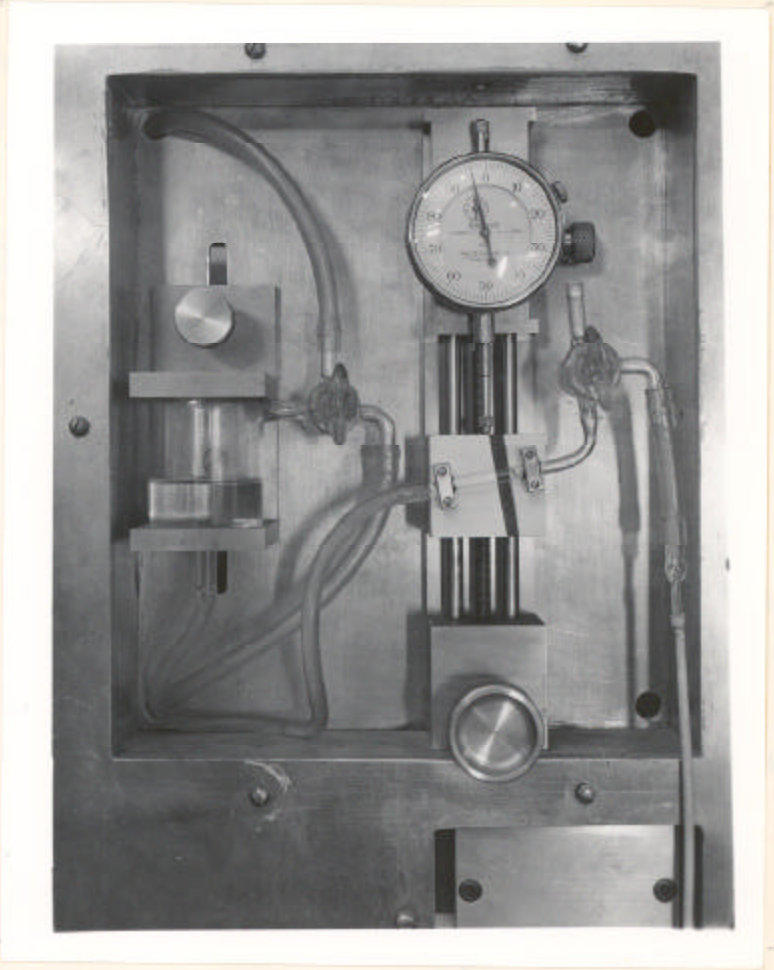

Fig. 6. Micromanometer

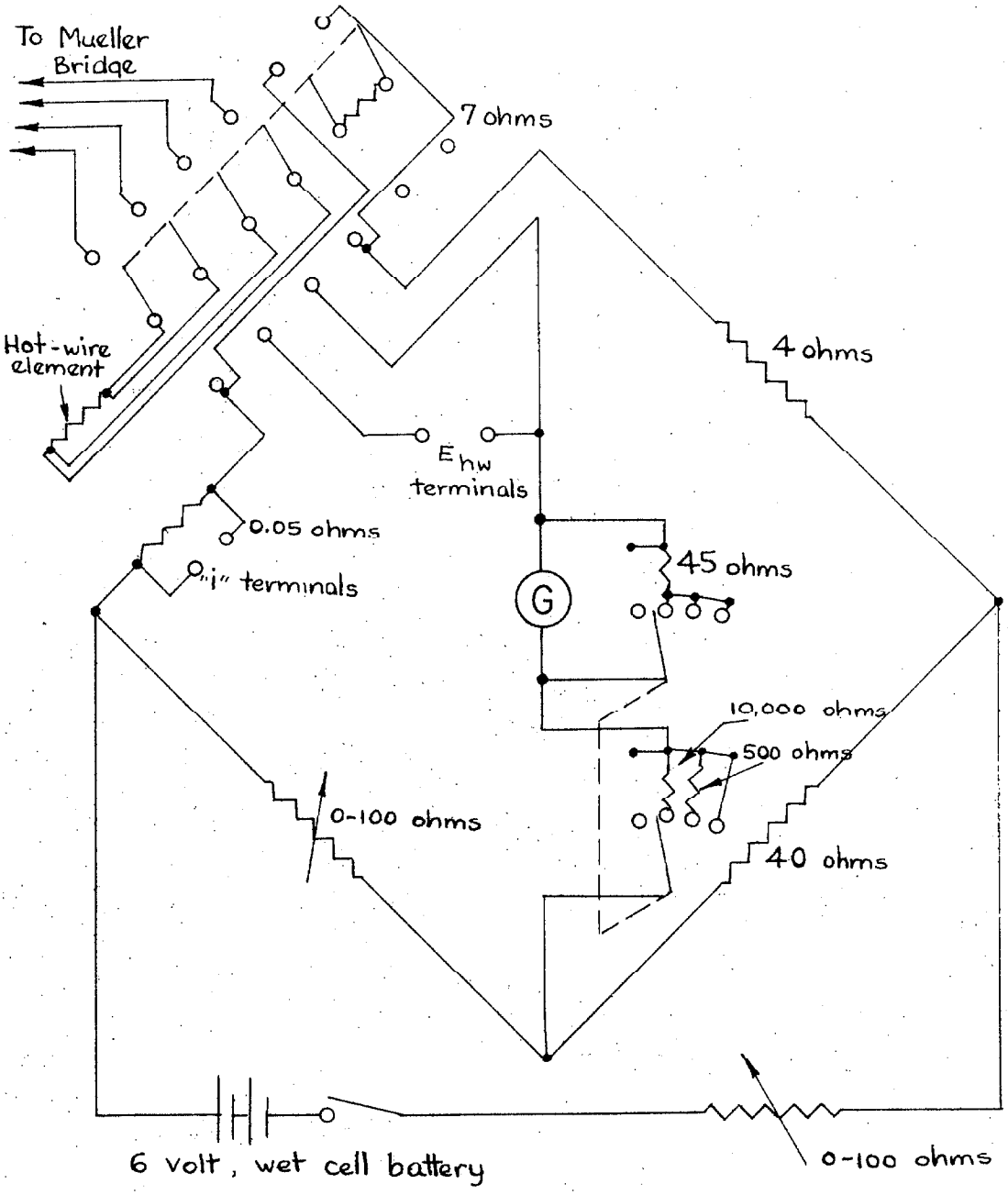

FIGURE 7

THERMANEMOMETER CIRCUIT DIAGRAM

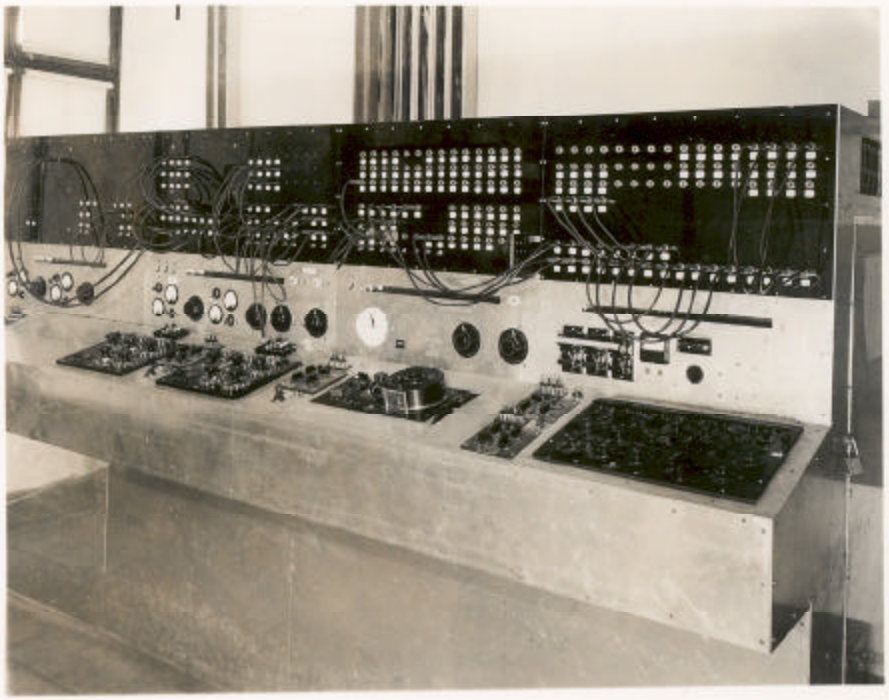

Fig. 8. Temperature Bench

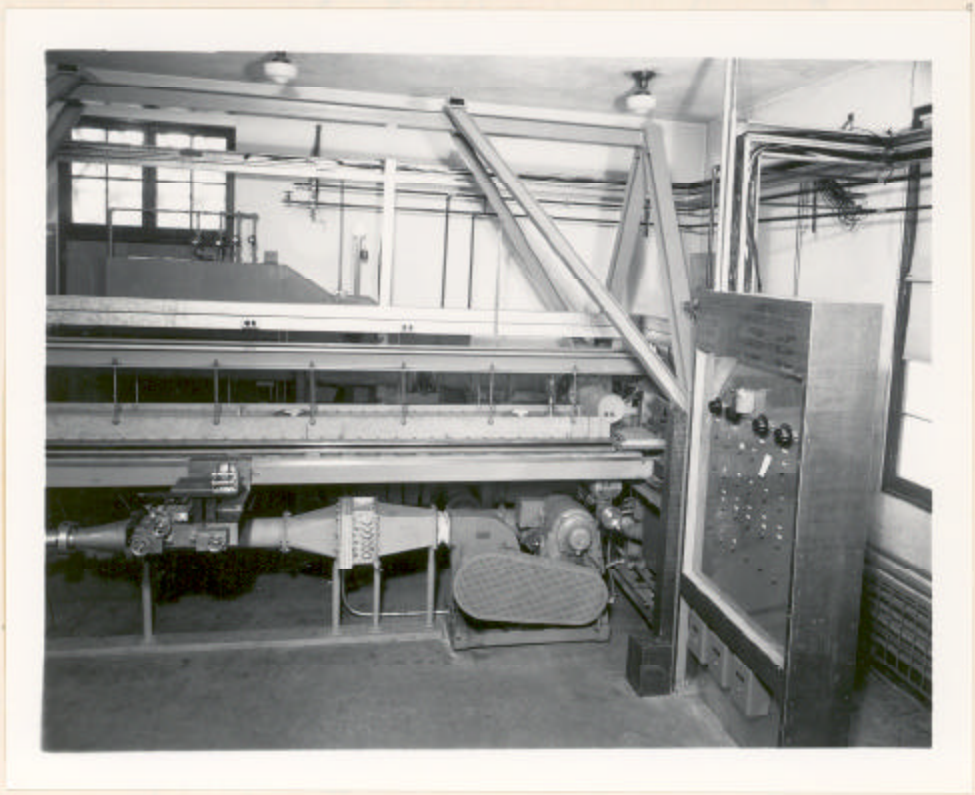

Fig. 9. Equipment, Downstream End

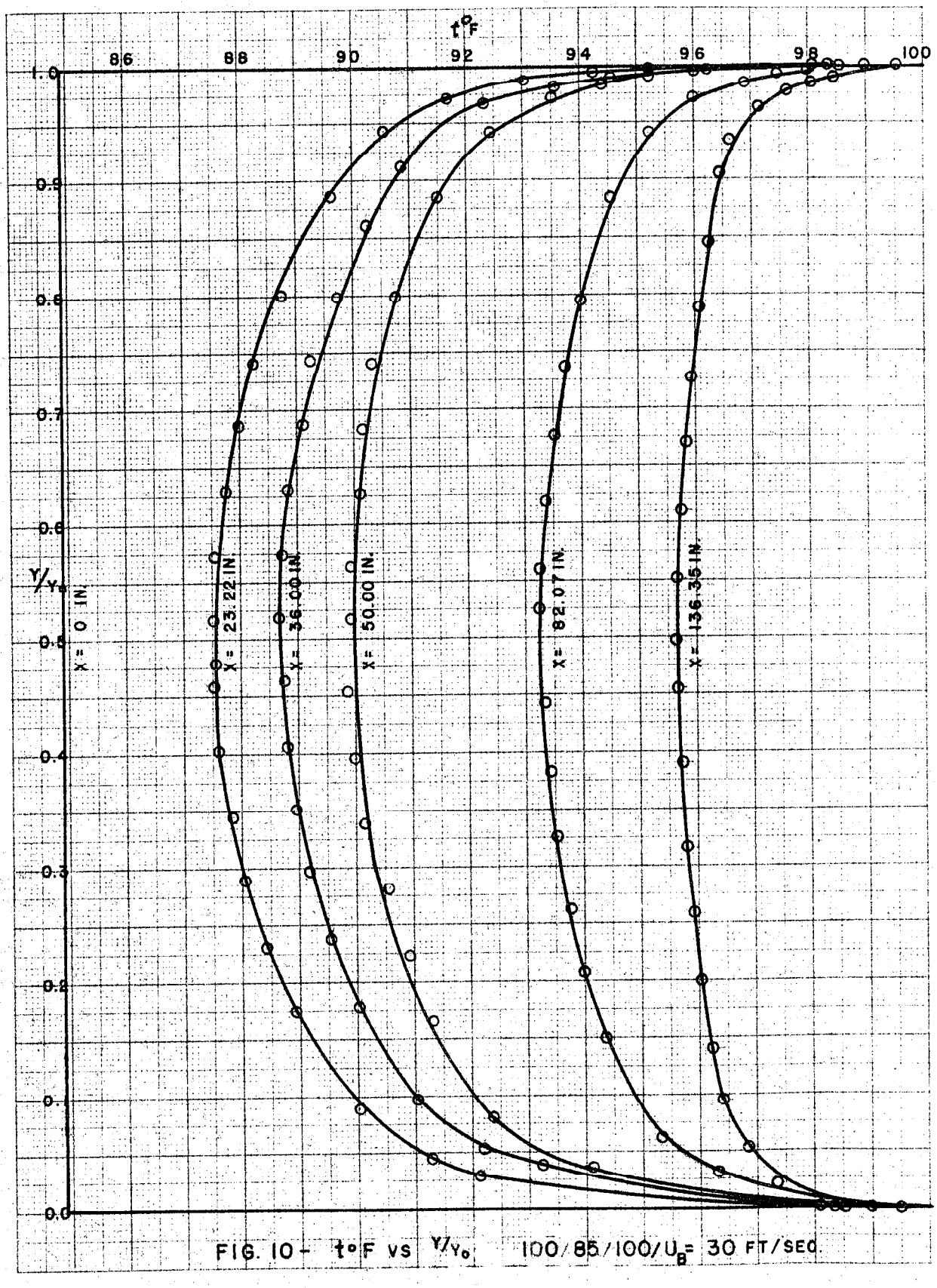

FIG. 10 - t°F vs Y/Y_0 100/85/100/U_B = 30 FT/SEC.

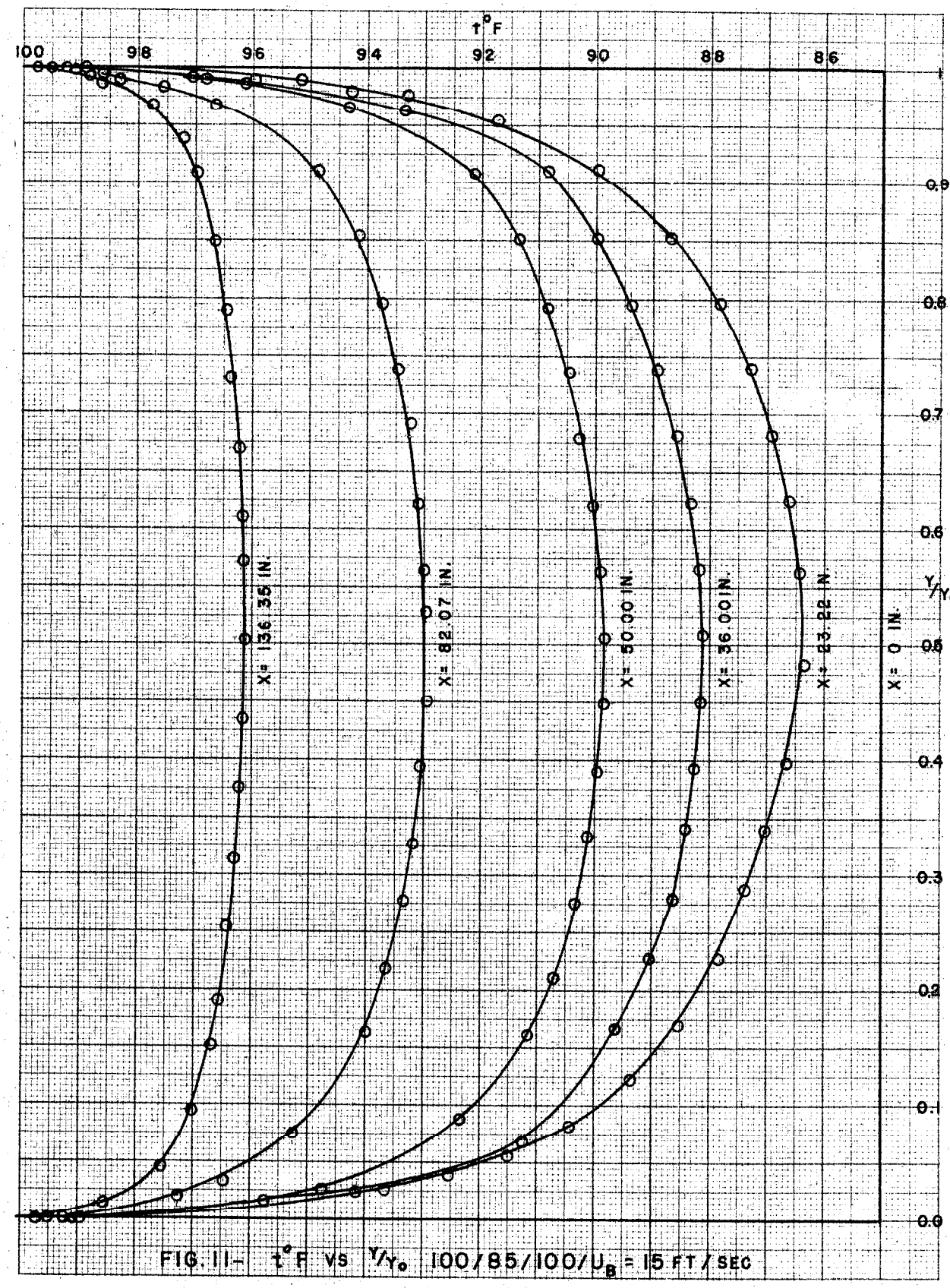

FIG. 11- $t°F$ VS Y/Y_o $100/85/100/U_B = 15$ FT/SEC

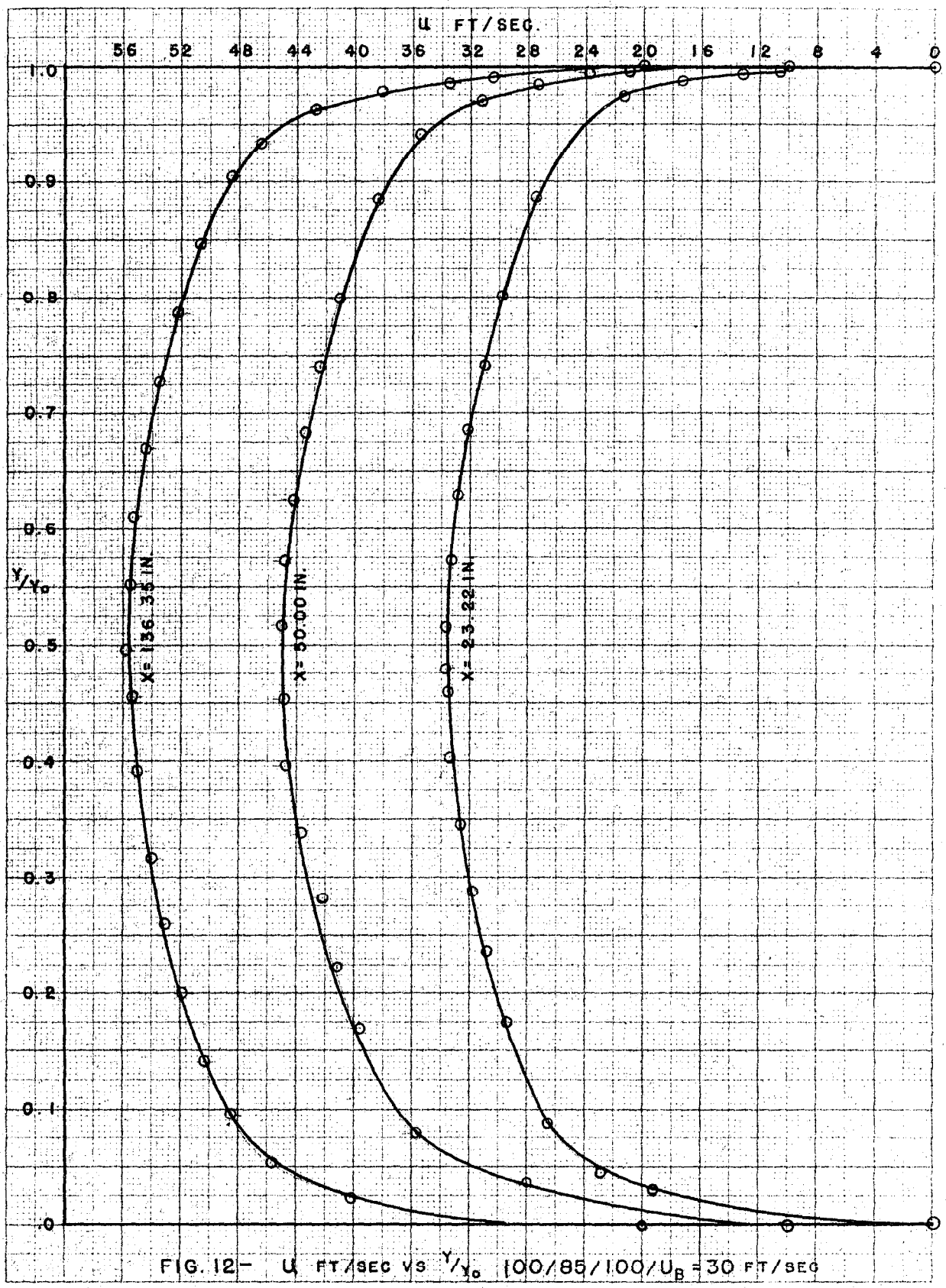

FIG. 12— U FT/SEC VS Y/Y_0 100/85/100/U_B = 30 FT/SEC

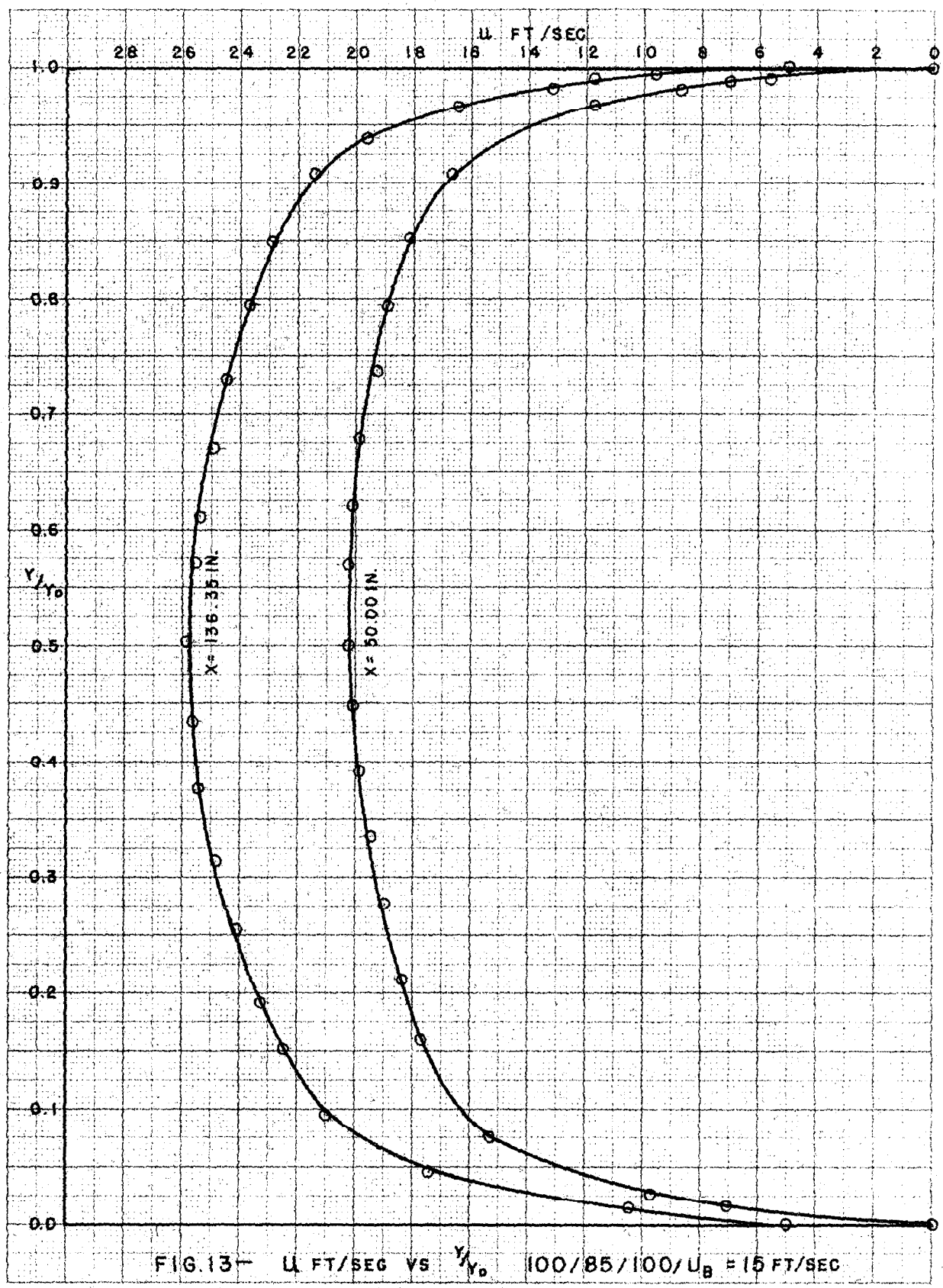

FIG.13— u FT/SEC VS Y/Y_0 100/85/100/U_B = 15 FT/SEC

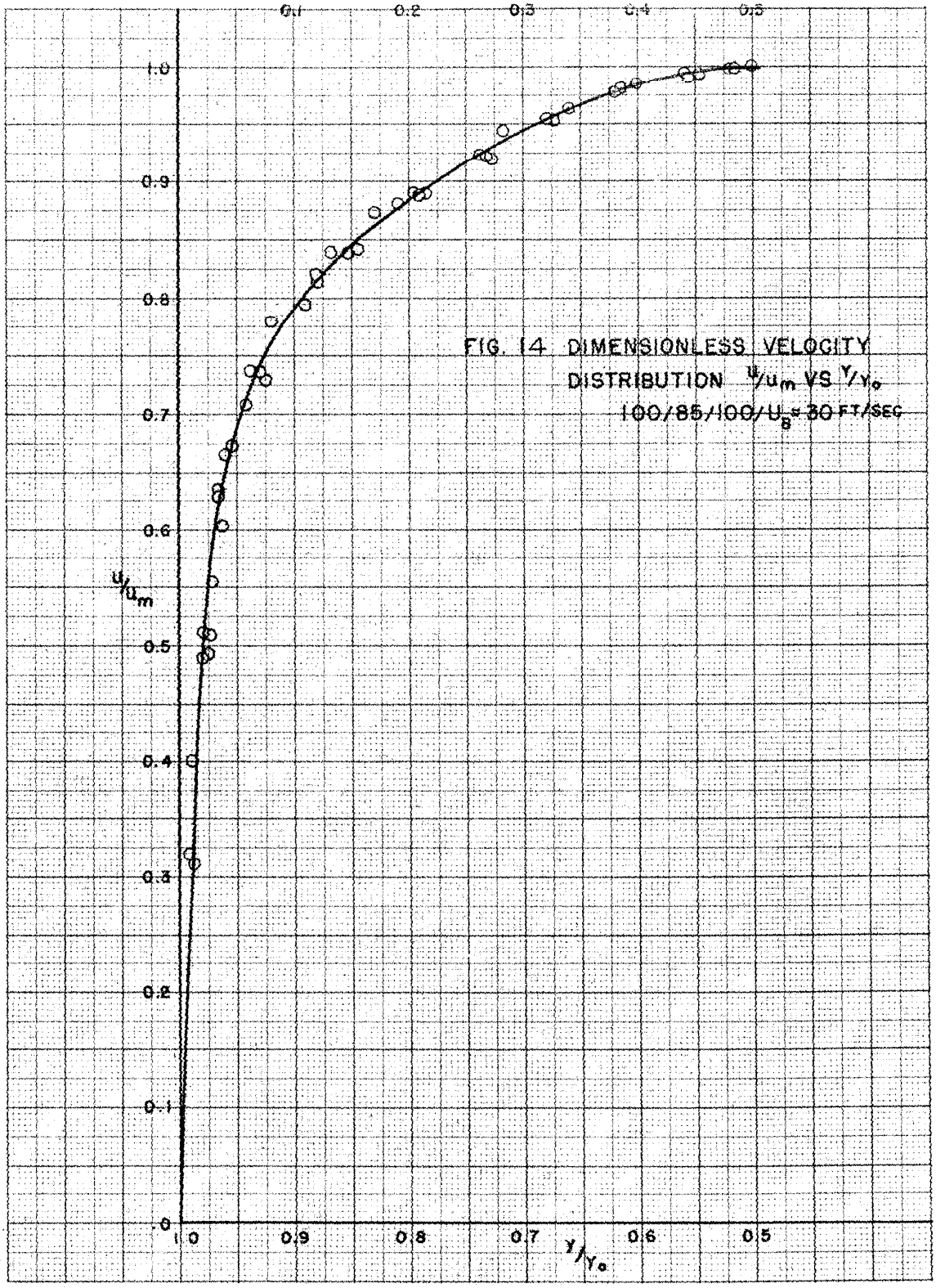

FIG. 14 DIMENSIONLESS VELOCITY DISTRIBUTION u/u_m VS y/y_o
100/85/100/U_B = 30 FT/SEC

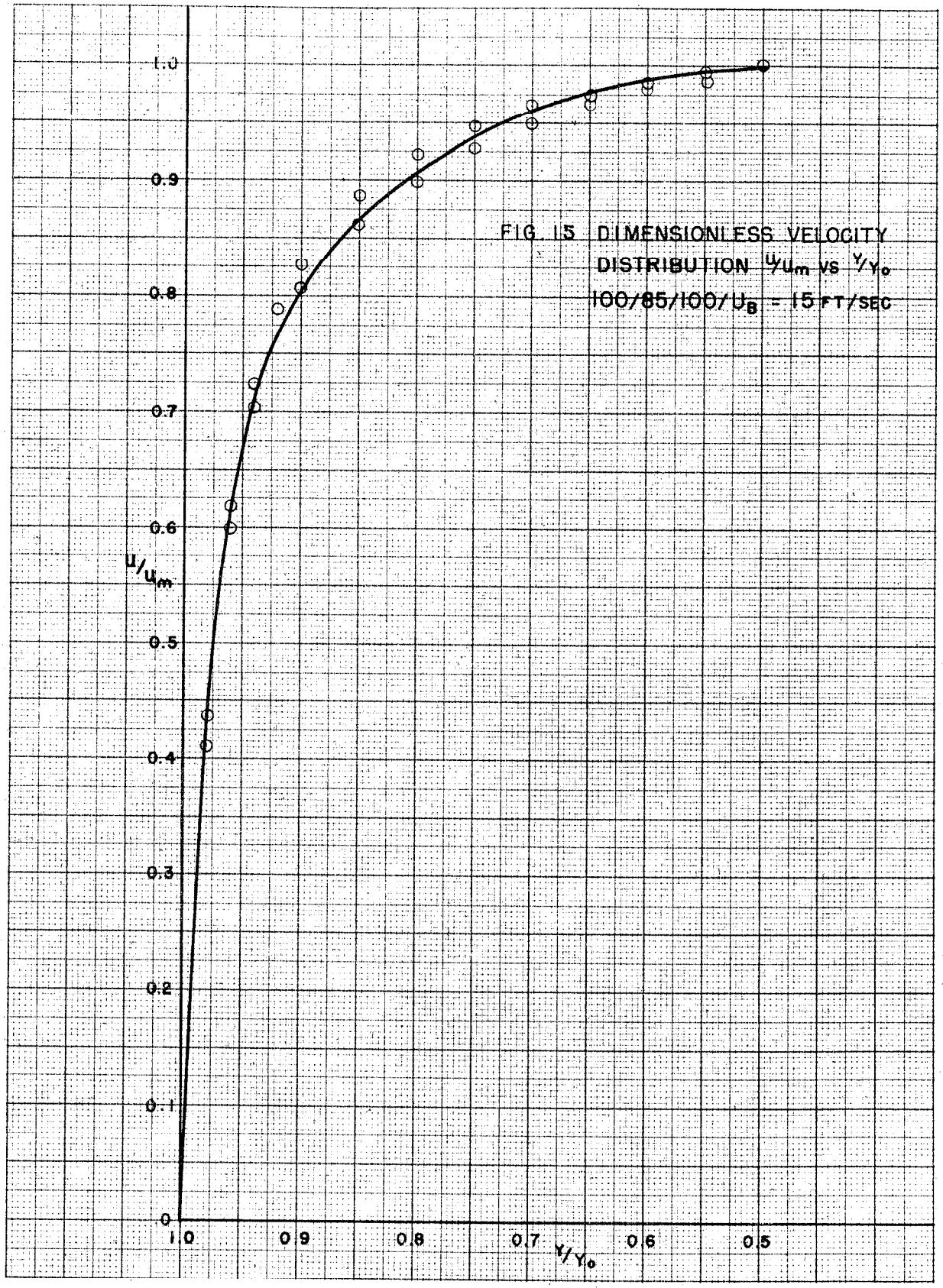

FIG. 15 DIMENSIONLESS VELOCITY DISTRIBUTION u/u_m VS y/y_o 100/85/100/U_B = 15 FT/SEC

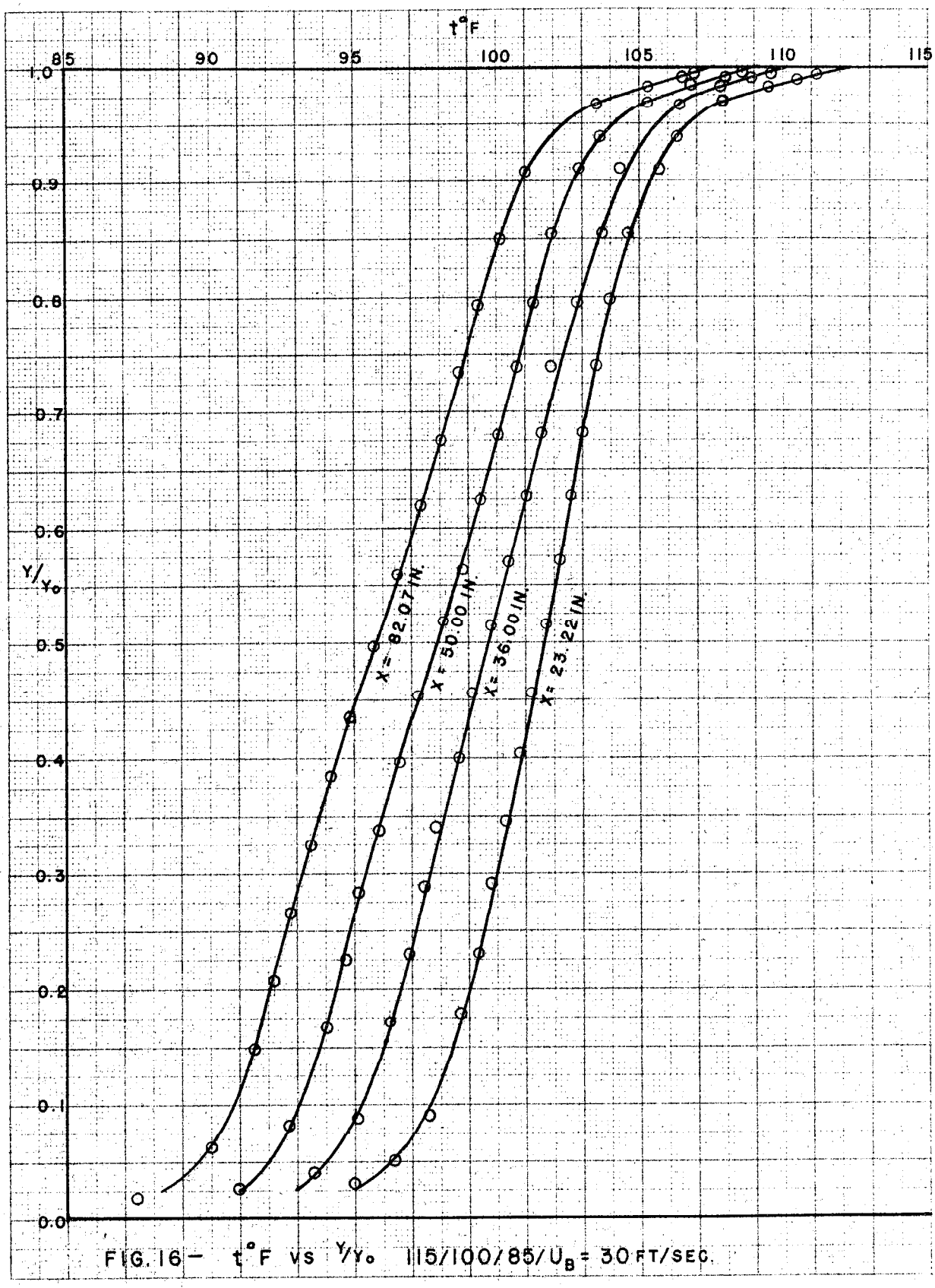

FIG. 16 — $t°F$ vs Y/Y_o $115/100/85/U_B = 30$ FT/SEC.

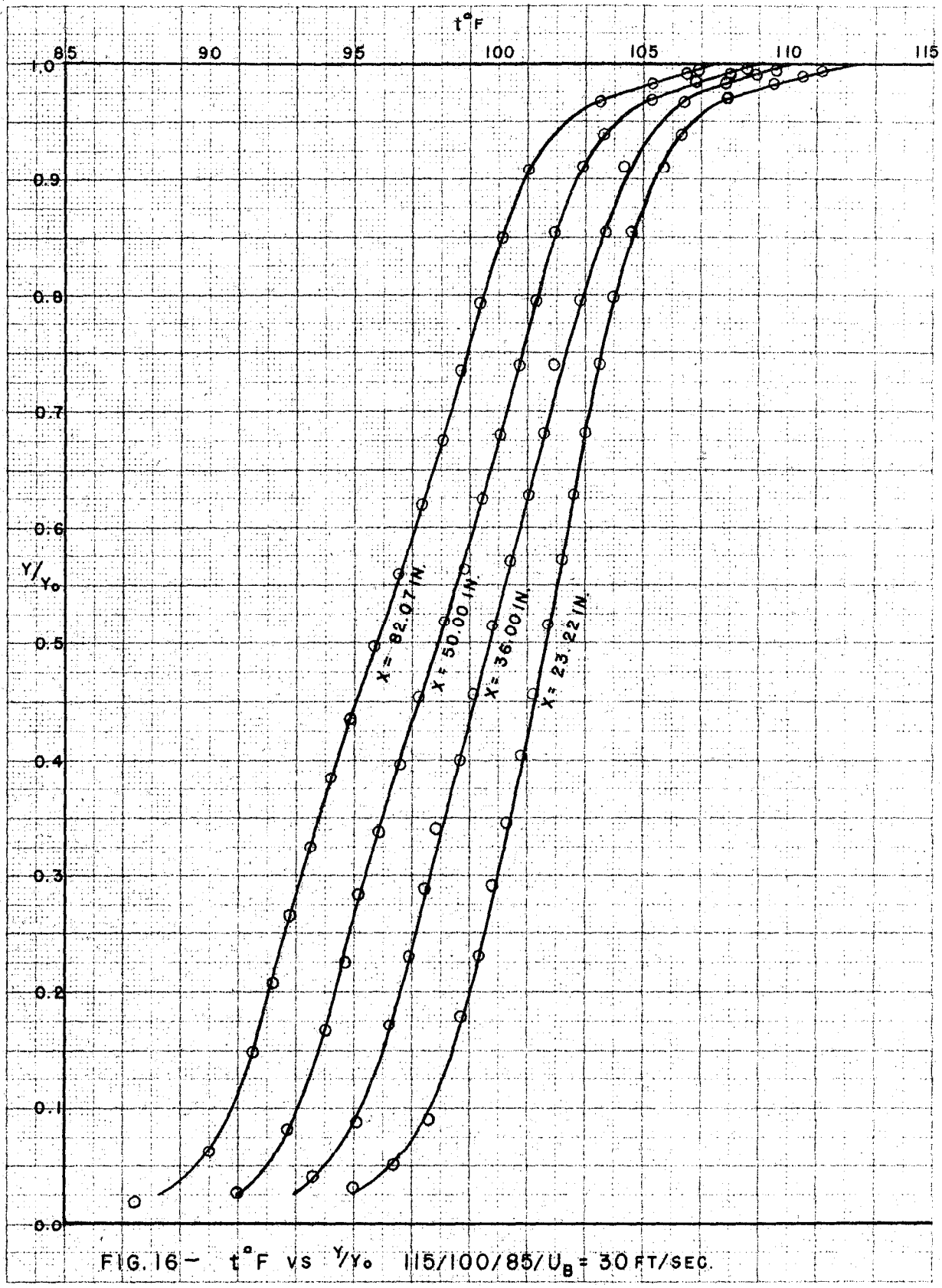

FIG. 16 – $t°F$ vs Y/Y_o 115/100/85/U_B = 30 FT/SEC.

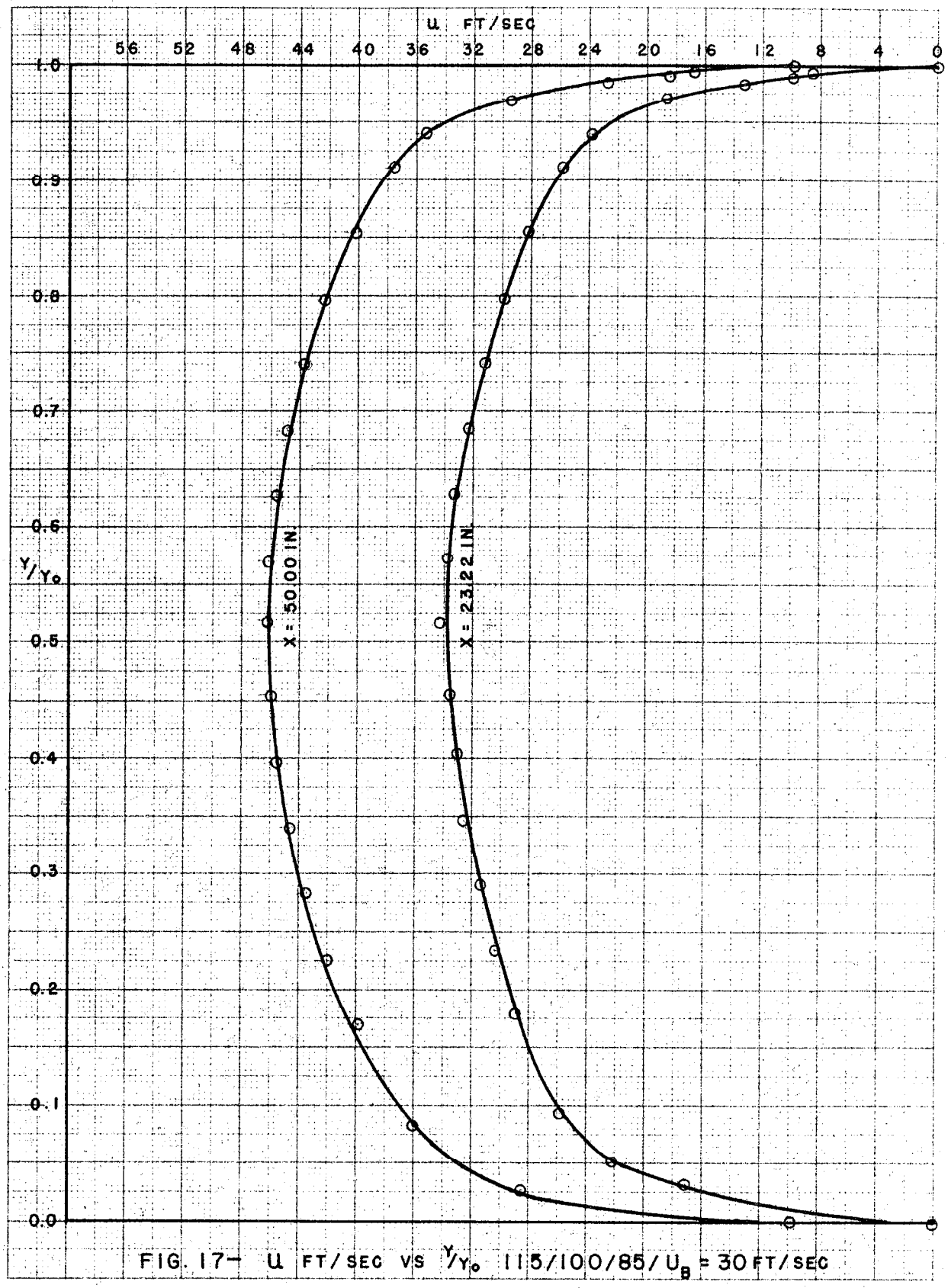

FIG. 17- u FT/SEC VS Y/Y_0 115/100/85/ U_B = 30 FT/SEC

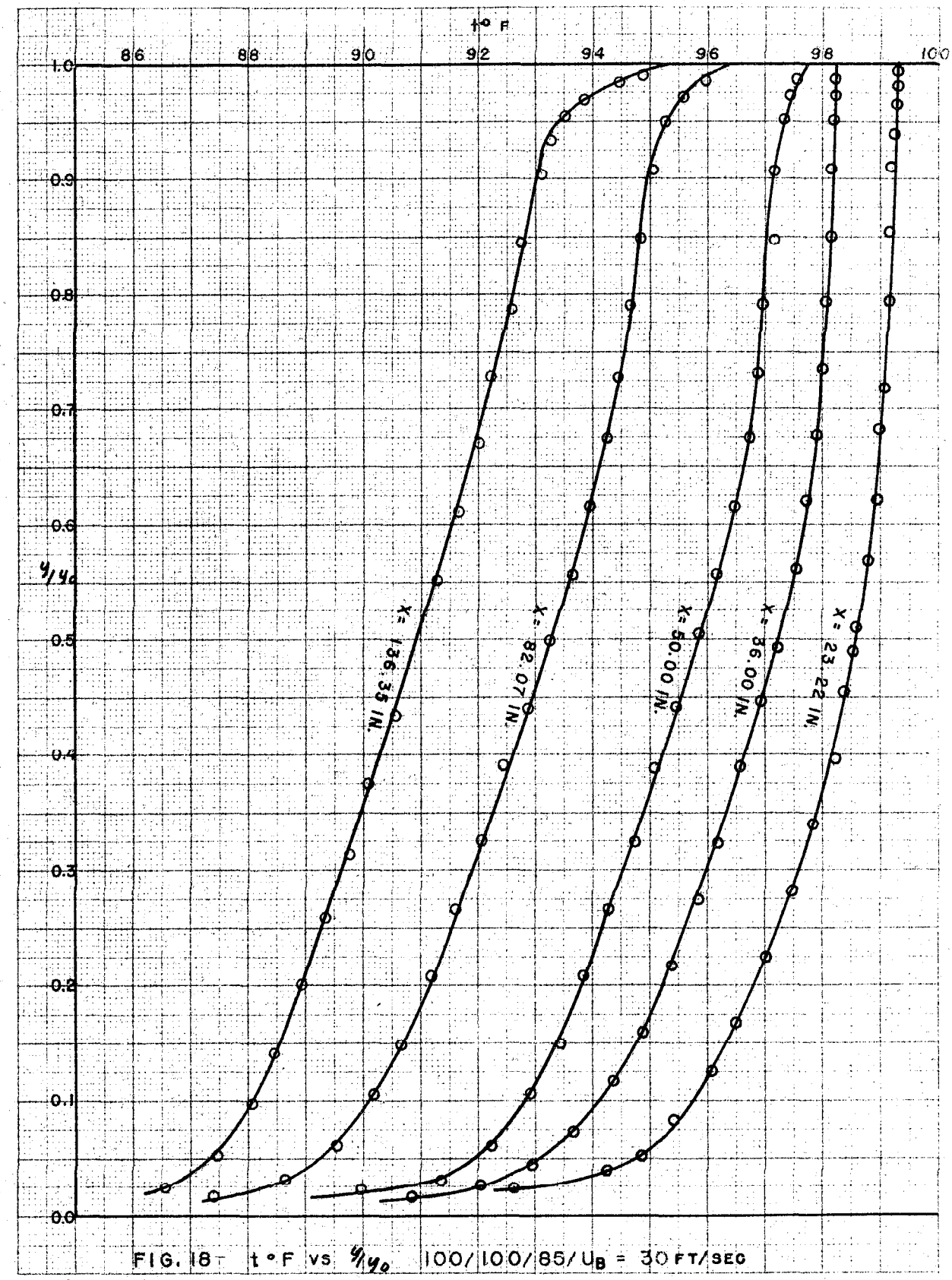

FIG. 18 - t °F vs y/y_0 100/100/85/U_B = 30 FT/SEC

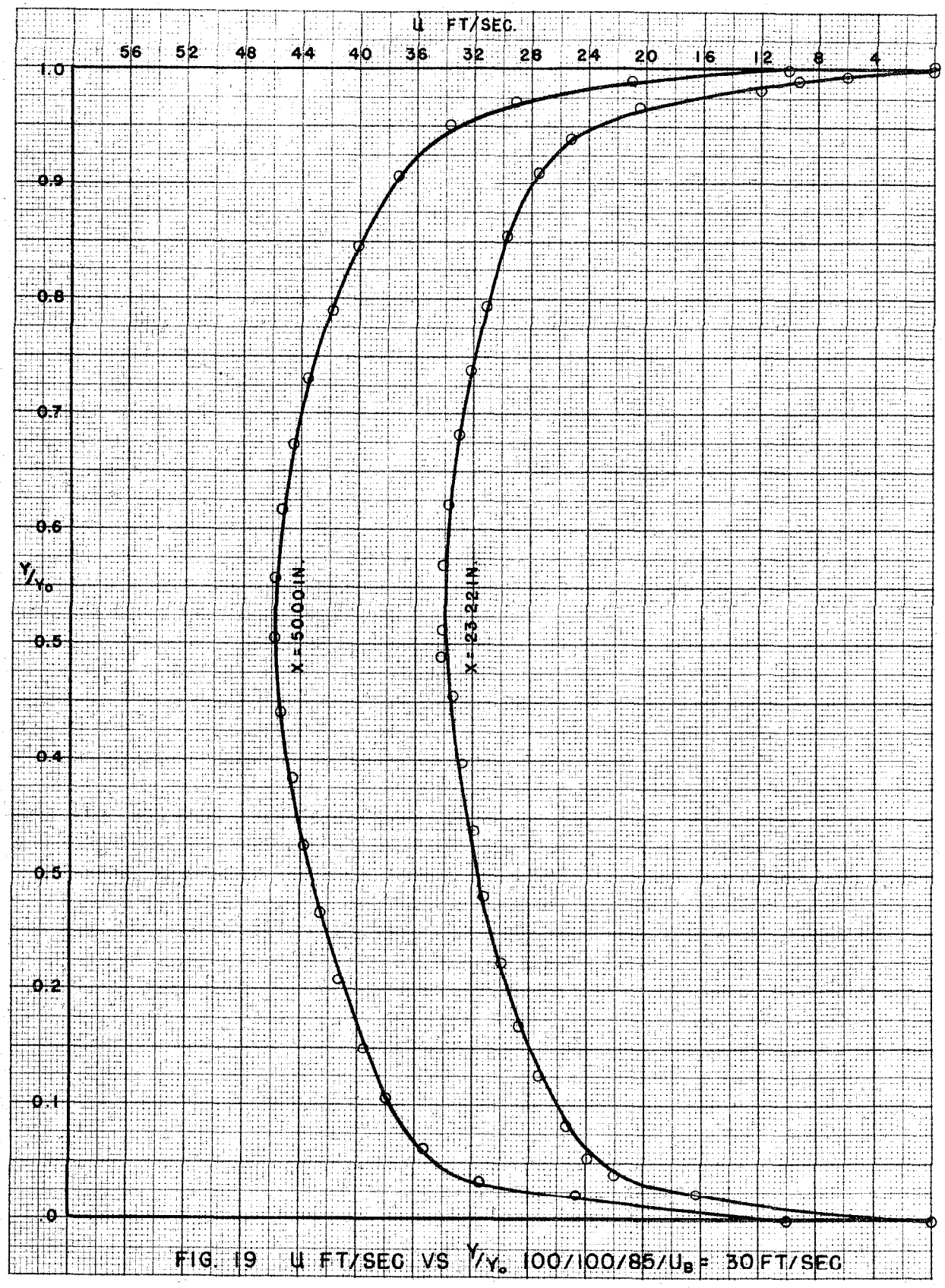

FIG. 19 U FT/SEC VS Y/Y_o 100/100/85/U_B = 30 FT/SEC

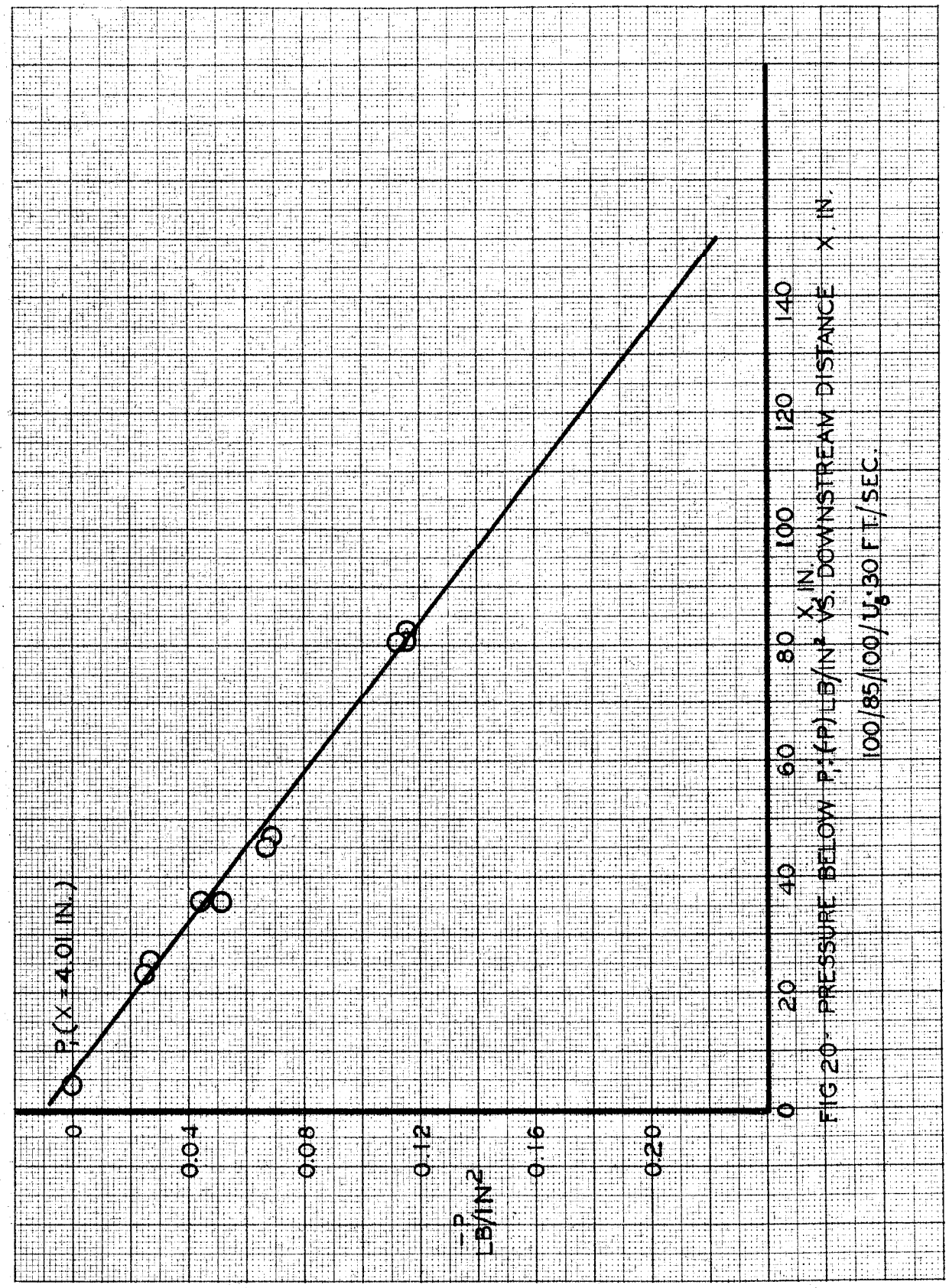

FIG 20- PRESSURE BELOW $P_f(P)$ LB/IN² VS. DOWNSTREAM DISTANCE X, IN.
100/85/100/U_∞ 30 FT./SEC.

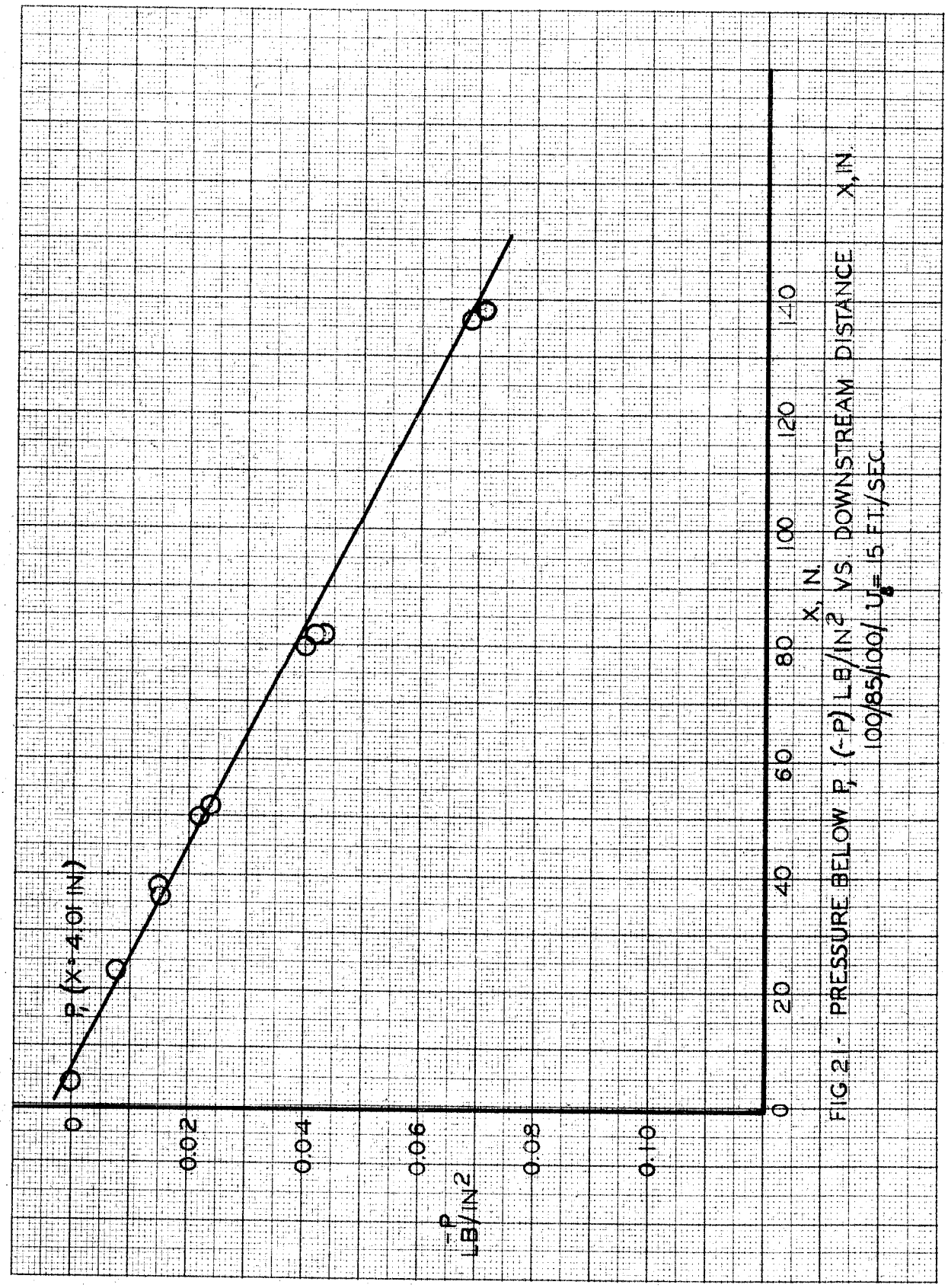

FIG. 21 - PRESSURE BELOW P, (-P) LB/IN^2 VS. DOWNSTREAM DISTANCE X, IN. 100/85/100/ U_∞ = 15 FT/SEC.

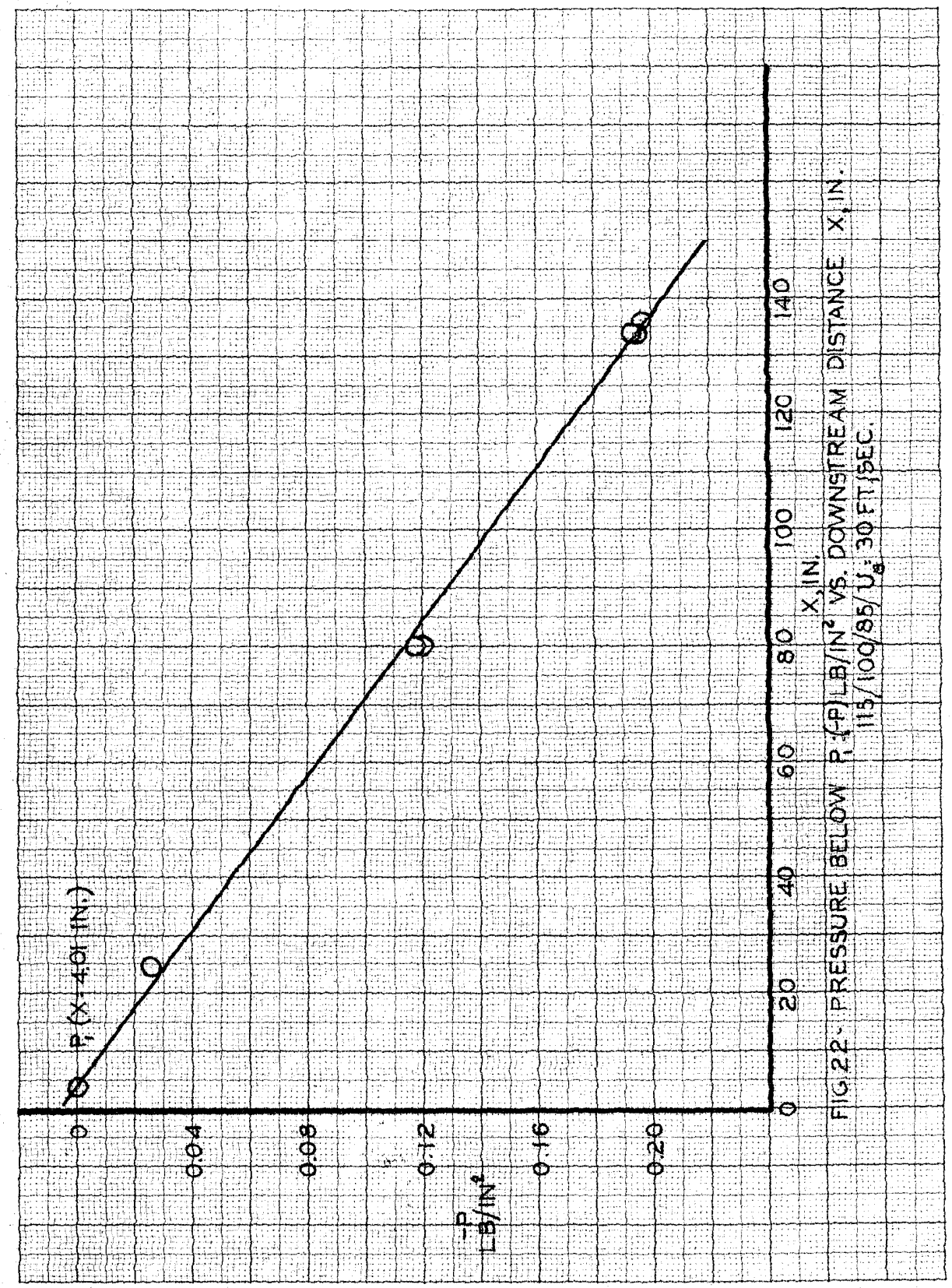

FIG. 22 - PRESSURE BELOW P_1, $-(P)$ LB/IN^2 VS. DOWNSTREAM DISTANCE X, IN.
115/100/85/U_∞ 30 FT/SEC.

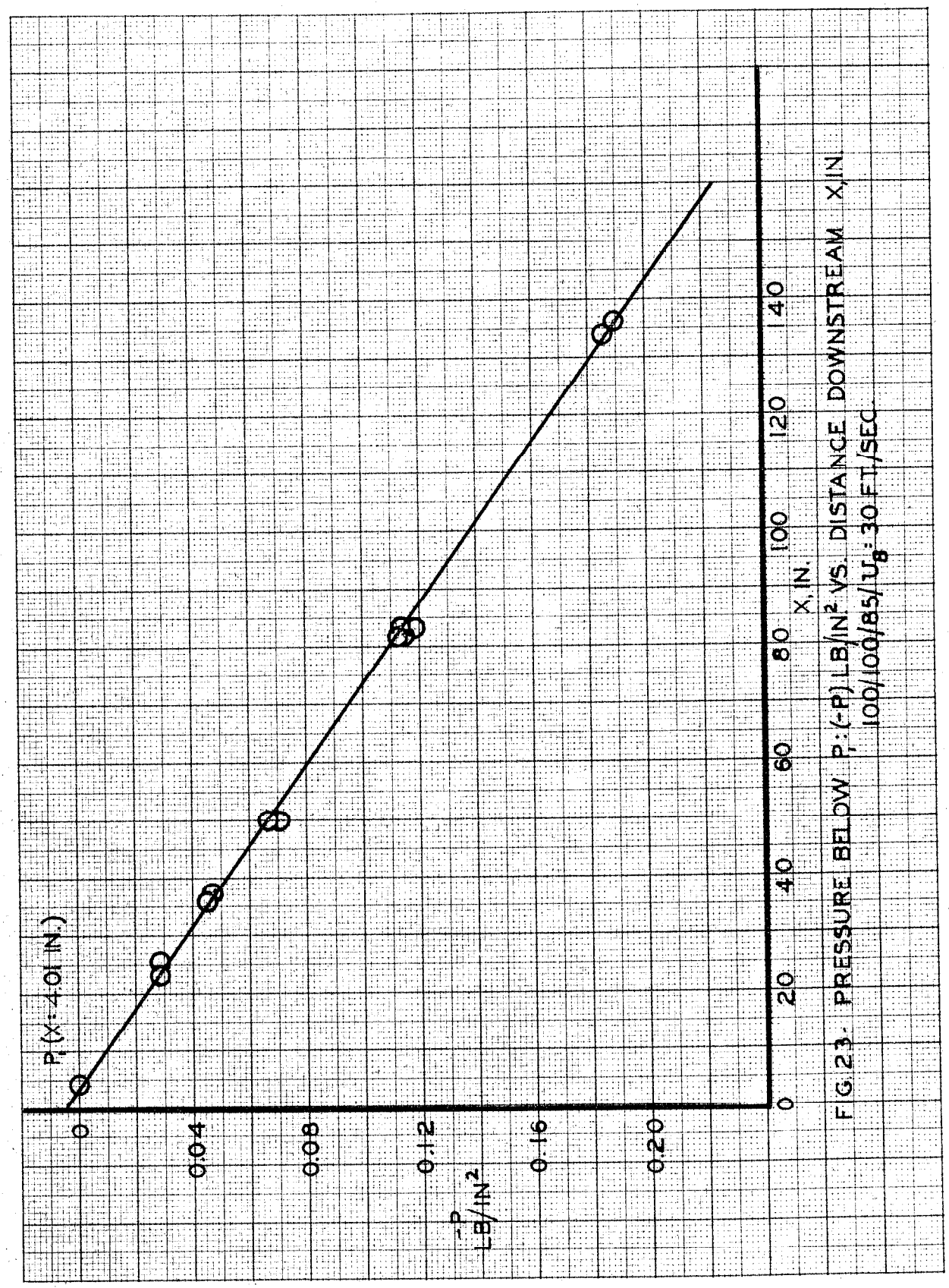

FIG 23- PRESSURE BELOW P_1: $(-P)$ LB/IN^2 VS. DISTANCE DOWNSTREAM X, IN.
100/100/85/U_∞ = 30 FT/SEC

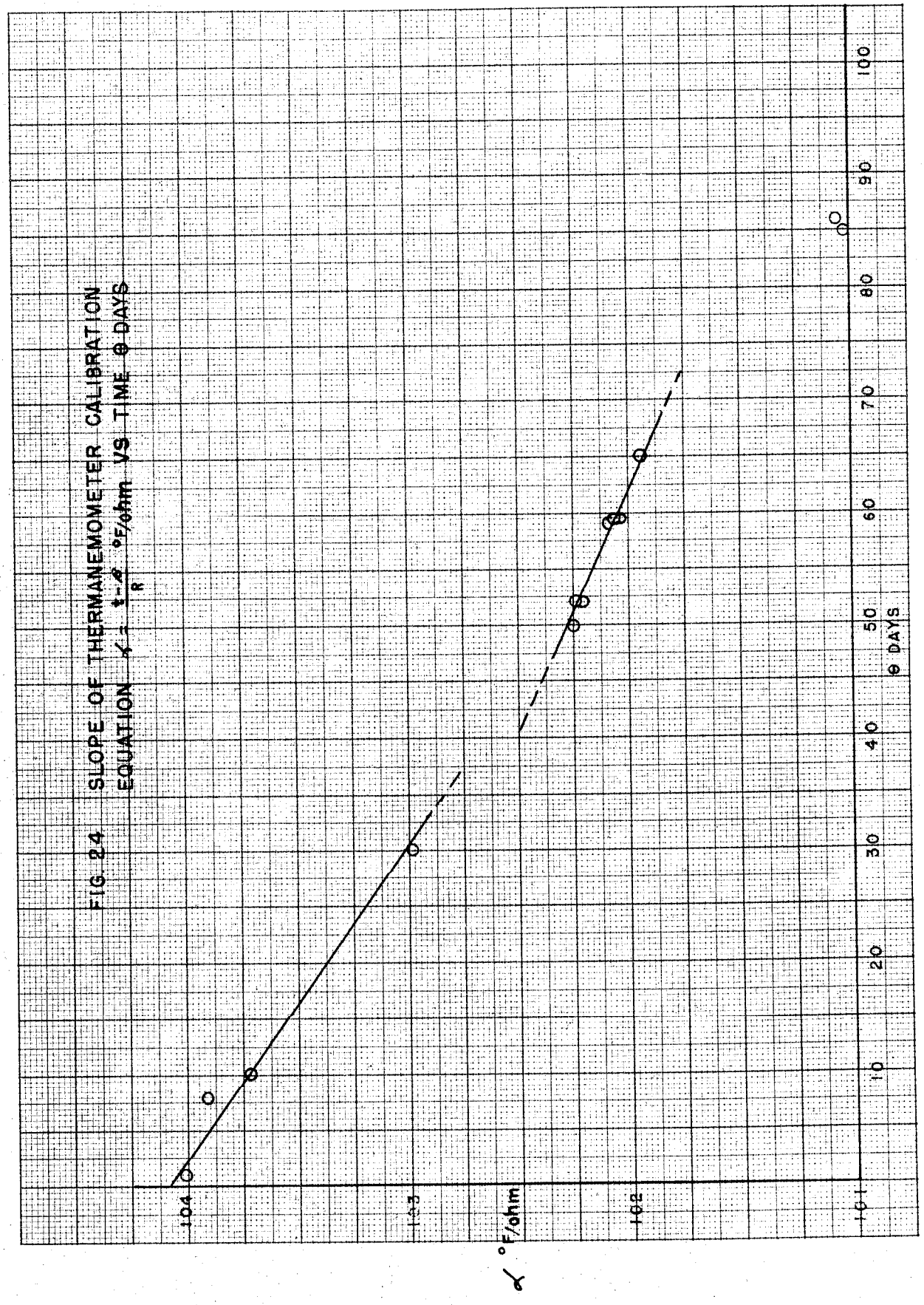
FIG 24 SLOPE OF THERMANEMOMETER CALIBRATION
EQUATION $\gamma = \frac{1-\phi}{R}$ °F/ohm VS TIME Θ DAYS
γ °F/ohm
10⁴
10³
10²
10¹
Θ DAYS
10
20
30
40
50
60
70
80
90
100

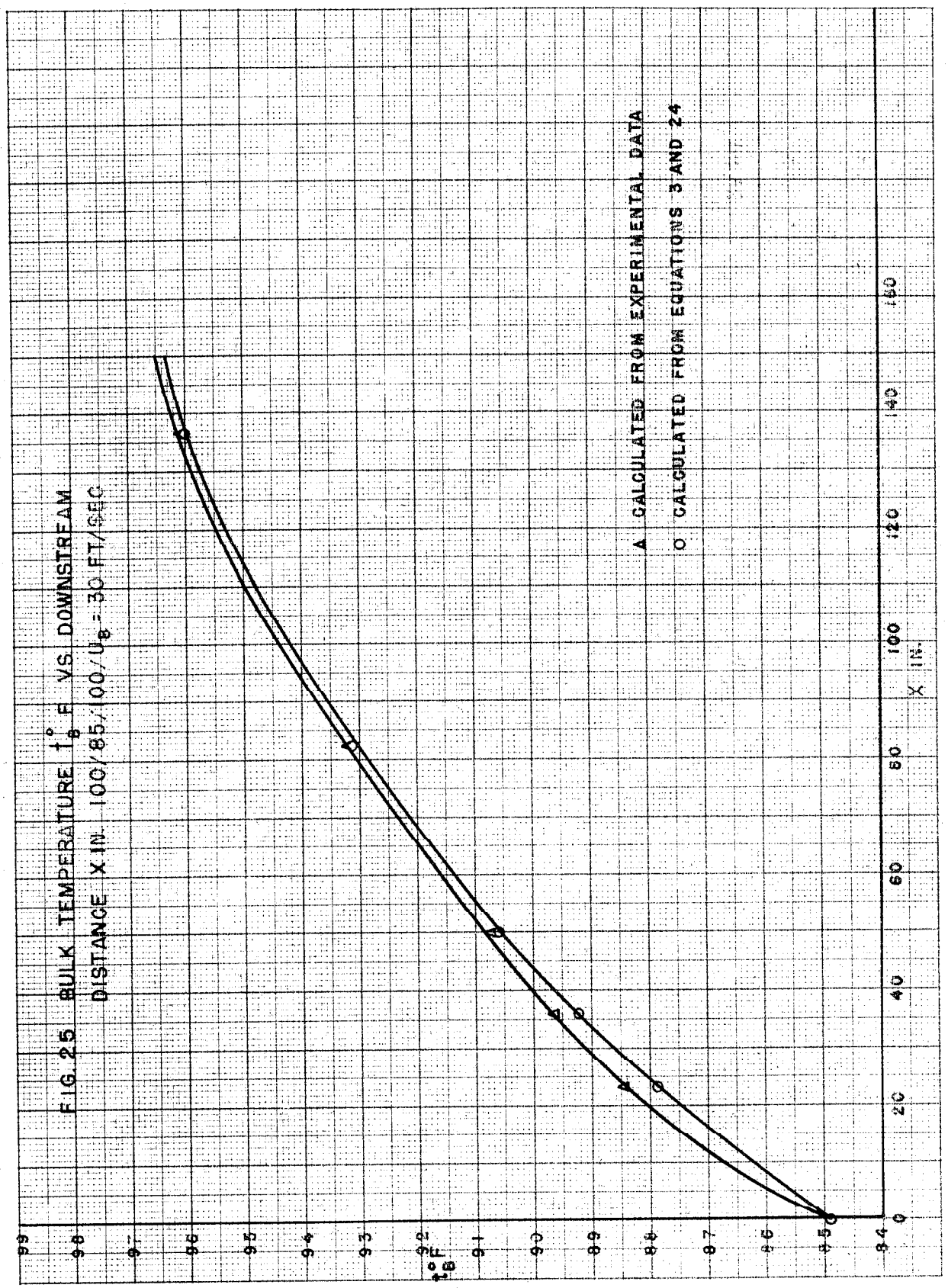
FIG. 25 BULK TEMPERATURE t_B° F VS. DOWNSTREAM DISTANCE X IN. 100/85/100/U_B = 30 FT/SEC
A CALCULATED FROM EXPERIMENTAL DATA
O CALCULATED FROM EQUATIONS 3 AND 24
t_B °F
X IN.
99
98
97
96
95
94
93
92
91
90
89
88
87
86
85
84
0
20
40
60
80
100
120
140
160

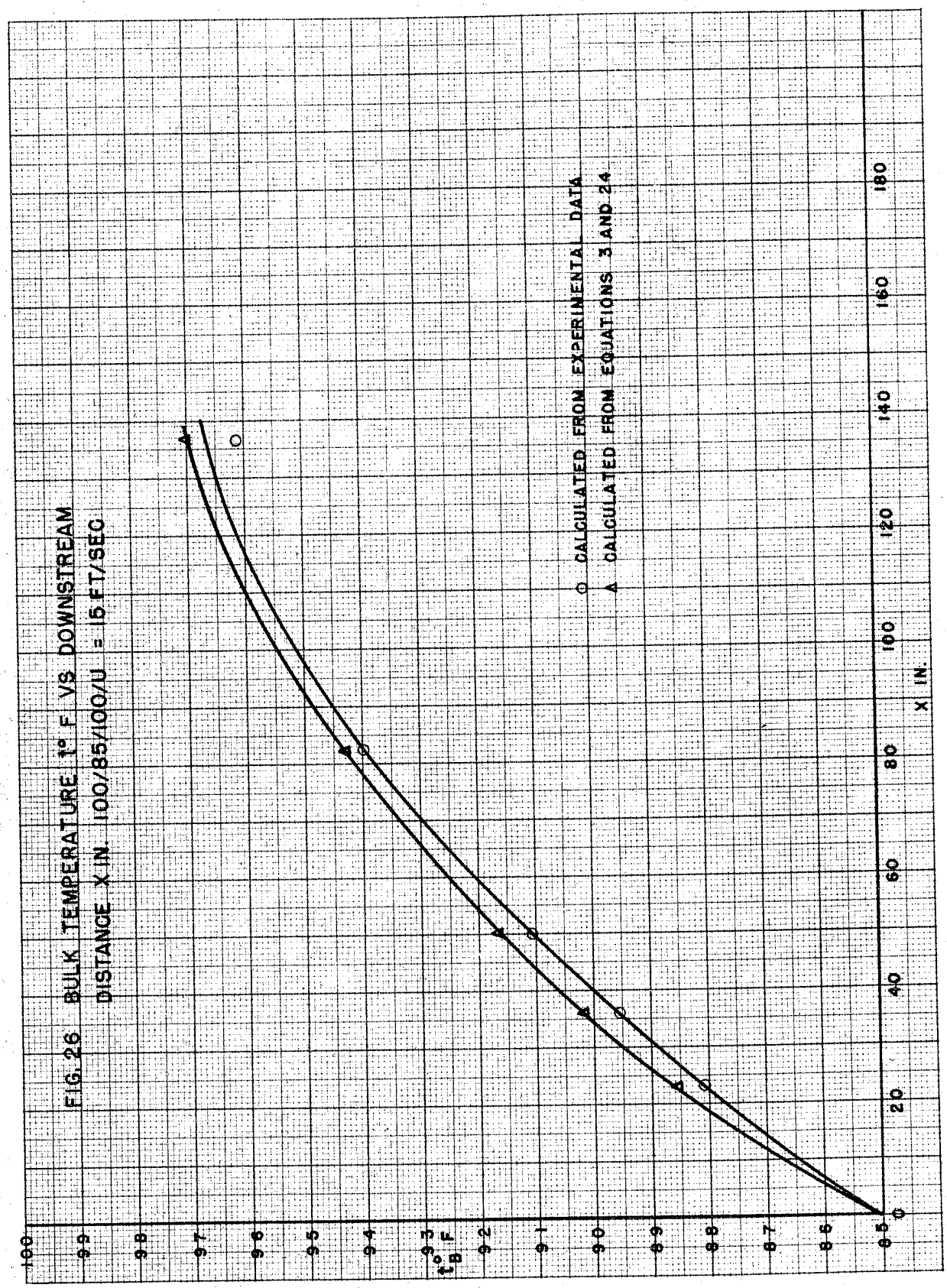
FIG. 26 BULK TEMPERATURE t° F VS DOWNSTREAM DISTANCE X IN. 100/85/100/U = 15 FT/SEC
O CALCULATED FROM EXPERIMENTAL DATA
Δ CALCULATED FROM EQUATIONS 3 AND 24
t°B F
X IN.
100
99
98
97
96
95
94
93
92
91
90
89
88
87
86
85
0
20
40
60
80
100
120
140
160
180

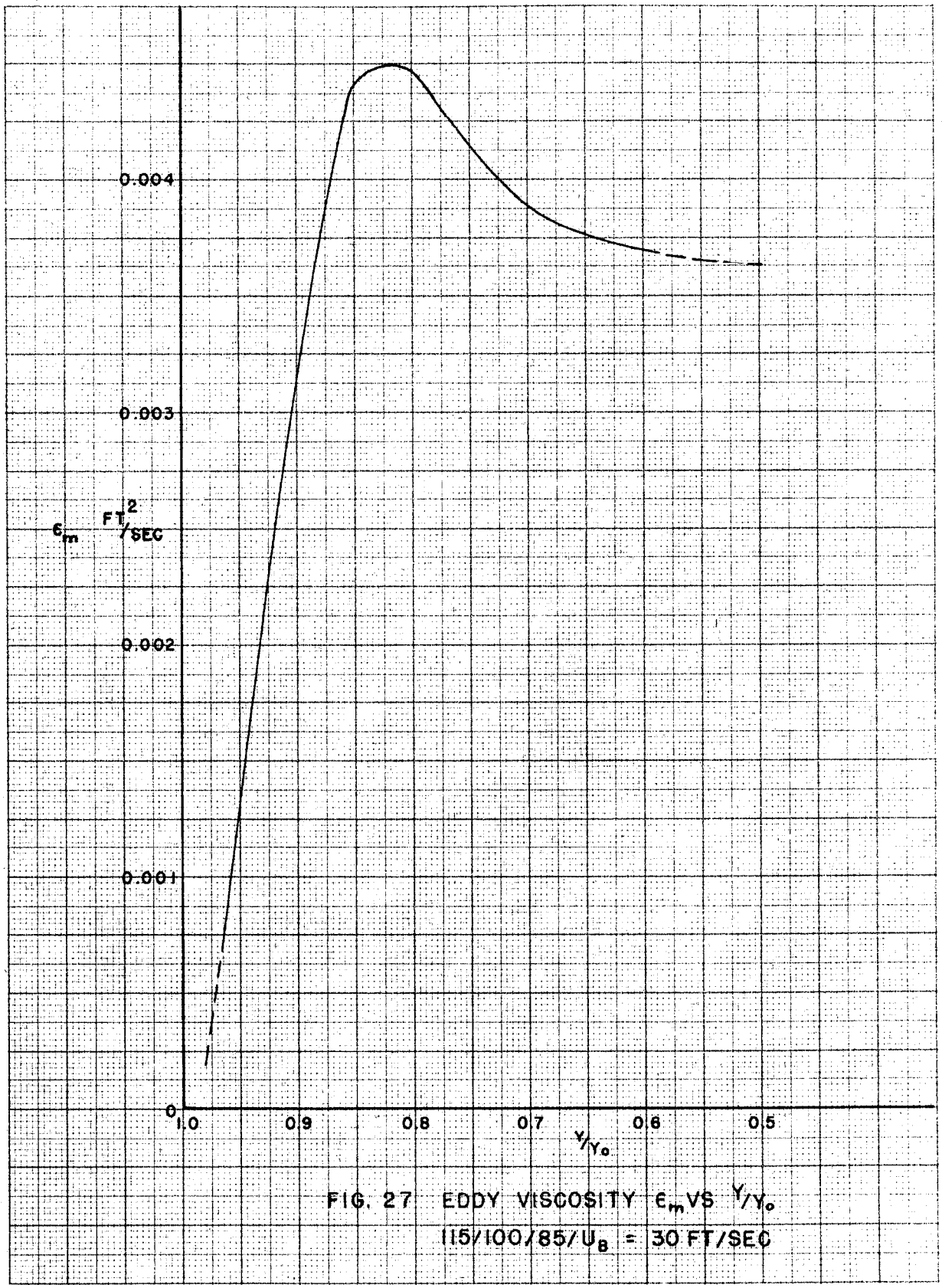

FIG. 27 EDDY VISCOSITY ϵ_m VS Y/Y_o
115/100/85/U_B = 30 FT/SEC

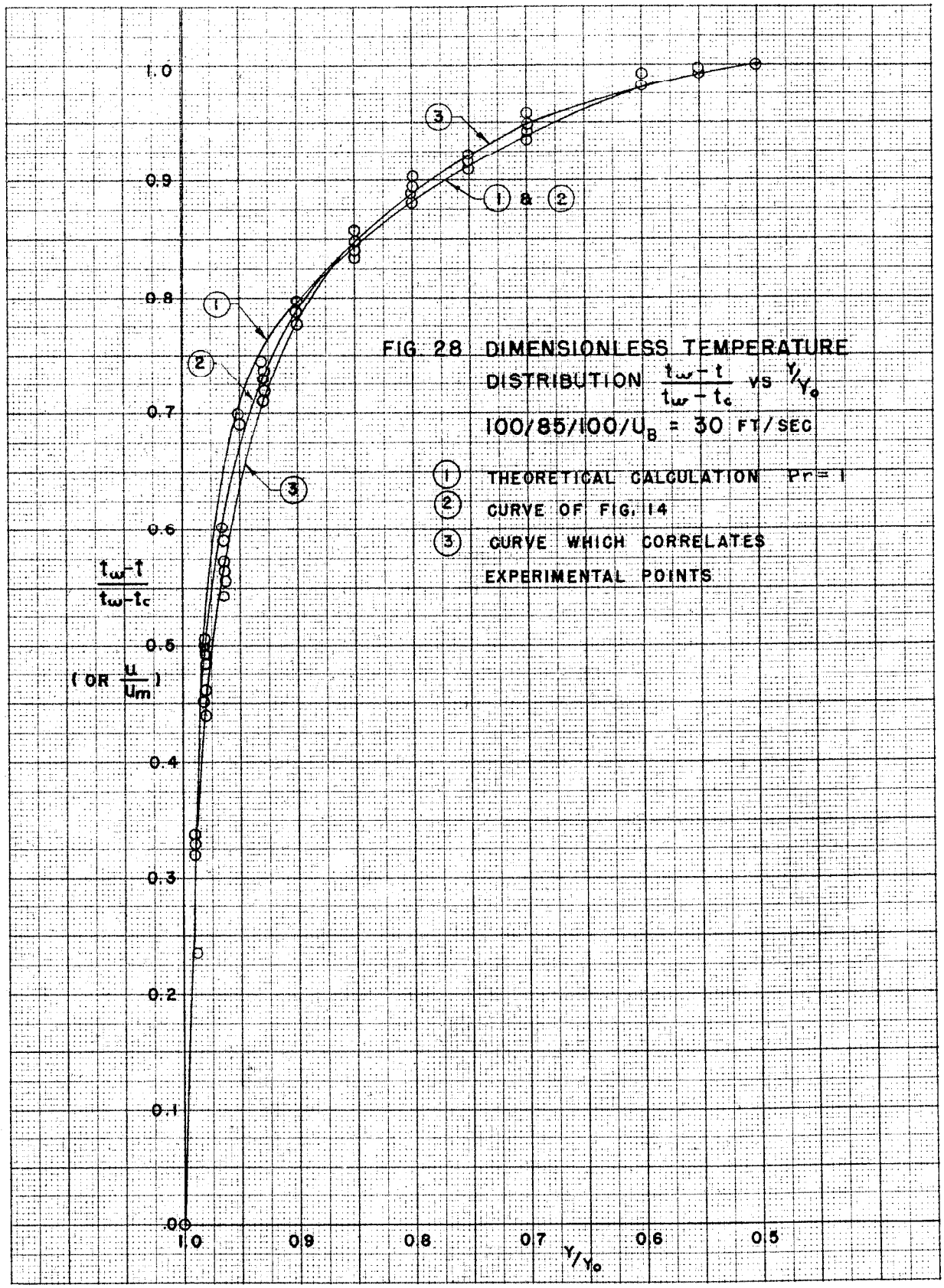

FIG. 28 DIMENSIONLESS TEMPERATURE DISTRIBUTION $\frac{t_\omega - t}{t_\omega - t_c}$ VS Y/Y_o

100/85/100/U_B = 30 FT/SEC

(1) THEORETICAL CALCULATION Pr = 1

(2) CURVE OF FIG. 14

(3) CURVE WHICH CORRELATES EXPERIMENTAL POINTS

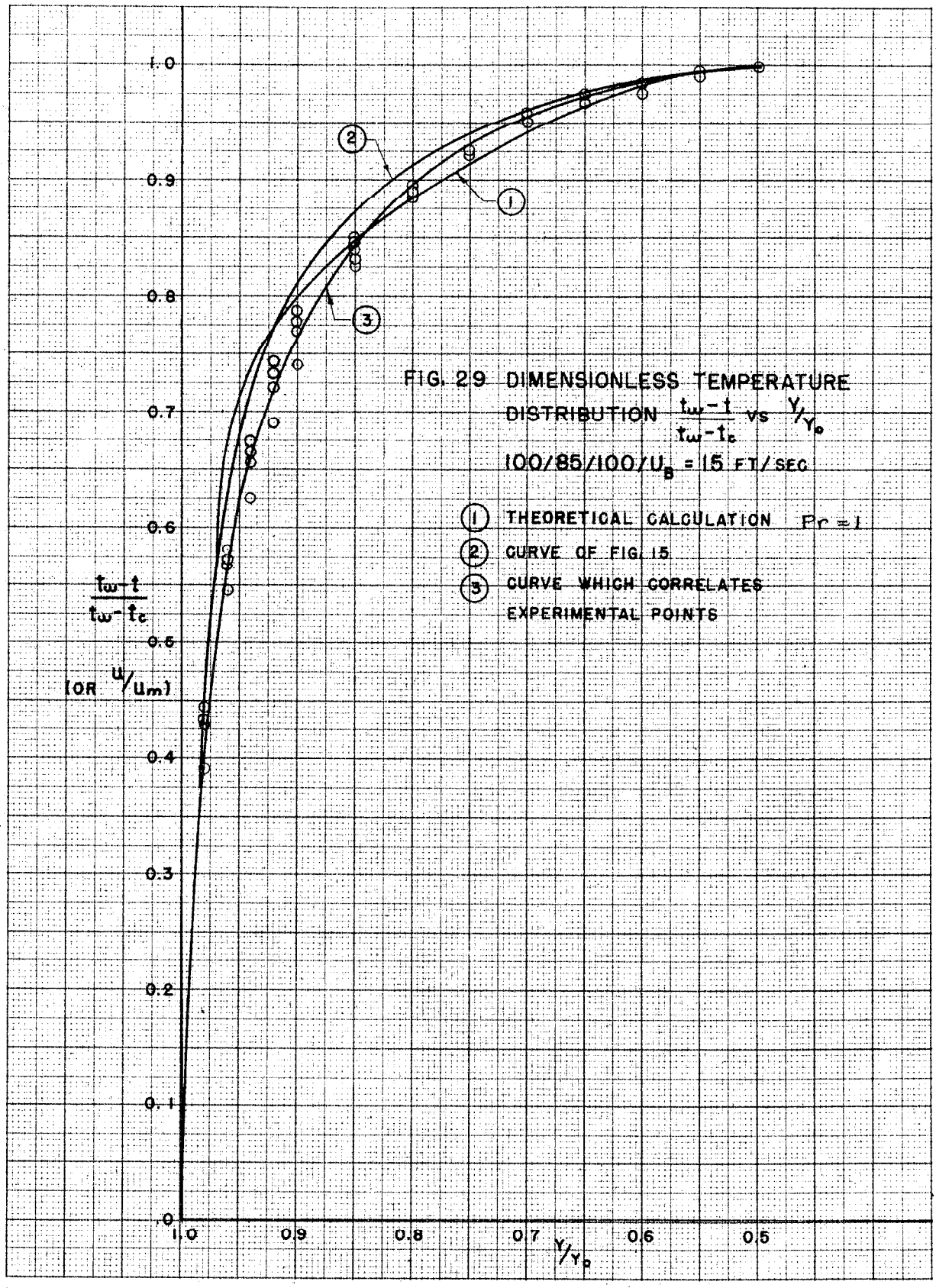

FIG. 29 DIMENSIONLESS TEMPERATURE DISTRIBUTION $\frac{t_w - t}{t_w - t_c}$ VS Y/Y_o

100/85/100/U_B = 15 FT/SEC

(1) THEORETICAL CALCULATION Pr = 1

(2) CURVE OF FIG. 15

(3) CURVE WHICH CORRELATES EXPERIMENTAL POINTS

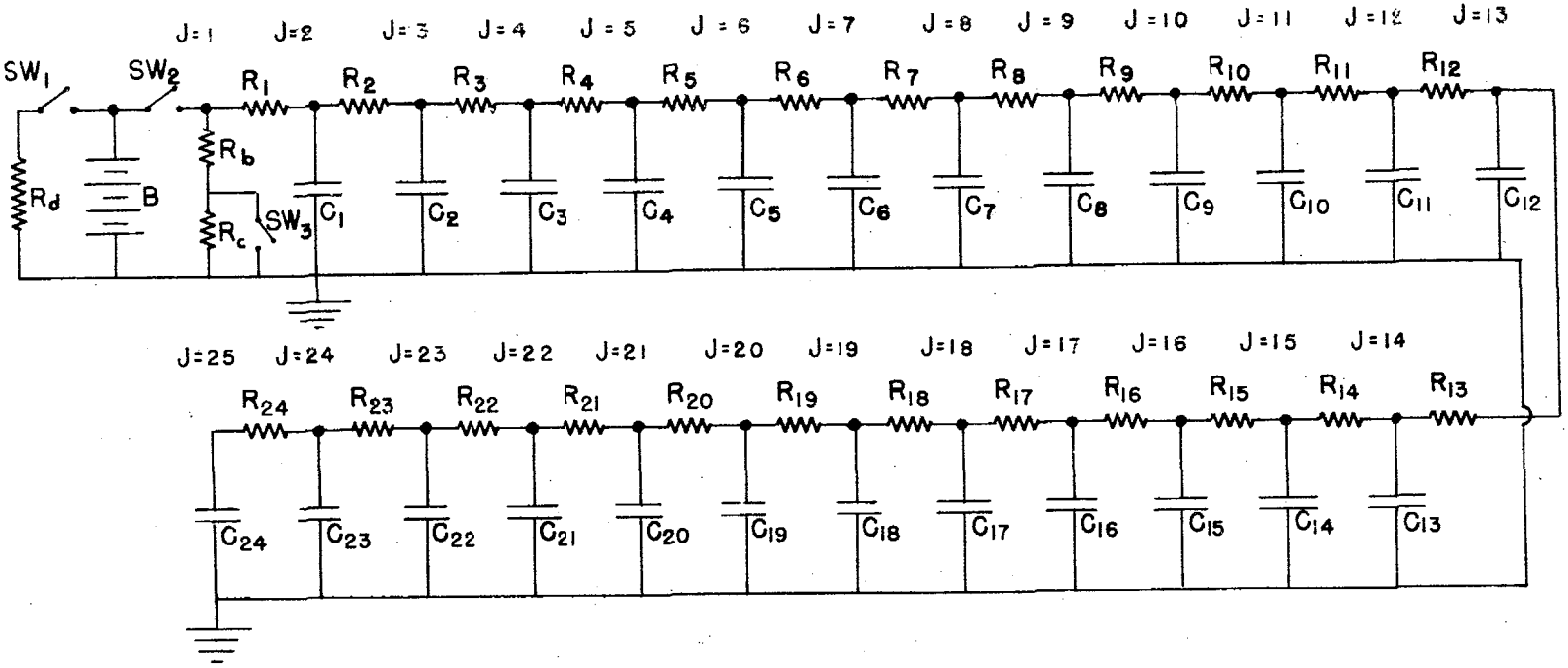

LEGEND:

$R_1, R_2 \ldots R_{24} = \Delta R = 136$ ohms
$C_1 = 0.01$ mfd
$C_2 = 0.02$
$C_3 = 0.03$
$C_4 = 0.04$
$C_5 = 0.07$
$C_6 = 0.11$
$C_7 = 0.25$
$C_8 = 0.38$
$C_9 = 0.56$
$C_{10} = 0.81$
$C_{11} = 1.12$
$C_{12} = 1.58$
$C_{13} = 2.15$
$C_{14} = 2.76$
$C_{15} = 3.34$
$C_{16} = 3.70$
$C_{17} = 3.96$
$C_{18} = 3.84$
$C_{19} = 3.69$
$C_{20} = 3.48$
$C_{21} = 3.28$
$C_{22} = 3.15$
$C_{23} = 1.56$
J = 1,2.....25 CIRCUIT JUNCTION POINTS
J = 1 ~ WALL OF CHANNEL
J = 25~MIDSTREAM OF CHANNEL

FIG. 30 CIRCUIT DIAGRAM, ANALOG EQUIPMENT

FIG. 31 EDDY CONDUCTIVITY ϵ_c FT^2/SEC VS Y/Y_a
(TEST 40 UNIFORM FLOW)

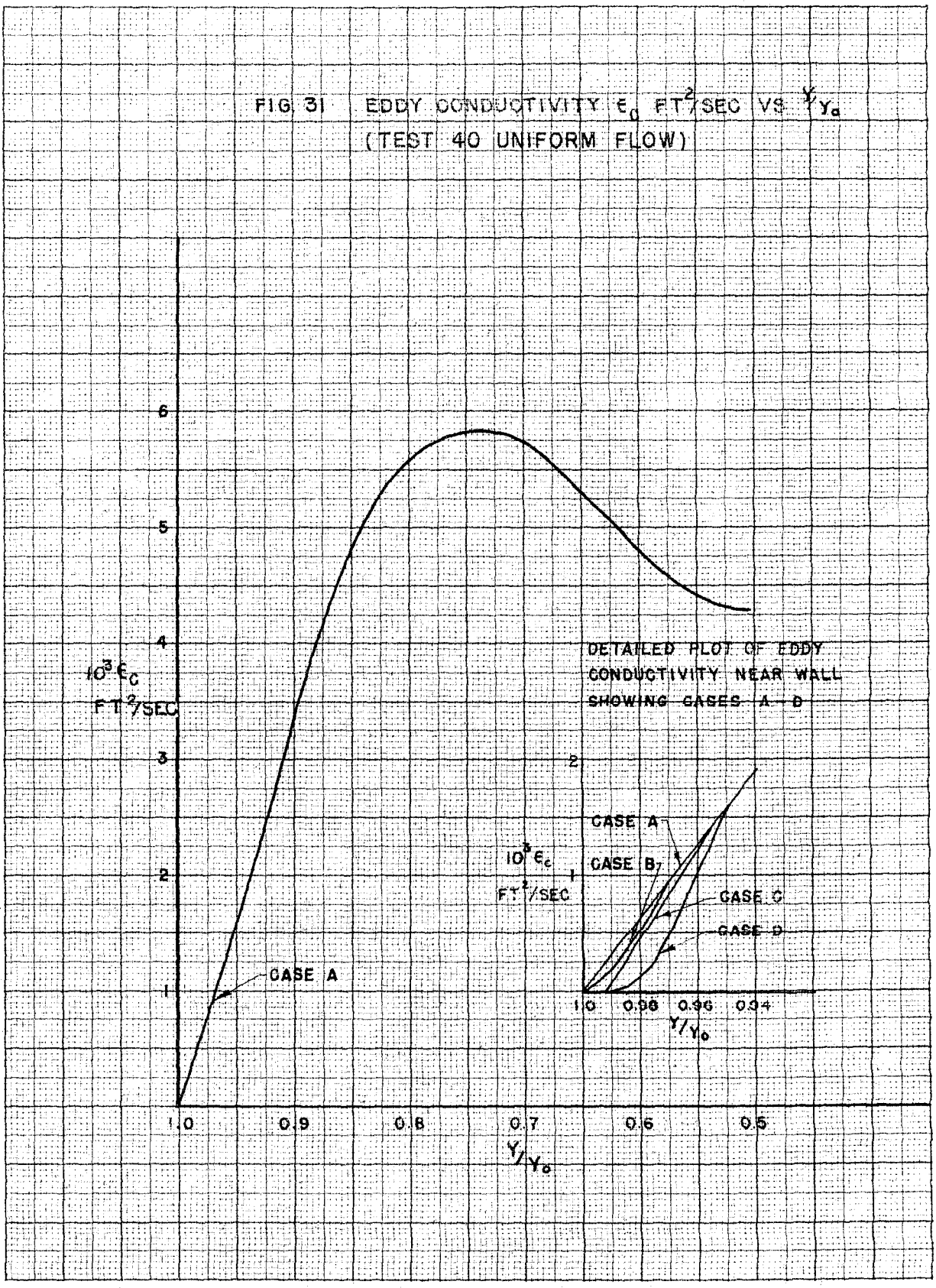

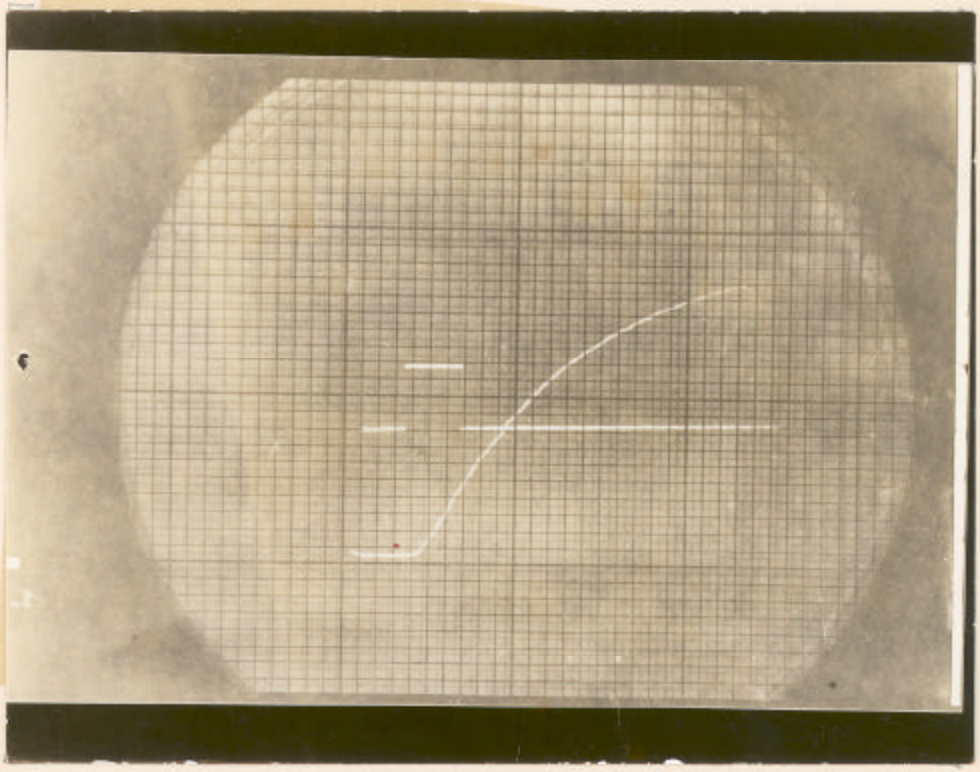

Fig. 32. Oscilloscope Trace, E vs. θ , $y/y_o = 0.5$

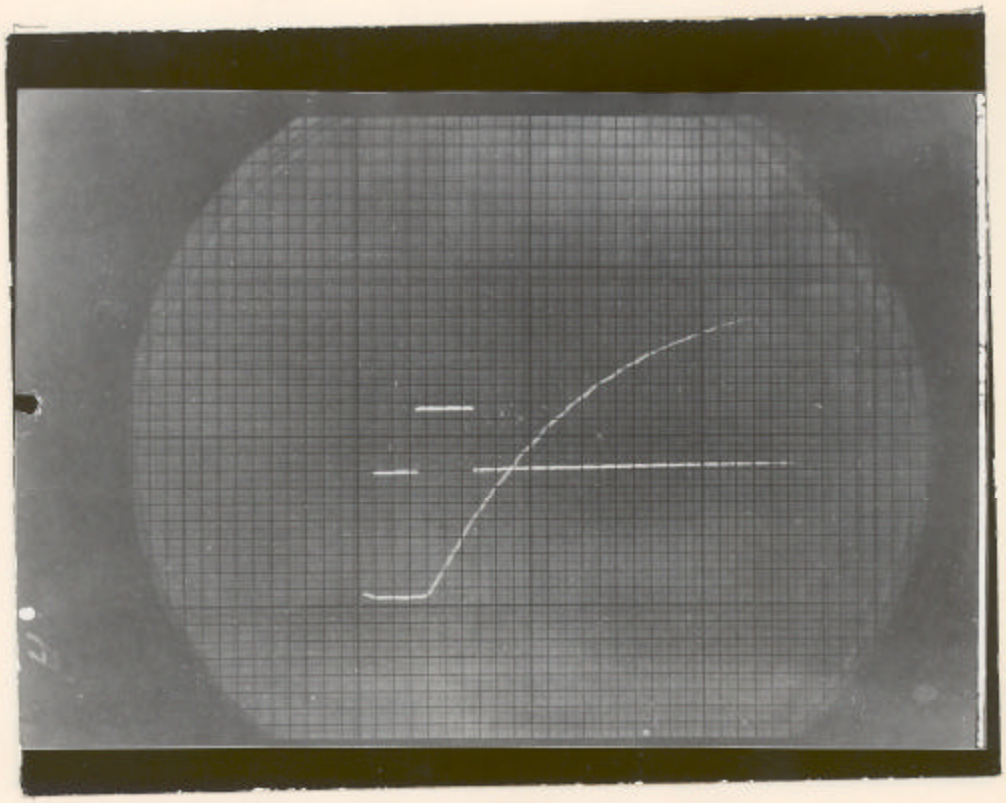

Fig. 33. Oscilloscope Trace, E vs. θ , $y/y_o = 0.643$

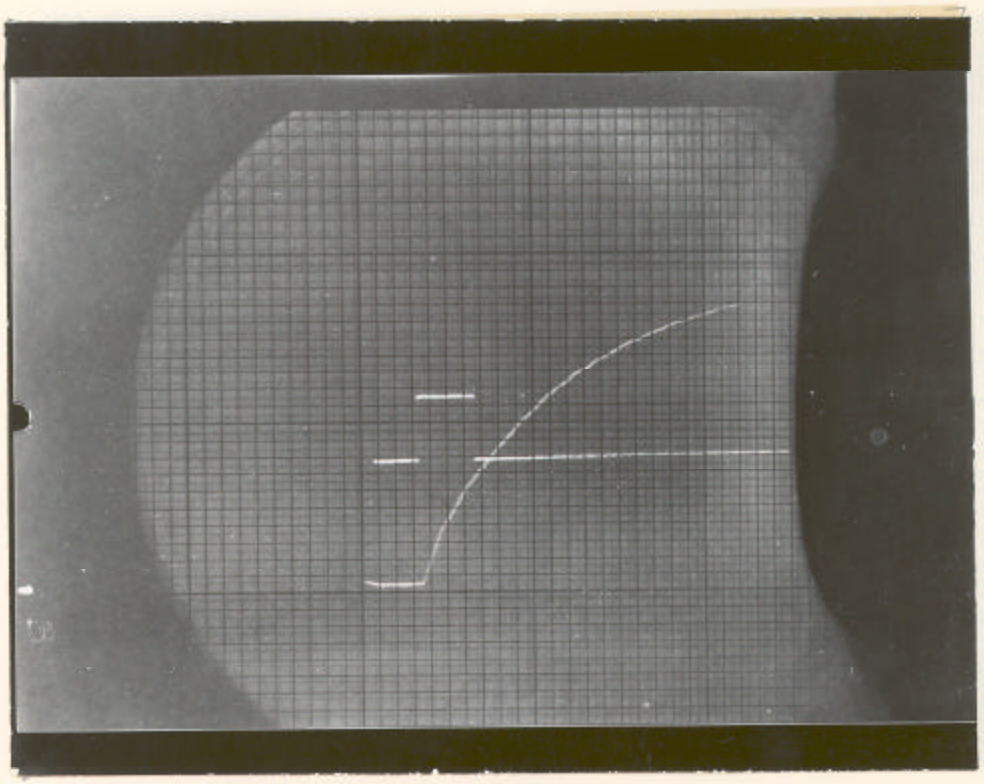

Fig. 34. Oscilloscope Trace, E vs. θ , $y/y_o = 0.821$

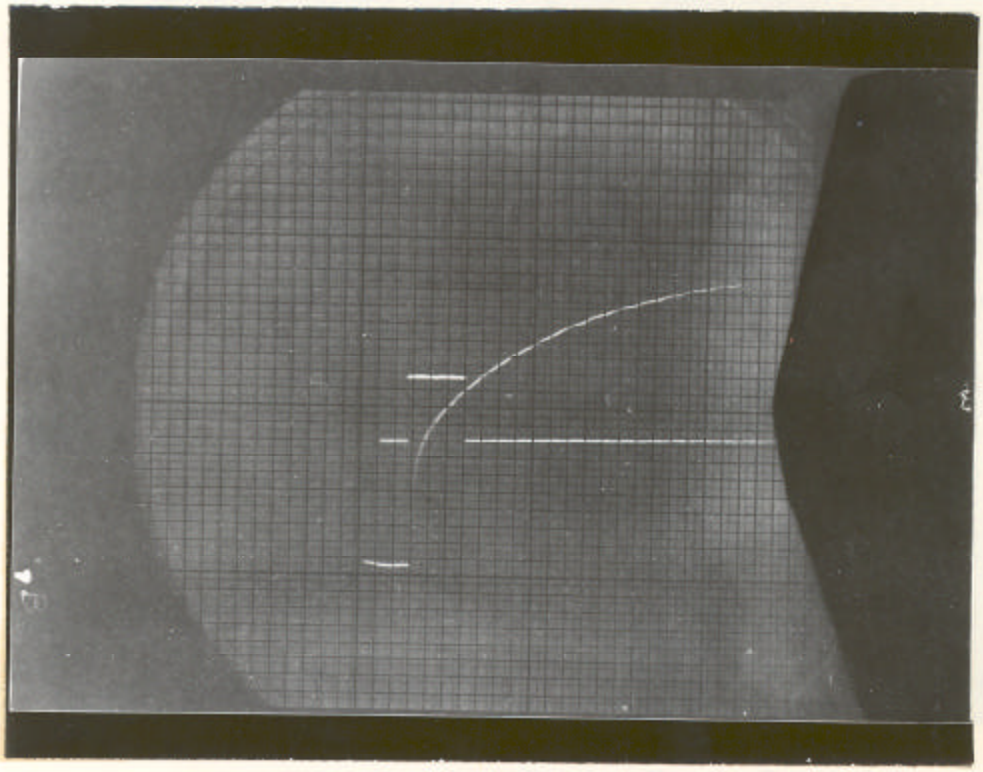

Fig. 35. Oscilloscope Trace, E vs. θ, $y/y_o = 0.964$

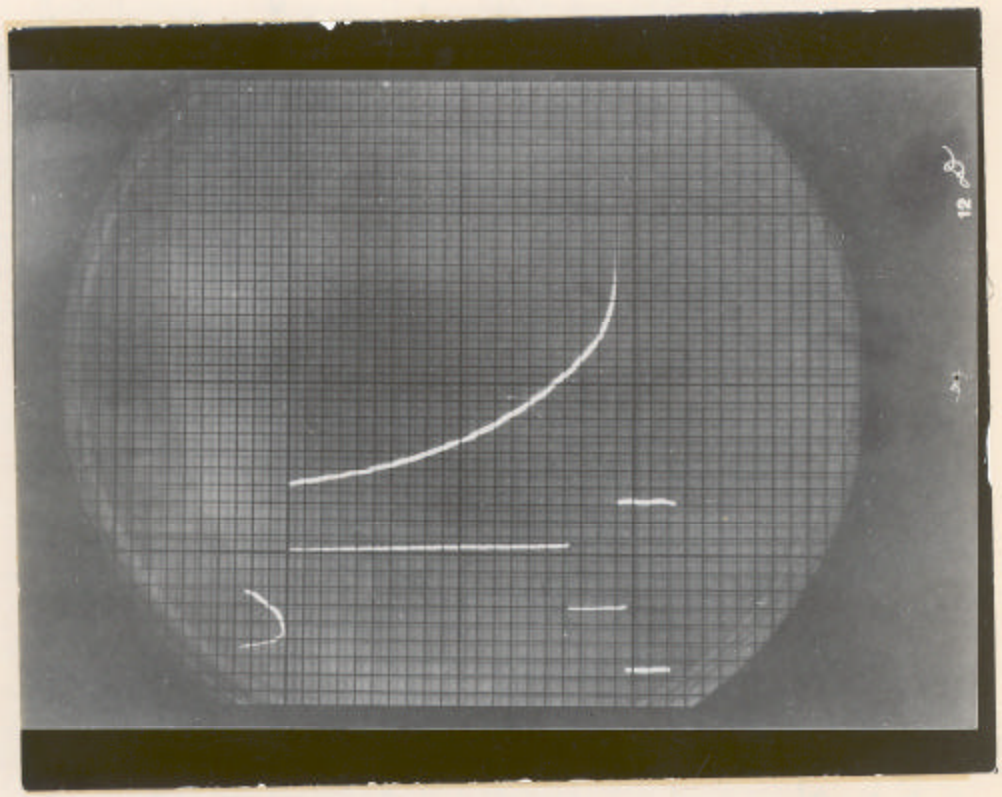

Fig. 36. Oscilloscope Trace, E_{12} vs. θ

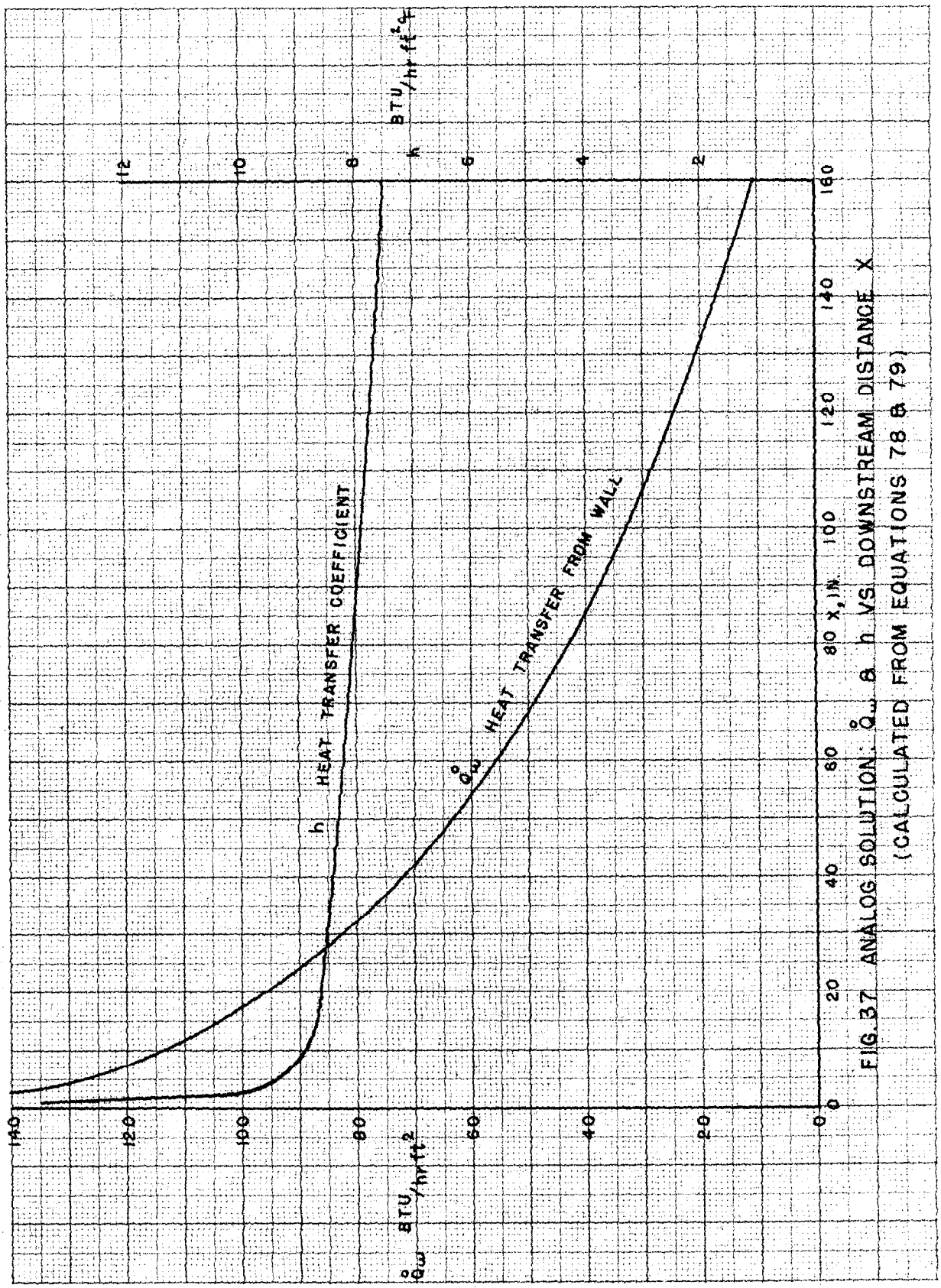

FIG. 37 ANALOG SOLUTION: $\dot{Q}_w$ & h VS DOWNSTREAM DISTANCE X
(CALCULATED FROM EQUATIONS 78 & 79)

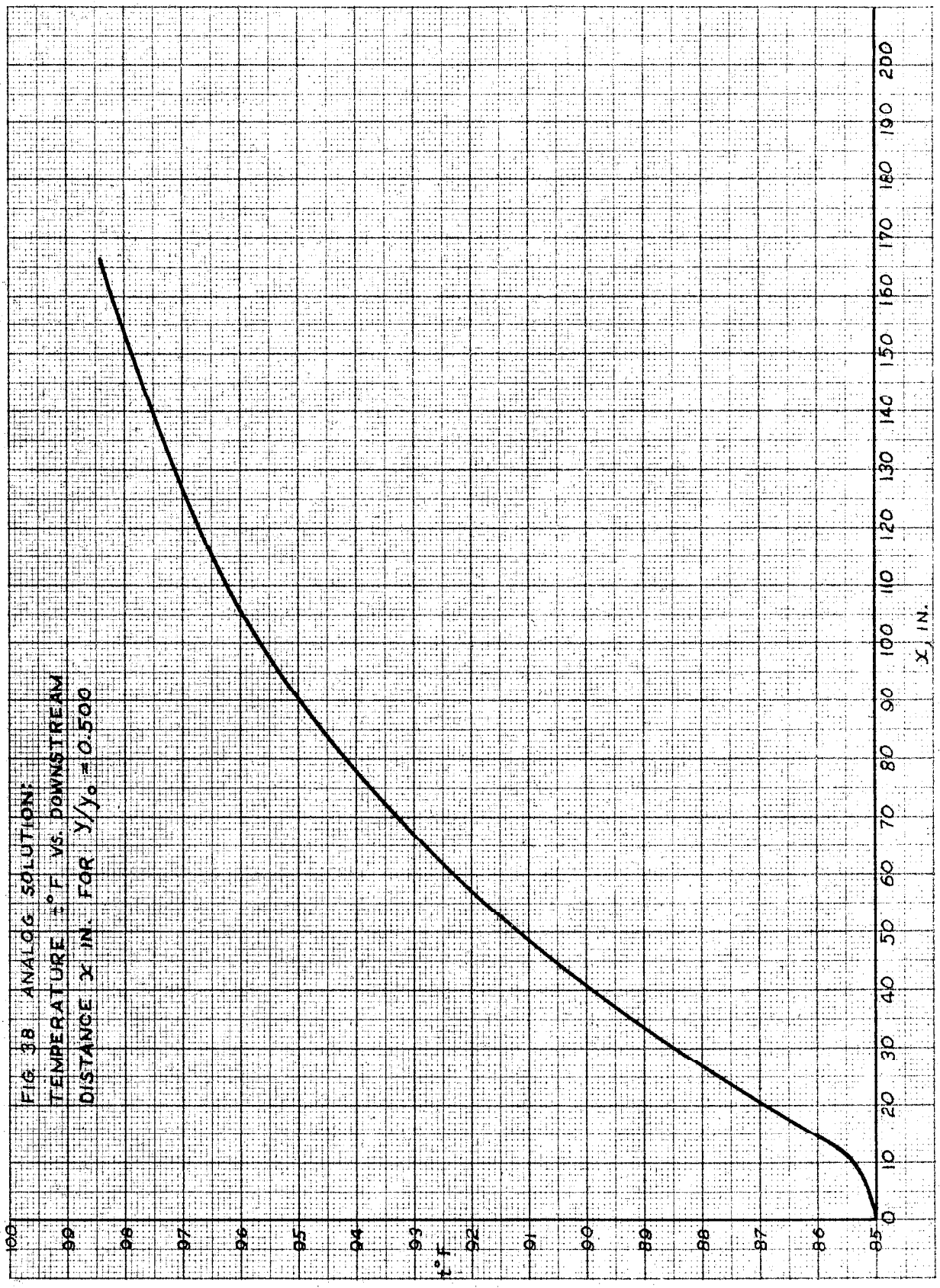

FIG. 38 ANALOG SOLUTION:
TEMPERATURE t°F VS. DOWNSTREAM
DISTANCE X IN. FOR $Y/Y_o = 0.500$

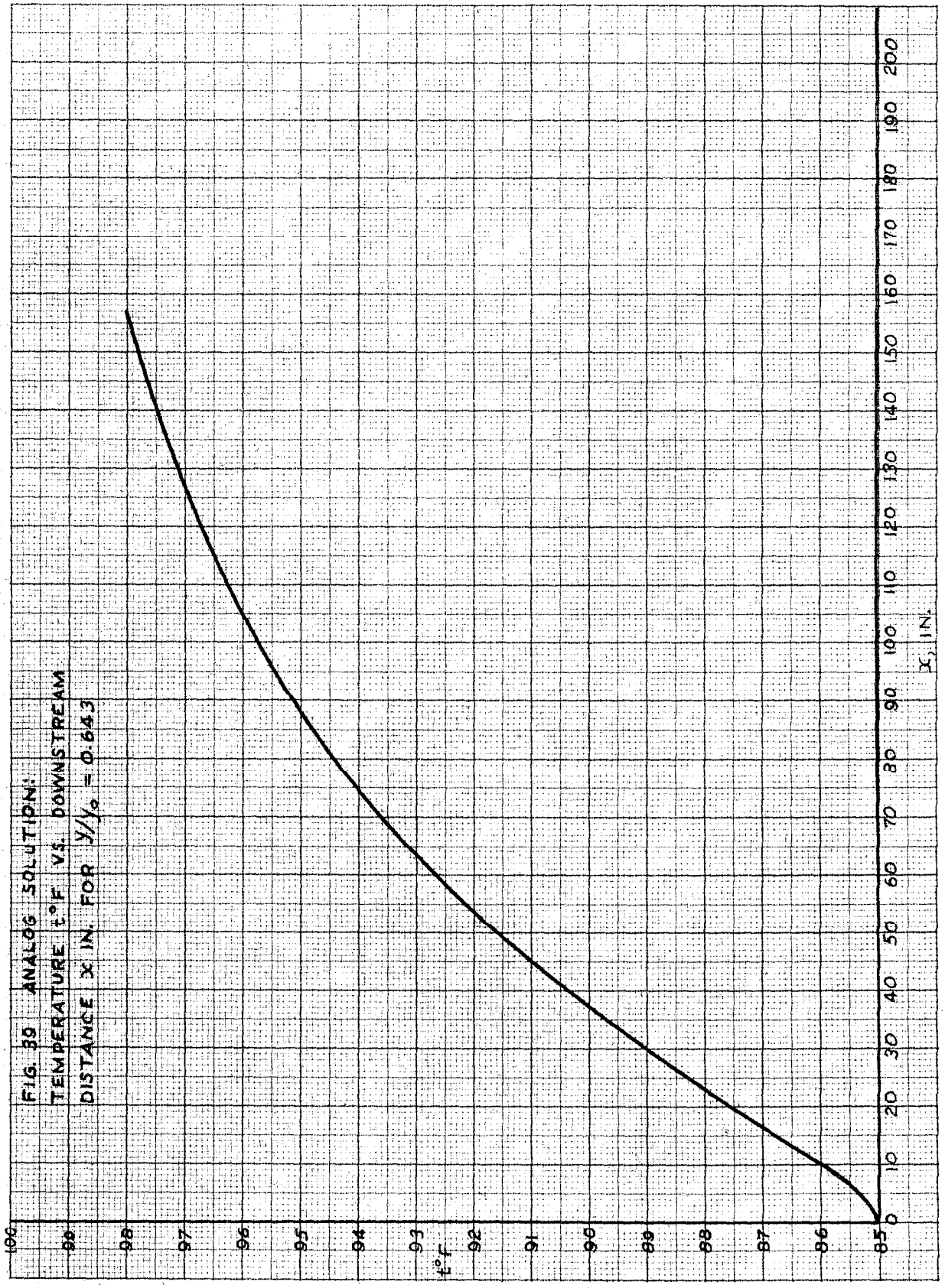
FIG. 39 ANALOG SOLUTION:
TEMPERATURE t°F VS. DOWNSTREAM
DISTANCE X IN. FOR y/y_o = 0.643
t°F
X_2 IN.
100
99
98
97
96
95
94
93
92
91
90
89
88
87
86
85
0
10
20
30
40
50
60
70
80
90
100
110
120
130
140
150
160
170
180
190
200

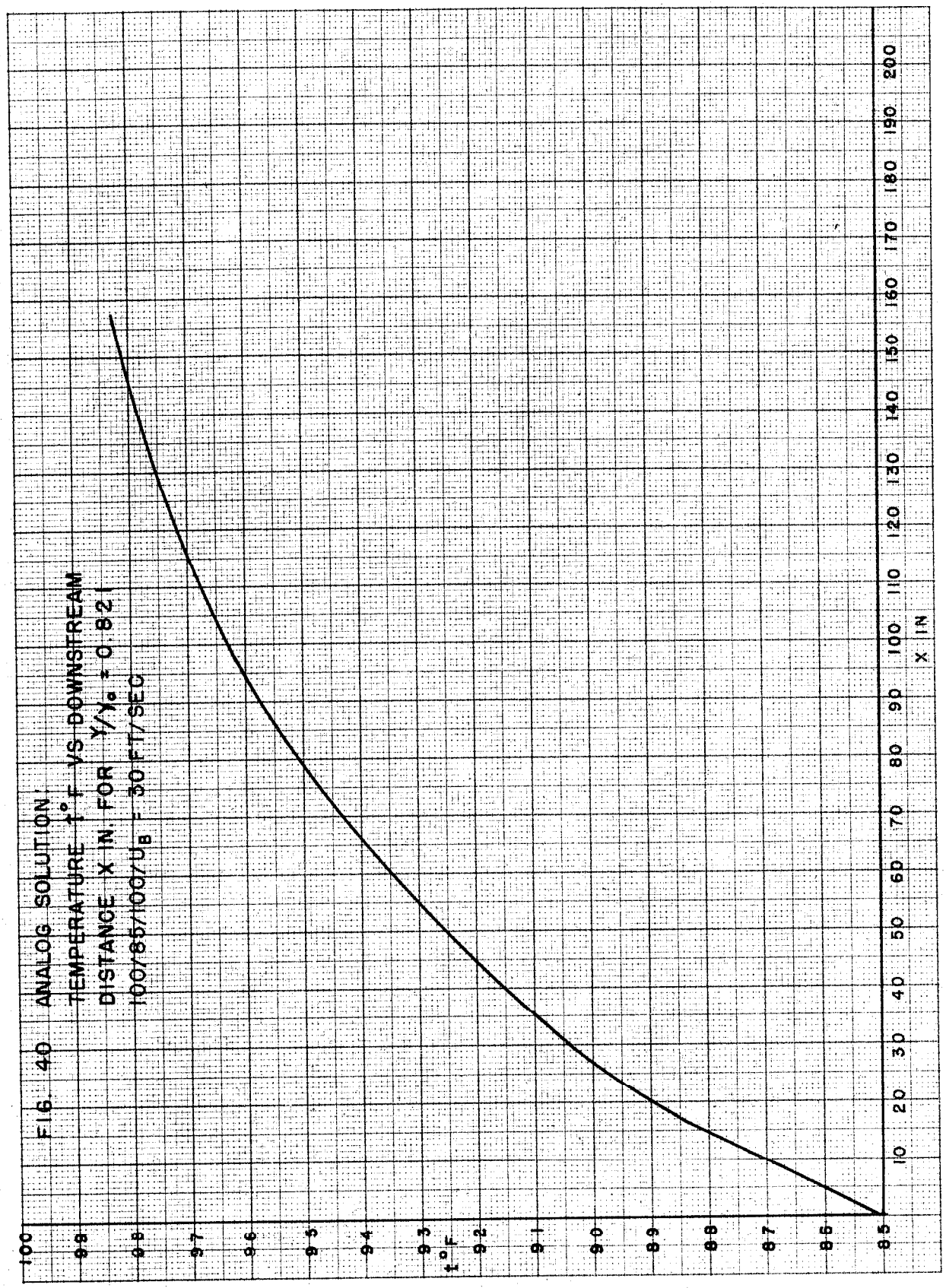
FIG 40 ANALOG SOLUTION
TEMPERATURE t°F VS DOWNSTREAM DISTANCE X IN. FOR Y/Y₀ = 0.821
100/85/100/U_B = 30 FT/SEC
t°F
X IN
100
98
97
96
95
94
93
92
91
90
89
88
87
86
85
10
20
30
40
50
60
70
80
90
100
110
120
130
140
150
160
170
180
190
200

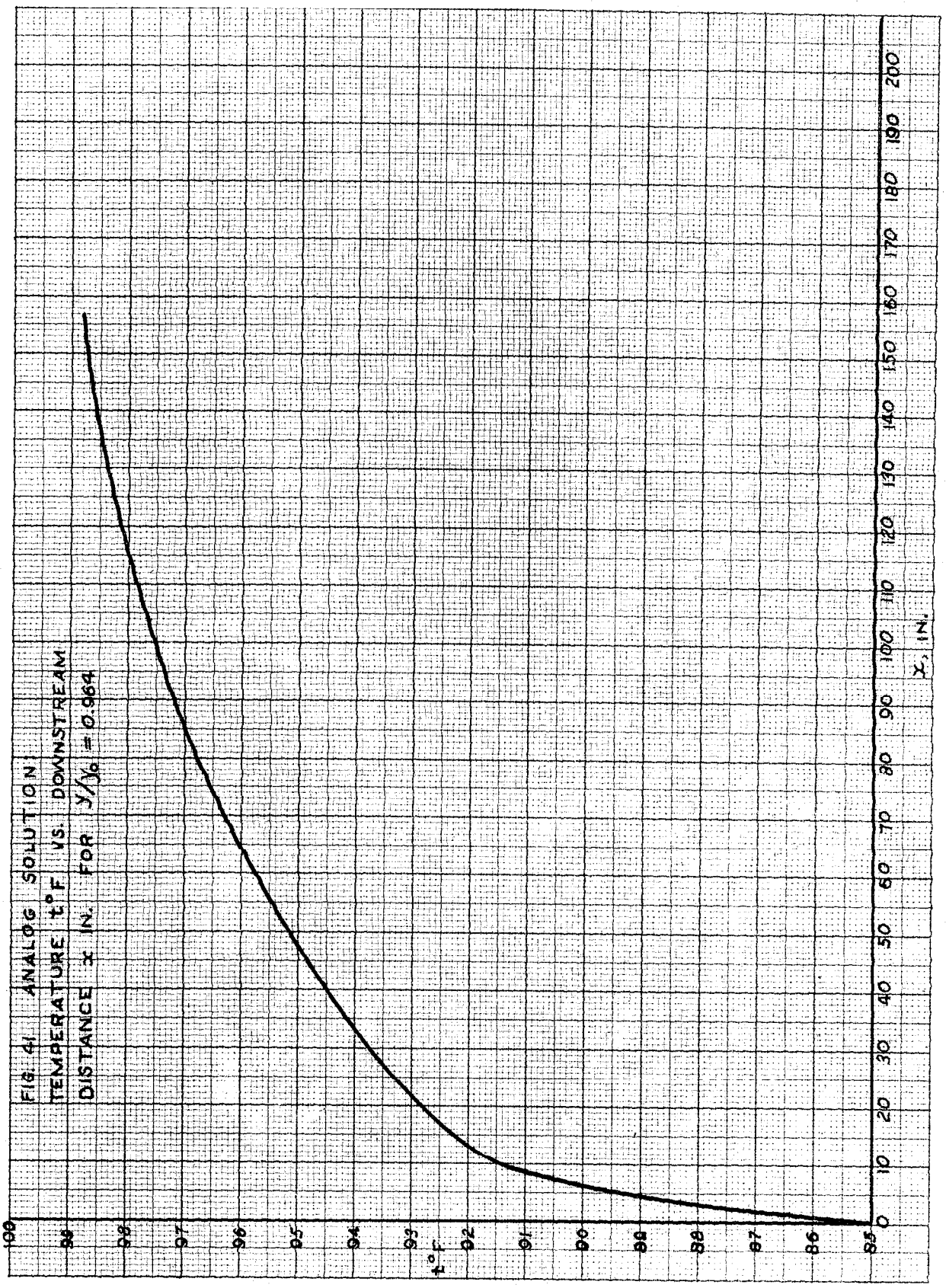
FIG. 41 ANALOG SOLUTION:
TEMPERATURE t°F VS. DOWNSTREAM
DISTANCE x IN. FOR y/y0 = 0.964
t°F
x, IN.
100
99
98
97
96
95
94
93
92
91
90
89
88
87
86
85
0
10
20
30
40
50
60
70
80
90
100
110
120
130
140
150
160
170
180
190
200

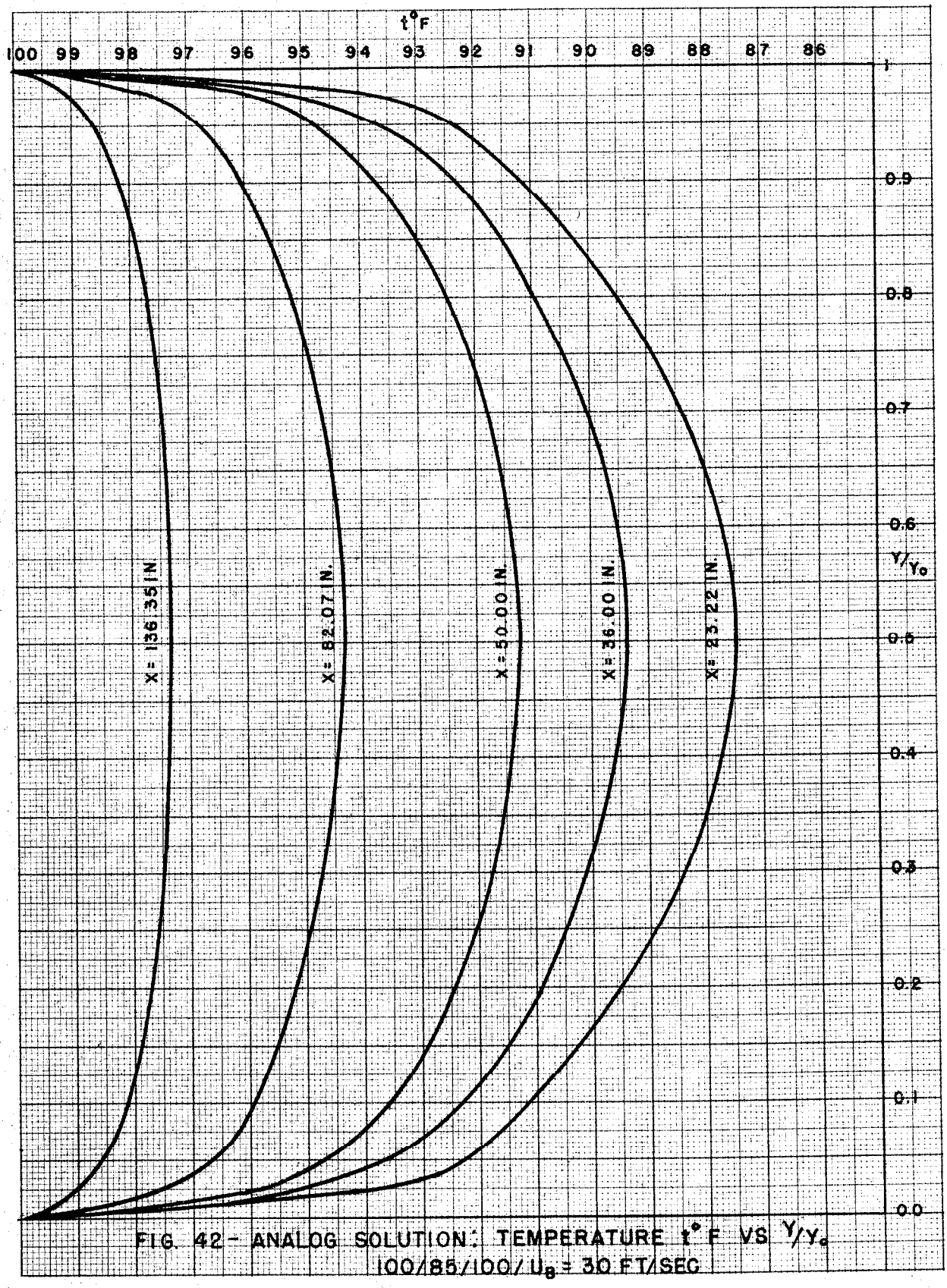

FIG. 42 - ANALOG SOLUTION: TEMPERATURE t° F VS Y/Y_o
100/85/100/ U_s = 30 FT/SEC

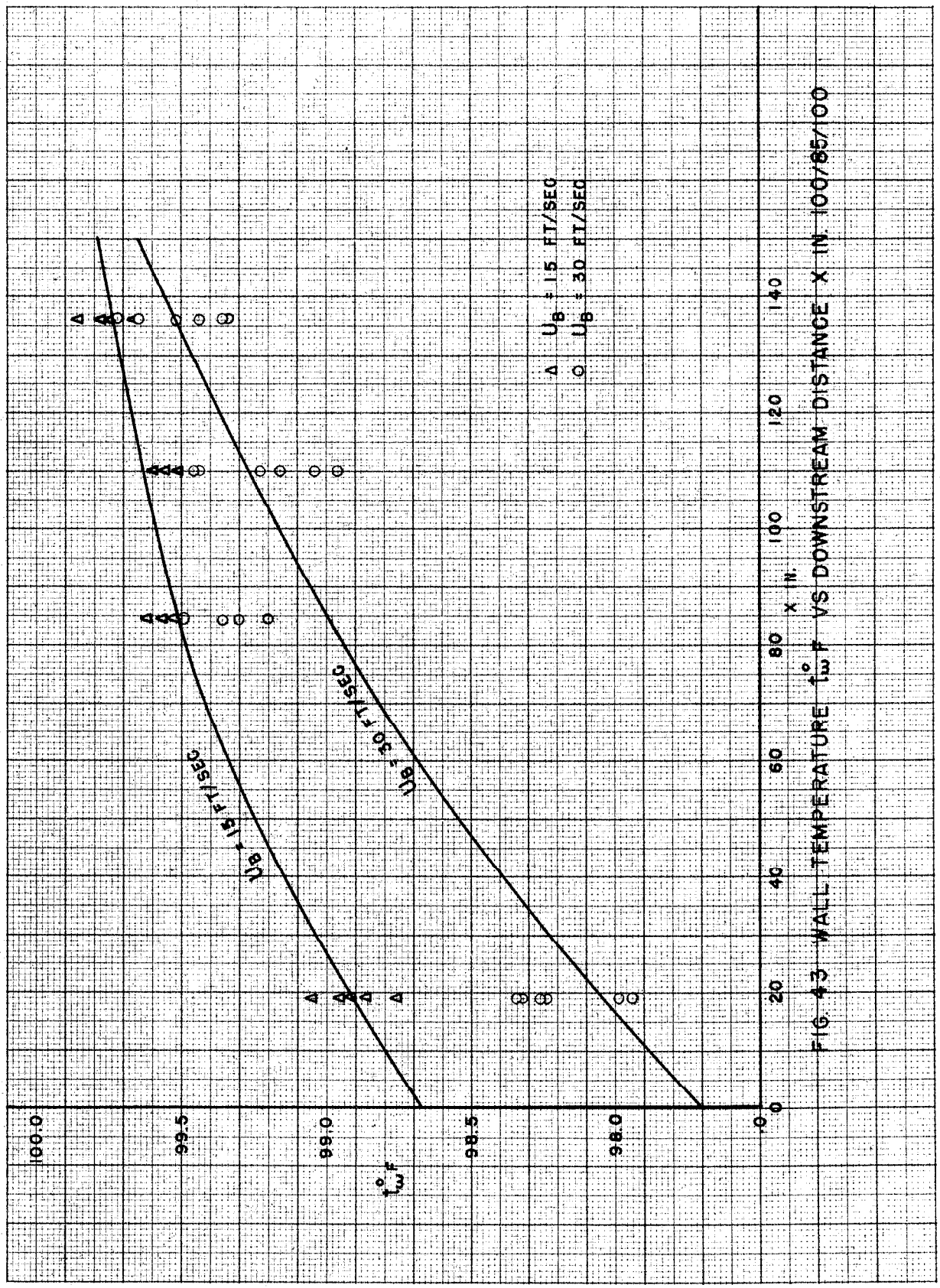

FIG. 43 WALL TEMPERATURE t°F VS DOWNSTREAM DISTANCE X IN. 100/85/100

List of Tables

Table I: Part 1
Temperature and Velocity

a. $100/85/100/U_B$ = 30 ft/sec
x = 23.22 in.
y_o = 0.703 in.

y/y_o	t^oF	u ft/sec
0.997	95.22	10.61
0.993	94.24	13.15
0.986	93.01	17.31
0.972	91.68	21.37
0.943	90.57	24.61
0.886	89.61	27.52
0.801	88.76	29.95
0.741	88.26	31.15
0.687	87.99	32.18
0.630	87.75	32.88
0.573	87.56	33.32
0.516	87.53	33.71
0.479	87.58	33.73
0.479		33.76*
0.459	87.52	33.56
0.403	87.60	33.30
0.346	87.85	32.68
0.289	88.06	31.88
0.232	88.41	30.78
0.175	88.92	29.42
0.088	90.01	26.34
0.045	91.29	22.49
0.031	92.14	19.32

b. $100/85/100/U_B$ = 30 ft/sec
x = 36.00 in.
y_o = 0.713 in.

y/y_o	t^oF
0.993	96.12
0.989	94.57
0.982	93.57
0.968	92.33
0.912	90.89
0.856	90.24
0.799	89.69
0.743	89.23
0.687	89.10
0.631	88.82
0.575	88.72
0.519	88.65
0.463	88.72
0.407	88.76
0.351	88.92
0.295	89.16
0.238	89.53
0.178	90.02
0.098	90.99
0.053	92.21
0.039	93.22

Table I: Part 1 (cont)

c. 100/85/100/U_B = 30 ft/sec
x = 50.00 in.
y_o = 0.695 in.

y/y_o	t^oF	u ft/sec
0.997	96.02	10.92
0.993	95.21	13.79
0.984	94.40	17.34
0.971	93.51	21.20
0.942	92.43	25.52
0.885	91.50	28.44
0.799	90.77	31.10
0.741	90.34	32.42
0.683	90.19	33.47
0.626	90.12	34.38
0.568	89.93	34.89
0.517	89.99	35.08
0.517		35.05*
0.453	89.90	34.83
0.396	90.00	34.40
0.338	90.17	33.66
0.281	90.59	32.23
0.223	90.92	31.14
0.165	91.34	29.54
0.079	92.40	25.68
0.036	94.13	17.97

d. 100/85/100/U_B = 30 ft/sec
x = 82.07 in.
y_o = 0.682 in.

y/y_o	t^oF	u ft/sec
0.997	98.00	11.54
0.993	97.47	14.36
0.985	96.89	17.55
0.971	96.01	22.46
0.941	95.21	26.32
0.883	94.56	29.11
0.795	94.00	31.73
0.736	93.73	32.96
0.677	93.54	34.06
0.619	93.37	35.07
0.560	93.26	35.40
0.526	93.25	35.71
0.526		35.64*
0.443	93.31	35.59
0.384	93.41	35.01
0.326	93.57	34.13
0.267	93.78	33.02
0.208	94.00	31.72
0.150	94.36	30.01
0.062	95.32	25.35
0.032	96.34	19.83

Table I: Part 1 (cont)

e. 100/85/100/U_B = 30 ft/sec
x = 136.35 in.
y_o = 0.681 in.

y/y_o	t^oF	u ft/sec
0.990	98.57	10.45
0.985	98.17	13.76
0.978	97.71	18.17
0.963	97.22	22.77
0.934	96.71	26.52
0.905	96.47	28.56
0.846	96.24	30.79
0.787	96.06	32.23
0.727	95.92	33.56
0.670	95.82	34.50
0.611	95.74	35.35
0.552	95.68	35.55
0.496	95.62	35.80
0.496		35.79*
0.455	95.65	35.33
0.391	95.75	34.86
0.317	95.80	34.02
0.258	95.93	33.14
0.200	96.03	31.97
0.141	96.24	30.36
0.097	96.43	28.24
0.053	96.83	25.67
0.023	97.33	20.28

f. 100/85/100/U_B = 15 ft/sec
x = 23.22 in.
y_o = 0.701 in.

y/y_o	t^oF	u ft/sec
0.990	95.08	6.05
0.976	93.31	10.71
0.954	91.72	15.48
0.912	89.97	20.27
0.854	88.68	21.87
0.797	87.84	23.22
0.740	87.29	24.47
0.683	86.90	25.38
0.626	86.65	26.23
0.569	86.45	26.54
0.484	86.37	26.39
0.484		26.36*
0.398	86.67	26.26
0.341	87.04	25.68
0.284	87.37	24.84
0.227	87.82	23.79
0.170	88.51	22.47
0.123	89.39	21.05
0.084	90.44	18.70
0.056	91.51	16.35
0.041	92.55	13.78
0.027	93.64	9.79

Table I: Part 1 (cont)

g. 100/85/100/U_B = 15 ft/sec
x = 36.00 in.
y_o = 0.696 in.

y/y_o	t^oF
0.994	97.08
0.990	95.98
0.980	94.30
0.968	93.37
0.911	90.83
0.853	89.99
0.796	89.40
0.739	88.93
0.681	88.59
0.624	88.36
0.566	88.20
0.509	88.16
0.451	88.15
0.394	88.24
0.336	88.41
0.279	88.66
0.227	89.06
0.164	89.61
0.069	91.25
0.023	94.15

h. 100/85/100/U_B = 15 ft/sec
x = 50.00 in.
y_o = 0.714 in.

y/y_o	t^oF	u ft/sec
0.991	96.76	5.60
0.987	96.04	7.07
0.981	95.38	8.66
0.967	94.24	11.71
0.909	92.11	16.63
0.852	91.27	18.16
0.794	90.76	18.93
0.737	90.39	19.27
0.679	90.21	19.89
0.622	89.93	20.01
0.564	89.86	20.21
0.506	89.75	20.18
0.506		20.15*
0.449	89.76	20.02
0.391	89.87	19.85
0.334	90.05	19.42
0.276	90.28	18.97
0.212	90.63	18.31
0.161	91.07	17.70
0.075	92.28	15.32
0.027	94.63	9.71
0.017	95.58	7.06

Table I: Part 1 (cont)

i. 100/85/100/U_B = 15 ft/sec
x = 82.07 in.
y_o = 0.695 in.

y/y_o	t°F
0.994	98.63
0.990	98.36
0.983	97.56
0.968	96.68
0.911	95.85
0.853	94.16
0.796	93.72
0.738	93.47
0.681	93.22
0.623	93.10
0.565	93.00
0.529	92.97
0.450	92.95
0.393	93.08
0.328	93.19
0.278	93.36
0.220	93.67
0.163	94.00
0.076	95.26
0.033	96.48
0.019	97.25

j. 100/85/100/U_B = 15 ft/sec
x = 136.35 in.
y_o = 0.681 in.

y/y_o	t°F	u ft/sec
0.994	98.80	4.60
0.990	98.54	5.75
0.982	98.21	8.17
0.967	97.67	11.45
0.938	97.12	14.81
0.908	96.89	16.43
0.849	96.56	17.94
0.790	96.38	18.77
0.731	96.31	19.48
0.670	96.19	19.97
0.612	96.12	20.39
0.572	96.09	20.59
0.504	96.06	20.84
0.504		20.81*
0.435	96.09	20.62
0.376	96.14	19.38
0.314	96.21	19.70
0.254	96.33	19.16
0.192	96.47	18.22
0.151	96.61	17.46
0.095	96.92	15.97
0.046	97.48	12.40
0.015	98.44	5.44

Table I: Part 1 (cont)

k. 115/100/85/U_B = 30 ft/sec
x = 23.22 in.
y_o = 0.695 in.

y/y_o	t°F	u ft/sec
0.993	109.15	8.44
0.989	108.49	9.89
0.982	107.46	13.83
0.968	105.86	19.33
0.939	104.33	23.80
0.911	103.66	25.88
0.855	102.60	28.21
0.798	102.03	29.84
0.742	101.49	31.08
0.685	101.01	32.22
0.629	100.56	33.21
0.573	101.16	33.70
0.516	99.67	34.25
0.516		34.32*
0.456	99.20	33.59
0.403	98.79	33.04
0.347	98.30	32.47
0.291	97.80	31.38
0.234	97.35	30.33
0.178	96.68	28.85
0.093	95.62	25.86
0.051	94.43	22.25
0.032	92.93	17.21

l. 115/100/85/U_B = 30 ft/sec
x = 36.00 in.
y_o = 0.705 in.

y/y_o	t°F
0.993	109.63
0.990	108.92
0.982	107.81
0.967	106.43
0.911	104.28
0.854	103.72
0.797	102.75
0.740	101.91
0.684	101.62
0.627	101.04
0.570	100.45
0.513	99.79
0.454	99.13
0.400	98.60
0.343	97.85
0.287	97.44
0.230	96.91
0.173	96.26
0.088	95.05
0.041	93.57
0.027	92.30

Table I: Part 1 (cont)

m. 115/100/85/U_B = 30 ft/sec
x = 50.00 in.
y_o = 0.700 in.

y/y_o	t^oF	u ft/sec
0.994	110.62	6.83
0.990	110.00	8.42
0.983	108.81	12.84
0.969	107.23	19.51
0.940	105.60	25.27
0.911	104.89	27.55
0.854	103.96	30.21
0.797	103.33	32.22
0.740	102.70	33.64
0.683	102.11	34.92
0.626	101.45	35.58
0.569	100.82	36.11
0.569		35.98*
0.519	100.14	36.18
0.454	99.22	35.89
0.397	98.60	35.52
0.340	97.88	34.64
0.283	97.19	33.39
0.226	96.65	32.00
0.169	96.06	29.83
0.083	94.76	26.05
0.027	92.91	18.52

n. 115/100/85/U_B = 30 ft/sec
x = 82.07 in.
y_o = 0.685 in.

y/y_o	t^oF
0.994	110.91
0.990	110.51
0.982	109.32
0.968	107.47
0.909	104.97
0.851	104.07
0.793	103.35
0.734	102.69
0.676	102.05
0.618	101.34
0.559	100.50
0.498	99.72
0.436	98.84
0.384	98.18
0.326	97.45
0.267	96.82
0.209	96.19
0.150	95.54
0.063	94.02
0.019	91.43

Table I: Part 1 (cont)

o. 100/100/85/U_B = 30 ft/sec
x = 23.22 in.
y_o = 0.701in.

y/y_o	t°F	u ft/sec
0.994	99.29	5.89
0.989	99.29	9.38
0.981	99.29	11.96
0.967	99.28	20.47
0.939	99.22	25.18
0.910	99.17	27.38
0.853	99.16	29.68
0.793	99.12	31.10
0.739	99.04	32.08
0.682	98.98	32.92
0.621	98.93	33.67
0.568	98.79	34.12
0.511	98.59	34.01
0.489		34.06*
0.489	98.53	34.15
0.454	98.38	33.29
0.397	98.11	32.73
0.340	97.81	31.92
0.282	97.46	31.13
0.225	97.01	29.91
0.168	96.49	28.55
0.126	96.05	27.27
0.083	95.40	25.55
0.054	94.83	23.94
0.040	94.23	22.03
0.024	92.64	16.34

p. 100/100/85/U_B = 30 ft/sec
x = 36.00 in.
y_o = 0.694 in.

y/y_o	t°F
0.987	99.21
0.973	99.21
0.951	99.19
0.908	99.18
0.850	99.14
0.793	99.06
0.735	99.00
0.677	98.90
0.620	98.71
0.562	98.52
0.492	98.22
0.447	97.91
0.389	97.58
0.323	97.18
0.274	96.83
0.217	96.39
0.159	95.86
0.116	95.36
0.073	94.67
0.044	93.95
0.027	93.03
0.017	92.86

Table I: Part 1 (cont)

q. 100/100/85/U_B = 30 ft/sec
x = 50.00 in.
y_o = 0.687 in.

y/y_o	t°F	u ft/sec
o.987	99.58	11.06
0.972	99.42	19.12
0.951	99.32	23.67
0.907	99.16	27.38
0.847	99.13	30.10
0.790	98.94	31.93
0.732	98.87	33.50
0.674	98.73	34.54
0.616	98.47	35.32
0.557	98.15	35.78
0.505	97.83	35.78
0.505		35.81*
0.441	97.48	35.37
0.383	97.09	34.48
0.325	96.72	33.80
0.266	96.28	32.49
0.208	95.81	31.25
0.150	95.42	29.54
0.106	94.99	28.01
0.063	94.27	25.44
0.033	93.35	21.22
0.023	91.98	14.62

r. 100/100/85/U_B = 30 ft/sec
x = 82.07 in.
y_o = 0.686 in.

y/y_o	t°F
0.987	98.95
0.972	98.56
0.950	98.26
0.907	98.05
0.849	97.83
0.790	97.65
0.728	97.45
0.674	97.23
0.615	96.96
0.557	96.65
0.499	96.26
0.441	95.87
0.381	95.42
0.324	95.04
0.266	94.61
0.208	94.18
0.149	93.67
0.106	93.19
0.062	92.53
0.031	91.63
0.017	90.40

Table I: Part 1 (cont)

s. 100/100/85/U_B = 30 ft/sec
x = 136.35 in.
y_o = 0.683 in.

y/y_o	t°F	u ft/sec
0.990	98.81	8.20
0.984	98.43	11.63
0.969	97.87	18.85
0.955	97.51	23.26
0.933	97.27	26.08
0.903	97.10	27.93
0.845	96.75	30.46
0.786	96.55	32.44
0.728	96.21	33.61
0.669	96.00	33.81
0.611	95.68	34.22
0.552	95.26	34.63
0.493	94.89	34.62
0.493		34.62*
0.435	94.54	33.41
0.376	94.08	33.06
0.318	93.75	32.25
0.259	93.32	31.37
0.201	92.93	30.29
0.142	92.45	28.91
0.098	92.09	27.78
0.054	91.44	25.09
0.025	90.55	20.00

* Pitot tube measurement

Table I: Part 2
Pressure, Pressure Gradient,
Weight Rate of Flow, Mass Velocity,
Reynolds Number

$100/85/100/U_B$ = 30 ft/sec

	x, in	$-P_1$ lb/in^2	$-P_2$ lb/in^2	$-P_3$ lb/in^2	$-P_4$ lb/in^2	$-P_5$ lb/in^2	$-P_6$ lb/in^2
a.	23.22	0	0.01486	0.02823	0.00257	---	---
b.	36.00	0	0.01501	0.02660	---	---	---
c.	50.00	0	0.01573	0.02679	0.00700	---	---
d.	82.07	0	0.01198	0.02734	0.01179	---	---
e.	136.35	0	0.01196	0.02751	0.01969	0.01944	0.01936

	x, in.	y_o, in.	m lb/sec	G lb/sec ft^2	
a.	23.22	0.703	0.1331	2.203	
b.	36.00	0.713	0.1349	2.202	
c.	50.00	0.695	0.1335	2.235	
d.	82.07	0.682	0.1336	2.280	
e.	136.35	0.681	0.1336	2.283	
	average	0.694	0.1337	2.241	$(Re)_{av}$ = 19290;
					$-(dP/dx)_{av}$ = 0.001796 psi/ft

Location of static pressure taps:

Fixed taps:

P_1 is measured at x_1 = 4.01 in.

P_2 is measured at x_2 = 82.07 in.

P_3 is measured at x_3 = 158.07 in.

Taps on traversing gear:

P_4 is measured at x_4 = (x-0.44) in.

P_5 is measured at x_5 = (x-2.25) in.

P_6 is measured at x_6 = (x-2.25) in.

Pressures are measured in lb/in^2 referred to P_1.

Table I: Part 2 (Cont)

100/85/100/U_B = 15 ft/sec

	x, in.	$-P_1$ lb/in^2	$-P_2$ lb/in^2	$-P_3$ lb/in^2	$-P_4$ lb/in^2	$-P_5$ lb/in^2	$-P_6$ lb/in^2
f.	23.22	0	0.00796	0.01285	0.00251	0.00230	---
g.	36.00	0	0.00584	0.01025	0.00238	0.00220	0.00220
h.	50.00	0	0.00594	0.01035	0.00148	0.00145	0.00148
i.	82.07	0	0.00430	0.01028	---	0.00401	0.00401
j.	136.35	0	0.00417	0.01042	0.00710	0.00691	0.00685

	x, in.	y_o in.	m lb/sec	G lb/sec ft^2	
f.	23.22	0.701	0.06854	---	
g.	36.00	0.696	---	---	
h.	50.00	0.714	0.06876	1.121	
i.	82.07	0.695	0.06829	1.143	
j.	136.35	0.681	0.06684	1.142	
	average	0.697	0.06796	1.135	$(Re)_{av}$ = 9750
					$-(dP/dx)_{av}$ = 0.000641 psi/ft

Location of static pressure taps:

Fixed taps:

P_1 is measured at x_1 = 4.01 in.

P_2 is measured at x_2 = 82.07 in.

P_3 is measured at x_3 = 158.07 in.

Taps on traversing gear:

P_4 is measured at x_4 = (x-0.44) in.

P_5 is measured at x_5 = (x-2.25) in.

P_6 is measured at x_6 = (x-2.25) in.

Pressures are measured in lb/in^2 referred to P_1.

Table I: Part 2 (cont)

115/100/85/U_B = 30 ft/sec

	x, in.	$-P_1$ lb/in^2	$-P_2$ lb/in^2	$-P_3$ lb/in^2	$-P_4$ lb/in^2	$-P_5$ lb/in^2	$-P_6$ lb/in^2
k.	23.22	0	0.01533	0.02616	0.00272	0.00249	0.00248
l.	36.00	0	0.01614	0.02726	0.00686	0.00673	0.00677
m.	50.00	0	0.01627	0.02740	---	0.00483	0.00453
n.	82.07	0	0.01167	0.02694	---	0.01117	0.01141

	x, in.		y_o in	m lb/sec	G lb/sec ft^2
k.	23.22	0	0.695	0.1330	2.227
l.	36.00	0	0.705	0.1350	2.228
m.	50.00	0	0.700	0.1344	2.234
n.	82.07	0	0.685	0.1335	2.268
	average		0.696	0.1340	2.239

$(Re)_{av}$ = 19200

$-(dP/dx)_{av}$ = 0.001784 psi/ft

Location of static pressure taps:

Fixed taps:

P_1 is measured at x_1 = 4.01 in.

P_2 is measured at x_2 = 82.07 in.

P_3 is measured at x_3 = 158.07 in.

Taps on traversing gear:

P_4 is measured at x_4 = (x-0.44) in.

P_5 is measured at x_5 = (x-2.25) in.

P_6 is measured at x_6 = (x-2.25) in.

Pressures are measured in lb/in^2 referred to P_1.

Table I: Part 2 (cont)

100/100/85/U_B = 30 ft/sec

	x, in.	$-P_1$ lb/in^2	$-P_2$ lb/in^2	$-P_3$ lb/in^2	$-P_4$ lb/in^2	$-P_5$ lb/in^2	$-P_6$ lb/in^2
o.	23.22	0	0.01485	0.02588	0.00255	0.00252	0.00247
p.	36.00	0	0.01602	0.02707	0.00474	0.00445	0.00444
q.	50.00	0	0.01600	0.02718	0.00706	0.00667	0.00659
r.	82.07	0	0.01188	0.02697	---	0.01146	0.01124
s.	136.35	0	0.01145	0.02635	0.01892	0.01858	0.01849

	x, in.	y_o, in	m lb/sec	G lb/sec ft^2	
o.	23.22	0.701	.1334	2.214	
p.	36.00	0.694	.1335	2.238	
q.	50.00	0.687	.1335	2.261	
r.	82.07	0.686	.1335	2.264	
s.	136.35	0.683	.1334	2.273	
	average	0.690	.1335	2.250	$(Re)_{av}$ = 19130

$-(dP/dx)_{av}$ = 0.001804 psi/ft

Location of static pressure taps:

Fixed taps;

P_1 is measured at x_1 = 4.01 in.

P_2 is measured at x_2 = 82.07 in.

P_3 is measured at x_3 = 158.07 in.

Taps on traversing gear:

P_4 is measured at x_4 = (x-0.44) in.

P_5 is measured at x_5 = (x-2.25) in.

P_6 is measured at x_6 = (x-2.25) in.

Pressures are measured in lb/in^2 referred to P_1.

Table II. Bulk Temperature, °F
(defined by Equation 6)

Part 1. $100/85/100/U_B$ = 30 ft/sec

x, in.	t_{B1}	t_{B2}	t_{B3}	t_{B4}	t_{B5}
00.00	84.90	84.90	84.90	85.00	85.00
23.22	88.43	87.86	88.47	89.16	88.55
36.00	89.65	89.24	90.03	90.74	89.95
50.00	90.67	90.58	91.49	92.32	91.41
82.07	93.18	93.11	94.08	95.07	94.10
136.35	96.06	96.00	96.80	97.69	96.89

t_{B1} Experimental bulk temperatures, $100/85/100/U_B$ = 30 ft/sec

t_{B2} Bulk temperatures calculated from Equations 3 and 24, experimental plate temperature distribution (Fig. 43) assumed.

t_{B3} Bulk temperatures calculated from Equations 3 and 24, plate temperature assumed uniform at 100°F.

t_{B4} Bulk temperatures calculated from analog solution; eddy conductivities used were Case C, Fig. 31.

t_{B5} Analog bulk temperatures corrected to experimental plate temperature distribution.

Table II (cont)

Part 2. $100/85/100/U_B = 15$ ft/sec

x, in.	t_{B6}	t_{B7}	t_{B8}
00.00	85.00	85.00	85.00
23.22	88.03	88.56	89.08
36.00	89.54	90.16	90.60
50.00	91.07	91.67	92.15
82.07	93.99	94.33	94.82
136.35	96.13	97.02	97.39

t_{B6} Experimental bulk temperatures, $100/85/100/U_B = 15$ ft/sec

t_{B7} Bulk temperatures calculated from Equations 3 and 24, experimental plate temperature distribution (Fig. 43) assumed.

t_{B8} Bulk temperatures calculated from Equations 3 and 24, plate temperature assumed uniform at 100°F.

Table III

Rate of Heat Transfer from Wall to Air Stream, $\overset{\circ}{Q}_w$, BTU/hr ft^2

Heat Transfer Coefficient h, BTU/hr ft^2 $^\circ$F

Part I. 100/85/100 U_B = 30 ft/sec

x, in.	$\overset{\circ}{Q}_{w1}$	$\overset{\circ}{Q}_{w2}$	$\overset{\circ}{Q}_{w3}$	h_1	h_2	h_3
23.22	60.0	82.5	78.3	6.21	7.61	7.22
36.00	55.6	76.2	76.5	6.43	8.23	8.26
50.00	50.6	68.5	64.0	6.43	8.92	8.33
82.07	41.3	42.6	41.7	7.10	8.65	8.46
136.35	30.4	30.2	18.3	8.83	13.10	7.92

$\overset{\circ}{Q}_{w1}$ and h_1 were computed from experimental bulk temperatures by Equation 20.

$\overset{\circ}{Q}_{w2}$ and h_2 were computed from analog bulk temperatures by Equation 20.

$\overset{\circ}{Q}_{w3}$ and h_3 were obtained directly from the analog solution.

See page 45.

Table III (cont)

Part II. 100/85/100/U_B = 15 ft/sec

x, in.	$\overset{\circ}{Q}_{w1}$	h_1
23.22	48.2	4.45
36.00	43.1	4.51
50.00	41.0	5.02
82.07	27.9	5.02
136.35	11.4	3.49

$\overset{\circ}{Q}_{w1}$ and h_1 were computed from experimental bulk temperatures by Equation 20.

Table IV
Eddy Conductivity, ϵ_c,
Eddy Viscosity, ϵ_m, and the Ratio ϵ_c/ϵ_m

Part 1. 100/85/100/U_B = 30 ft/sec

a. Eddy Conductivity, ϵ_c, ft^2/sec

y/y_o	x = 23.22 in.	x = 36.00 in.	x = 50.00 in.	x = 82.07 in.	x = 136.35 in.
0.90	0.00277	0.00324	0.00286	0.00319	0.00486
0.80	0.00387	0.00380	0.01052	0.00583	0.00755
0.70	0.00415	0.00484	0.00507	0.00532	0.00630
0.60	0.00390	0.00834	0.00774	0.00505	0.00517

b. Eddy Viscosity, ϵ_m, ft^2/sec

y/y_o	x = 23.22 in.	x = 36.00 in.	x = 50.00 in.	x = 82.07 in.	x = 136.35 in.
1.00	0.00000	0.00000	-0.00001	0.00000	0.00000
0.95	0.00131	0.00128	0.00128	0.00129	0.00131
0.90	0.00326	0.00320	0.00319	0.00322	0.00327
0.80	0.00451	0.00442	0.00440	0.00446	0.00453
0.70	0.00392	0.00385	0.00382	0.00390	0.00396
0.60	0.00375	0.00368	0.00366	0.00376	0.00381

Table IV: Part 1 (cont)

c. Ratio ϵ_e/ϵ_m

y/y_o	x = 23.22 in.	x = 36.00 in.	x = 50.00 in.	x = 82.07 in.	x = 136.35 in.
0.90	0.85	1.01	0.90	0.99	1.49
0.80	0.86	0.86	2.39	1.31	1.67
0.70	1.06	1.26	1.33	1.36	1.59
0.60	1.04	2.27	1.98	1.34	1.36

Part 2 $115/100/85/U_B$ = 30 ft/sec

Eddy conductivity, ϵ_e, ft^2/sec

y/y_o	x = 23.22 in.	x = 36.00 in.	x = 50.00 in.	x = 82.07 in.
0.98	0.00023	0.00017	0.00018	0.00005
0.96	0.00068	0.00061	0.00048	0.00040
0.94	0.00095	0.00096	0.00098	0.00098
0.92	0.00135	0.00138	0.00153	0.00160
0.90	0.00178	0.00205	0.00205	0.00218
0.80	0.00164	0.00312	0.00356	0.00359
0.70	0.00101	0.00293	0.00348	0.00347
0.60	0.00030	0.00236	0.00287	0.00300
0.50	0.00000	0.00219	0.00250	0.00293

Table V
Temperature, °F
Solution of Heat Transfer Equation
by Analog Computer

$100/85/100/U_B$ = 30 ft/sec

y/y_o	x = 23.22 in.	x = 36.00 in.	x = 50.00 in.	x = 82.07 in.	x = 136.35 in.
1.00	100.00	100.00	100.00	100.00	100.00
0.99	96.82	97.08	97.72	98.48	99.45
0.98	94.43	95.50	96.29	97.77	99.00
0.96	92.77	94.16	94.96	96.89	98.61
0.93	91.73	92.94	94.12	96.29	98.30
0.90	91.13	92.26	93.56	95.91	98.11
0.85	90.25	91.45	92.88	95.47	97.89
0.80	89.50	90.90	92.45	95.17	97.72
0.75	88.89	90.46	92.12	94.94	97.59
0.70	88.38	90.10	91.85	94.74	97.50
0.60	87.70	89.58	91.36	94.43	97.38
0.50	87.43	89.37	91.16	94.26	97.34

References

1. Reynolds, O., Proc. Lit. & Phil. Soc. of Manchester, 14, 7-12, (1874).

2. Mason, D.M., Ph. D. Thesis, California Institute, (1949).

3. Corcoran, W.H., Ph. D. Thesis, California Institute, (1948).

4. Page, F. Jr., Ph. D. Thesis, California Institute, (1950).

5. Cavers, S.D., Ph. D. Thesis, California Institute, (1950).

6. von Karman, Th., Proc. 3rd Int. Congress for App. Mech, 1, 85, (1930).

7. Durand, W.F., Aerodynamic Theory, VI, (1934).

8. Boelter, L.M.K., Martinelli, R.C., Jonassen, F., Trans. Am. Soc. Mech. Engrs., 63, 446-459, (1947).

9. Walker, W.H., Lewis, W.K., McAdams, W.H., Gilliland, E.R., Principles of Chemical Engineering, McGraw-Hill, (1937).

10. Billman, G.W., Ph. D. Thesis, California Institute, 1948).

11. Dryden, H.L., Kuethe, A.M., NACA Tech. Rpt. No. 320 (1929).

12. Wimmer, W., NACA Tech. Memo. No. 967 (1941).

13. Berry, V.B., Student Report, California Institute, (1949).

14. Mellor, F.W., Higher Mathematics for Students of Physics and Chemistry, Longman, Green & Co., (1905).

15. Martinelli, R.C., Trans. Am. Soc. Mech. Engrs., 69, 947-959, (1947).

16. Durand, W.F., Aerodynamic Theory, III, (1934).

17. Lamb, H., Hydrodynamics, Cambridge Press, (1879).

18. Navier, C., Mem. de l'Acad. des Sciences, 6, 389, (1822).

19. Stokes, G., Camb. Trans., 8, 287, (1845).

20. Lacey, W.N., Sage, B.H., Thermodynamics of One Component Systems, California Institute, (1940).

Propositions Submitted by John Latimer Mason

Ph.D. Oral Examination, May ~~26~~ 25, 1:00 P.M., Crellin Conference Room

Committee: Professors Sage (Chairman), Kirkwood, Lacey, McCann, Pauling, and Swift

Chemical Engineering

1. The heat transfer coefficient h as determined by the equation

$$h/c_p G = 0.023\ Re^{-0.2} Pr^{-0.6} \qquad (1)$$

is not applicable to heat transfer near a channel entrance or at any point where temperature boundary conditions are suddenly changed.

2. The concept of isotropic turbulence is of limited utility in practical fluid flow problems since isotropic turbulence can exist only in the absence of a velocity gradient.

3. The following observations are made regarding hot wire anemometry:

a. The use of a hot wire anemometer to measure velocities near a wall is subject to error because of heat transfer from the wire to the wall. A method of correction has been suggested (2) involving measurement of the function

$$\Phi_o = I^2 R_{HW} / (R_{HW} - R_A)$$

at successively smaller values of $(R_{HW} - R_A)$. A value of Φ_o corrected for the effect of the wall is obtained by extrapolating the curve Φ_o vs. $(R_{HW} - R_A)$ to $(R_{HW} - R_A) = 0$. The corrected velocity would then be calculated from King's equation:

$$u = (1/B^2)(\Phi_o - A)^2$$

This method of correction for the effect of the wall is operationally unsatisfactory since the constants A and B in King's equation have been found experimentally (3) to be functions of the hot wire operating resistance R_{HW}.

b. The hot wire method of measurement of the intensity of turbulence is inaccurate at any point where the velocity gradient normal to the wire is appreciable, since the fluctuations in velocity due to vibrations of the hot wire are of the same order of magnitude as the turbulent velocity fluctuations.

4. Present correlations for natural convection heat transfer are seriously in error when applied to small wires (diameter less than 0.001 in.). The equation recommended by McAdams (4) for natural convection from horizontal cylinders

$$h = 0.27(\Delta t/D_o)^{0.25}$$

results in a calculated rate of heat transfer which is less than 10% of the experimental value. It is proposed that natural convection heat transfer from small wires of various sizes be investigated to determine the effect of wire size on heat transfer.

5. Attempts to represent the eddy viscosity as a scalar or a vector are theoretically unsatisfactory. Reference to the fundamental defining equations indicates that the eddy viscosity is a symmetric tensor of the second rank analogous to the stress tensor.

Chemistry

6. A simple proof for the equation

$$\overline{xF_x} = 0$$

has been devised. This equation is used in a derivation of the diffusion displacement equation

$$\overline{\Delta x^2} = 2D\theta$$

without adequate proof (5).

7. The temperature distribution within a solid body in which heat is generated at a variable rate may be solved for analytically by operating successively on the energy balance equation by means of a substitution of variable and a Laplace transform. This analysis is applicable to an arbitrary heat generation function. Previous solutions to this problem (6) have been applicable only to a heat generation function corresponding to a first order chemical reaction.

8. The induction time for the first order decomposition of azomethane has been estimated (7) by assuming that the heat generated does not vary with time. A better approximation has been devised which takes the variation of Q_g with time into account:

$$\theta_i = \int_{T_o}^{T_o+25} \frac{e^{\frac{E}{RT}}\, dT}{K'(A-T)}$$

Mechanical Engineering

9. It is proposed that a flow meter measuring the rate of gasoline consumption be provided as optional equipment for automobiles.

10. Lamb (8) defines a mean pressure as follows:

$$P = 1/3 \left(\tau_{xx} + \tau_{yy} + \tau_{zz} \right)$$

Regarding P, he states: "The question remains open as to whether, in the case of a gas, the mean pressure is a function of the density and temperature only or whether it depends also on the rate of expansion at the point (x,y,z)."

It may readily be shown that for the case of flow of a compressible fluid, the mean pressure P does depend on the rate of expansion as well as on the density and temperature of the fluid. The only necessary assumption is the validity of the Navier-Stokes equations of motion.

11. The work expended in frictionless isothermal compression of a gas by means of a reciprocating pump discharging into a receiver may be expressed in terms of a geometric mean pressure $\bar{P}$:

$$W_t = bT\Delta m \left[1 + \frac{n-1}{n} \ln \frac{\bar{P}}{P_0} \right]$$

where

$$\bar{P} = \left(\prod_{k=2}^{n} P_k \right)^{\frac{1}{n-1}}$$

A method of determining $\bar{P}$ in terms of the total number of piston strokes n and the path of the fluid in the receiver is proposed.

Nomenclature, Propositions

A, B	Dimensional constants in King's equation
A', K'	Dimensional constants in induction time equation
c_p	Specific heat at constant pressure, BTU/lb $^{\circ}F$
D	Diffusion coefficient, ft^2/sec
D_o	Outside diameter of cylinder, ft
E	Energy of activation, cal/gm mol
e	Base of natural logarithms
F_x	x component of force, lb
G	Mass velocity, lb/ft^2 sec
h	Heat transfer coefficient, BTU/hr ft^2 $^{\circ}F$
I	Current, amperes
k	Dummy index
Δm	Total weight of gas compressed, lbs
n	Total number of piston strokes in compression
P	Mean pressure as defined in Prop. 10, lb/ft^2
P	Geometric mean pressure as defined in Prop. 11, lb/ft^2
Pr	Prandtl number, dimensionless
$\dot{Q}_g$	Heat generated by chemical reaction, cal/sec
Re	Reynolds number, dimensionless
R	Gas constant, cal/gm mol $^{\circ}K$
R_A	Resistance of thermanemometer at airstream temperature, ohms
R_{HW}	Resistance of thermanemometer at its operating temperature, ohms
Δt	Temperature difference between cylinder and airstream, $^{\circ}F$
T	Temperature, $^{\circ}K$ (Prop. 8) or $^{\circ}R$ (Prop. 11)
T_o	Initial temperature, $^{\circ}K$
u	x component of velocity, ft/sec
W_r	Work expended in frictionless compression, BTU
$\overline{\Delta x^2}$	Mean square displacement, ft^2

References, Propositions

1. Walker, Lewis, McAdams, and Gilliland, Principles of Chemical Engineering, McGraw-Hill, (1937).

2. Willis, Australian Council for Aeronautics Report ACA-19, (1945).

3. Berry, Student Report, California Institute, (1949).

4. McAdams, Heat Transmission, McGraw-Hill, (1942).

5. Loeb, Kinetic Theory of Gases, McGraw-Hill, (1927).

6. Ingersoll and Zobell, Heat Conduction, McGraw-Hill, (1948).

7. Jost, Explosion and Combustion Processes in Gases, McGraw-Hill, (1946).

8. Lamb, Hydrodynamics, Cambridge Press, (1879).